



**UNIVERSIDADE FEDERAL DO CEARÁ  
CENTRO DE TECNOLOGIA  
DEPARTAMENTO DE ENGENHARIA DE TRANSPORTES  
PROGRAMA DE PÓS-GRADUAÇÃO EM ENGENHARIA DE TRANSPORTES**

**JORGE LUIZ OLIVEIRA LUCAS JÚNIOR**

**ADESIVIDADE AGREGADO-LIGANTE: EFEITO NO COMPORTAMENTO DE  
MISTURAS ASFÁLTICAS E NA PREVISÃO DE DESEMPENHO DE PAVIMENTOS**

**FORTALEZA  
2021**

JORGE LUIZ OLIVEIRA LUCAS JÚNIOR

ADESIVIDADE AGREGADO-LIGANTE: EFEITO NO COMPORTAMENTO DE  
MISTURAS ASFÁLTICAS E NA PREVISÃO DE DESEMPENHO DE PAVIMENTOS

Tese de Doutorado apresentada ao Programa de  
Pós-Graduação em Engenharia de Transportes  
da Universidade Federal do Ceará, como parte  
dos requisitos para a obtenção do título de  
Doutor em Engenharia de Transportes.  
Área de concentração: Infraestrutura de  
Transportes.

Orientador: Prof. Jorge B. Soares, PhD  
Coorientador: Prof. Dr. Lucas F. Babadopulos

FORTALEZA  
2021

Dados Internacionais de Catalogação na Publicação  
Universidade Federal do Ceará  
Biblioteca Universitária  
Gerada automaticamente pelo módulo Catalog, mediante os dados fornecidos pelo autor

---

L966i Lucas Júnior, Jorge Luiz Oliveira.

Adesividade agregado-ligante: efeito no comportamento de misturas asfálticas e na previsão de desempenho de pavimento / Jorge Luiz Oliveira Lucas Júnior. – 2021.  
96 f.: il. color.

Tese (doutorado) – Universidade Federal do Ceará, Centro de Tecnologia, Programa de Pós-Graduação em Engenharia de Transportes, Fortaleza, 2021.

Orientação: Prof. Dr. Jorge Barbosa Soares.

Coorientação: Prof. Dr. Lucas Feitosa de Albuquerque Lima Babadopoulos.

1. Adesividade. 2. Misturas asfálticas. 3. Previsão de desempenho do pavimento. I. Título.

CDD 388

---

JORGE LUIZ OLIVEIRA LUCAS JÚNIOR

ADESIVIDADE AGREGADO-LIGANTE: EFEITO NO COMPORTAMENTO DE  
MISTURAS ASFÁLTICAS E NA PREVISÃO DE DESEMPENHO DE PAVIMENTOS

Tese apresentada ao Programa de Pós-Graduação em Engenharia de Transportes da Universidade Federal do Ceará, como requisito parcial à obtenção do título de Doutor em Engenharia de Transportes. Área de concentração: Infraestrutura de Transportes.

Aprovada em: 26/02/2021.

BANCA EXAMINADORA

---

Prof. Dr. Jorge Barbosa Soares (Orientador)  
Universidade Federal do Ceará (UFC)

---

Prof. Dr. Lucas Feitosa de Albuquerque Lima Babadopulos (Coorientador).  
Universidade Federal do Ceará (UFC)

---

Profª. Drª. Suelly Helena de Araújo Barroso  
Universidade Federal do Ceará (UFC)

---

Profª. Drª. Juceline Batista dos Santos Bastos  
Instituto Federal de Educação, Ciência e Tecnologia do Ceará (IFCE)

---

Prof. Dr. David H. Allen  
Texas A&M University

---

Prof. Dr. Fernando Moreno Navarro  
Universidad de Granada

*“A imaginação é mais importante que o conhecimento.  
O conhecimento é limitado, enquanto a imaginação abraça o mundo.  
Ela é, rigorosamente falando, um fator real na pesquisa científica.”*

(Albert Einstein)

## AGRADECIMENTOS

Poderia dizer que meus agradecimentos deveriam começar pelo dia 16/03/2016, quando entrei no mestrado no PETRAN/UFC ou em 16/03/2018 quando defendi o mestrado e entrei no Doutorado no mesmo PETRAN, porém meus agradecimentos vão muito além deste período. Tive muita sorte na minha trajetória e por isso agradeço. Sorte de encontrar pessoas que acreditaram em mim, investiram em mim, e me ajudaram na medida de suas possibilidades.

As primeiras duas pessoas que gostaria de agradecer são talvez as pessoas que mais me conhecem na vida, minha Mãe e meu Pai. Vocês me apoiaram desde a 1ª série do antigo 1º grau e abdicam hoje da minha companhia sem nunca terem reclamado, por que sabem que eu precisava terminar essa etapa, mesmo que tenhamos praticamente perdido os últimos 5 anos de convivência. A vida é feita de escolhas e eu trocaria qualquer título para poder estar na companhia de vocês, diariamente, mas às vezes ou muitas vezes a vida vai nos afastando geograficamente daqueles que mais amamos, porém deixo claro aqui que todos os dias vocês estiveram comigo na construção e na desconstrução deste trabalho. Só o que eu desejo a vocês é que tenham muita saúde para que nessa nova etapa da minha vida nós possamos aproveitar nossa companhia e estarmos mais juntos.

Aos meus irmãos, cada um com suas qualidades, agradeço pela parceria de vida, pela união que temos devido às dificuldades que vivemos e acima de tudo pela maneira como torcemos uns pelos outros, e como ficamos felizes com cada vitória alcançada de cada um. Aos meus parentes mais próximos, acreditem, todos vocês foram exemplos em algum segmento da vida e formaram a pessoa que sou hoje. Como não agradecer por ter a sorte de fazer parte de uma família tão legal como a nossa.

Enfim cheguei em 16/03/2018, e não poderia começar essa história pelo Doutorado. Foi no Mestrado que se abriu um novo mundo para mim, conheci pessoas incríveis e que me ensinaram a evoluir no meu momento. A pós-graduação que nunca foi um desejo para mim se tornou minha realidade e como eu curti cada aula que tive, cada conhecimento novo que aprendi, cada ensaio novo no laboratório. Novamente a sorte esbarrou em mim e eu fui parar em um laboratório reconhecidamente inovador, o LMP. Cada história e cada nome de alunos que por lá passaram me fizeram ter a certeza de que estava no lugar certo. Mas como um Engenheiro Químico do Rio Grande do Sul, chamado por alguns como Gaúcho ou Tchê, foi parar no LMP/PETRAN? É uma longa história com duas explicações, a primeira é simples, pura sobrevivência misturada com pragmatismo. A segunda é uma contradição pessoal para alguém céítico como eu, a única explicação é que foi o destino ou era pra ser assim. Sem correr

o risco de esquecer alguém, agradeço a todos os alunos, funcionários, colaboradores e professores que encontrei ao longo dessa jornada da pós-graduação.

Agradeço às Professoras Suelly Barroso e Juceline Bastos e aos Professores David Allen e Fernando Navarro por aceitarem participar da banca e por terem de alguma forma servido de inspiração para a realização deste trabalho.

Foi em 2016 que conheci meu orientador, Prof. Jorge Soares, nas aulas de materiais betuminosos, e desde lá só fizemos uma coisa: trabalhar. E quando a gente pensa que o trabalho que está sendo bem feito não pode ficar melhor, novamente a sorte bate a minha porta e se junta ao time, no final de 2017, o Prof. Lucas Babadopoulos, que veio a ser meu coorientador de Doutorado. Para alguém extremamente autocrítico como eu foi um desafio atender a dois revisores tão exigentes. Se por um lado as exigências me demandavam um tempo grande, por outro, devido a elas, tivemos êxito nos principais periódicos de nossa área. Agradeço aos dois a liberdade e a independência que me deram no desenvolvimento do nosso trabalho. Novamente não sei se a vida vai me levar pra longe ou não, mas tenho certeza que essa parceria será duradoura.

Agradeço à Fundação Cearense de Apoio ao Desenvolvimento Científico e Tecnológico pela qual fui bolsista durante 4 anos, 2 de mestrado e 2 de doutorado, e à Agência Nacional do Petróleo, Gás Natural e Biocombustíveis que financiou esse trabalho de doutorado, a partir de maio de 2020. Agradeço ao PETRAN/DET por ter me proporcionado conhecer pessoas tão legais, pelo acolhimento, pelos aprendizados e evolução profissional que me possibilitou e pelas inúmeras oportunidades concedidas.

Agradeço ao meu filho Thiago por entender a mudança da sua rotina devido a esse trabalho e aceitar minhas cobranças. Por fim, queria registrar um agradecimento especial à minha mulher Angelina. Se há uma pessoa que sabe quantas horas de trabalho foram dedicadas nesses últimos 5 anos é ela. E digo isso pedindo desculpas e agradecendo-a pelos vários momentos de lazer abdicados por ela e pelo Thiago para que eu pudesse me envolver em mais uma coisa só, que seria a última, mas que duas semanas a frente se transformava na penúltima. Foi ela quem não me deixou desistir do mestrado quando eu quis parar porque a grana estava curta. Foi ela quem viu minhas frustrações com algum equipamento quebrado no laboratório que parava meus ensaios. Foi ela quem me ensinou a levar a vida mais tranquilo, sem me estressar tanto, e como minha gastrite agradeceu. Poderia dizer 1000 coisas em que ela me ajudou ou me fez uma pessoa melhor, mas simplesmente vou dizer OBRIGADO, sem você nada disso seria possível, te amo.

Tenho claro em minha mente que o sucesso é fruto de trabalho, mas não é só isso. Se fosse só pelo trabalho as olimpíadas só teriam medalhas de ouro. O que diferencia a medalha de ouro das demais não é somente o trabalho, a dedicação e a perseverança com que você se prepara para ela, mas acima de tudo o ambiente que nos rodeia, as pessoas que nos cercam e as oportunidades que nos são dadas. Eu diria que se você tiver tudo isso que citei, ainda assim, você só terá uns 80% do que é preciso para ter sucesso. Eu credito 20% a sorte em toda a caminhada, estar na hora e no lugar certo ou conhecer a pessoa certa pode revolucionar sua vida. Nunca considerei o Doutorado uma competição de quem publicava mais ou ia a mais congressos. Tudo o que fiz nesses 5 anos foi em busca de ser a minha melhor versão, pois sabia que assim teria sucesso. Sei que poderia ter feito mais ou melhor, mas terminei satisfeita e agradecida por toda ajuda que tive. Novos desafios virão e vamos em frente, em busca dos nossos sonhos.

## RESUMO

Inúmeras pesquisas já identificaram que o ligante asfáltico puro pode não produzir a devida qualidade da mistura asfáltica quando esta contém agregados ácidos, devido à fraca adesividade agregado-ligante. Uma alternativa para melhorar essa propriedade é utilizar um aditivo melhorador de adesividade. Por isso, o objetivo geral desta tese de doutorado foi determinar os efeitos e as inter-relações da adesividade agregado-ligante nas misturas asfálticas utilizando diferentes técnicas experimentais e seu impacto na previsão de desempenho dos pavimentos por meio de métodos mecanístico-empíricos. Quatro escalas foram analisadas: ligante e agregado separados, adesividade agregado-ligante, mistura asfáltica e estrutura do pavimento. Além dos ensaios básicos, foram utilizados 1 método de avaliação das propriedades morfológicas dos agregados, 1 método inovador de avaliação de propriedades de misturas baseado em processamento digital de imagens, 2 tipos de ensaios em ligantes asfálticos, 3 diferentes ensaios de adesividade agregado-ligante, 4 diferentes ensaios em misturas asfálticas e, por fim, 2 programas computacionais de análise e dimensionamento de pavimentos asfálticos.

Esta tese está organizada na forma de um compêndio de artigos. O artigo 1 aborda os efeitos das propriedades de forma dos agregados e da adesividade do ligante ao agregado nos resultados dos ensaios à compressão e à tração/compressão em misturas asfálticas a quente. O artigo 2 avalia o efeito do melhorador de adesividade na vida de fadiga de pavimentos. O artigo 3 se destina a determinar o efeito da temperatura, da espessura, da carga e da velocidade na previsão de área trincada de pavimentos asfálticos. O artigo 4 trata do efeito da reologia e da adesividade de ligantes asfálticos em diferentes substratos na resistência ao condicionamento por umidade. No artigo 1, a adesividade foi mais importante que a morfologia dos agregados para a fadiga medida à tração-compressão, enquanto que o tipo de agregado provou ser mais importante para os ensaios à compressão. No artigo 2, as misturas com melhorador à base de amina apresentaram maior vida de fadiga se comparadas às misturas com ligante puro. No artigo 3, cada variação de  $\pm 1\text{cm}$  de espessura do revestimento asfáltico produziu efeito na área trincada semelhante a variações de  $\pm 1,1^\circ\text{C}$ ,  $\pm 5,6\text{km/h}$  ou  $\pm 16,6\text{kN}$  de carga por roda de eixo simples. No artigo 4, apesar de o aditivo ter melhorado as propriedades adesivas do ligante ao agregado, ele ocasionou uma redução média de 9,5% na rigidez do ligante na condição seca e 8,7% após condicionamento à umidade, além de uma menor resistência à deformação permanente a  $82^\circ\text{C}$ .

**Palavras-chave:** adesividade, agregado, ligante, misturas asfálticas, previsão de desempenho do pavimento.

## ABSTRACT

Numerous researches have already identified that the neat asphalt binder may not produce the proper quality of the asphalt mixture when it contains acid aggregates, due to the poor aggregate-binder adhesiveness. An alternative to improve this property is to use an anti-stripping agent. Therefore, the objective of this work was to determine how the aggregate-binder adhesiveness affects the mechanical behavior of asphalt mixtures and consequently the prediction of pavement performance. Four scales were analyzed: separate binder and aggregate, aggregate-binder adhesiveness, asphalt mixture, and pavement structure. In addition to the basic tests themselves, 1 method for evaluating the morphological properties of the aggregates, 1 innovative method for evaluating the properties of mixtures based on digital image processing, 2 types of tests on asphalt binders, 3 different aggregate-binder adhesion tests, 4 different tests on asphalt mixtures, and 2 computer programs for analysis and design of asphalt pavements. This thesis is organized as a compendium of papers, including articles already published and others submitted to journals. Paper 1 addresses the effects of aggregate shape properties and the adhesion of the binder to the aggregate on the results of the compression and tension/compression tests in hot asphalt mixtures. Paper 2 assesses the effect of an amine-based anti-stripping agent on the fatigue life of pavements. Paper 3 presents the effect of temperature, thickness, load and speed in predicting cracked areas of asphalt pavements. Paper 4 deals with the effect of rheology and the adhesiveness of asphalt binders to different substrates on resistance to moisture conditioning. In paper 1, adhesiveness was indicated as more important than aggregate morphology for fatigue measured using tension-compression, while the type of aggregate proved to be more important for compression tests. In paper 2, mixtures with an amine-based anti-stripping agent showed a longer fatigue life when compared to mixtures with a neat binder. In paper 3, each variation of  $\pm 1\text{cm}$  in the thickness of the asphalt surface course produced in the cracked area an effect similar to variations of  $\pm 1.1^\circ\text{C}$ ,  $\pm 5.6\text{km/h}$  or  $\pm 16.6\text{kN}$  of load per single wheel axle. In paper 4, although the additive improved the adhesive properties of the binder to the aggregate, it caused an average reduction of 9.5% in the binder stiffness in the dry condition, and 8.7% after moisture conditioning and less resistance to permanent deformation at  $82^\circ\text{C}$ .

**Keywords:** adhesiveness, aggregate, binder, asphalt mixtures, pavement performance prediction.

## LISTA DE ABREVIATURAS

AASHTO	<i>American Association of State Highway and Transportation Officials</i>
ABNT	Associação Brasileira de Normas Técnicas
ABS	<i>Asphalt bond strength</i>
Additive	<i>Amine-based anti-stripping agent</i>
ANP	Agência Nacional do Petróleo, Gás Natural e Biocombustíveis
ASTM	<i>American Society for Testing and Materials</i>
CAP	Cimento asfáltico de petróleo
CAP3D-D	<i>Software</i> de dimensionamento e previsão de desempenho de pavimentos
CAPES	Coordenação de Aperfeiçoamento de Pessoal de Nível Superior
CNPq	Conselho Nacional de Desenvolvimento Científico e Tecnológico
DIP	<i>Digital image processing</i>
DNIT	Departamento Nacional de Infraestrutura de Transportes
FlexPAVE™	<i>Layered viscoelastic pavement analysis for critical distresses</i>
FN	<i>Flow Number</i>
FS	<i>Frequency sweep</i>
MSCR	<i>Multiple stress creep and recovery</i>
NCHRP	<i>National Cooperative Highway Research Program</i>
PATTI	<i>Pneumatic adhesion tensile testing instrument</i>
RTFO	<i>Rolling thin film oven</i>
SEINFRA-CE	Secretaria da Infraestrutura do Estado do Ceará
SHRP	<i>Strategic Highway Research Program</i>
Superpave	<i>Superior Performing Asphalt Pavement</i>
S-VECD	<i>Simplified viscoelastic continuum damage</i>
WLF	Modelo Williams-Landel-Ferry
2S2P1D	Modelo de comportamento viscoelástico de ligantes e misturas asfálticas

# SUMÁRIO

<b>1. INTRODUÇÃO .....</b>	<b>14</b>
<b>1.1. Considerações iniciais.....</b>	<b>14</b>
<b>1.2. Justificativa .....</b>	<b>14</b>
<b>1.3. Problema de pesquisa.....</b>	<b>15</b>
<b>1.4. Objetivo geral.....</b>	<b>16</b>
<b><i>1.4.1. Objetivos específicos .....</i></b>	<b>16</b>
<b>1.5. Estrutura do trabalho .....</b>	<b>16</b>
<b>1.6. Síntese dos resultados .....</b>	<b>17</b>
<b>1.7. Informações de trabalhos anteriores do autor que embasaram a tese .....</b>	<b>20</b>
<b>2. EFEITO DAS PROPRIEDADES DE FORMA DOS AGREGADOS E DA ADESIVIDADE DO LIGANTE AO AGREGADO NOS RESULTADOS DOS ENSAIOS A COMPRESSÃO E A TRAÇÃO/COMPRESSÃO EM MISTURAS ASFÁLTICAS A QUENTE .....</b>	<b>22</b>
<b>2.1. Introduction .....</b>	<b>22</b>
<b>2.2. Materials and tests.....</b>	<b>24</b>
<b><i>2.2.1. Shape properties of coarse aggregate .....</i></b>	<b>25</b>
<b><i>2.2.2. Aggregate-binder adhesion .....</i></b>	<b>26</b>
<b><i>2.2.3. Indirect tensile strength for axial compression and moisture induced damage .....</i></b>	<b>26</b>
<b><i>2.2.4. Uniaxial repeated load.....</i></b>	<b>27</b>
<b><i>2.2.5. Stiffness characterization .....</i></b>	<b>27</b>
<b><i>2.2.6. Damage characterization &amp; fatigue simulation .....</i></b>	<b>28</b>
<b>2.3. Results and discussions .....</b>	<b>29</b>
<b><i>2.3.1. Shape properties of the investigated aggregate sources .....</i></b>	<b>29</b>
<b><i>2.3.2. Adhesion properties of the investigated different combinations .....</i></b>	<b>30</b>
<b><i>2.3.3. Effect of aggregate and asphalt binder on its and rutting of HMA .....</i></b>	<b>31</b>
<b><i>2.3.4. Effect of aggregate and asphalt binder on the dynamic moduli of HMA .....</i></b>	<b>32</b>
<b><i>2.3.5. Effect of aggregate and asphalt binder on the fatigue life of HMA .....</i></b>	<b>34</b>
<b><i>2.3.6. Summary of test results and their relationships .....</i></b>	<b>36</b>
<b>2.4. Conclusions.....</b>	<b>39</b>
<b>REFERENCES .....</b>	<b>40</b>
<b>3. AVALIAÇÃO DO EFEITO DO ADITIVO MELHORADOR DE ADESIVIDADE A BASE DE AMINA NA VIDA DE FADIGA DE PAVIMENTOS ASFÁLTICOS.....</b>	<b>42</b>

<b>3.1. Introduction .....</b>	<b>42</b>
<b>3.2. Materials characterization and performance prediction method .....</b>	<b>44</b>
<i>3.2.1. Adhesiveness test, linear viscoelastic and fatigue damage characterization .....</i>	<b>46</b>
<i>3.2.2. FlexPAVETM 1.1<sup>Alpha</sup> simulation .....</i>	<b>48</b>
<b>3.3. Results and discussions .....</b>	<b>52</b>
<i>3.3.1. Fatigue cracking spatial distribution (damage contours) and percent damage .....</i>	<b>52</b>
<i>3.3.2. Average damage (<math>N/N_f</math> of 110 points) vs. time.....</i>	<b>54</b>
<i>3.3.3. Predicted cracked area of the pavement with the different combinations of asphalt mixtures .....</i>	<b>57</b>
<b>3.4. Conclusions.....</b>	<b>58</b>
<b>REFERENCES .....</b>	<b>60</b>
<b>4. EFEITO DA TEMPERATURA, DA ESPESSURA, DA CARGA E DA VELOCIDADE NA PREVISÃO DE ÁREA TRINCADA DE PAVIMENTOS ASFÁLTICOS.....</b>	<b>63</b>
<b>4.1. Introdução .....</b>	<b>64</b>
<b>4.2. Materiais e métodos.....</b>	<b>65</b>
<i>4.2.1. Ensaio de adesividade agregado-ligante .....</i>	<b>66</b>
<i>4.2.2. Caracterização viscoelástica linear e fadiga.....</i>	<b>67</b>
<i>4.2.3. Simulação no CAP3D-D.....</i>	<b>68</b>
<b>4.3. Resultados e discussões .....</b>	<b>70</b>
<i>4.3.1. Efeito da temperatura na previsão da área trincada .....</i>	<b>70</b>
<i>4.3.2. Efeito da espessura da camada asfáltica na previsão da área trincada .....</i>	<b>72</b>
<i>4.3.3. Efeito da carga na previsão da área trincada .....</i>	<b>73</b>
<i>4.3.4. Efeito da velocidade na previsão da área trincada .....</i>	<b>73</b>
<i>4.3.5. Avaliação do efeito unitário das diferentes variáveis analisadas na área trincada ....</i>	<b>74</b>
<i>4.3.6. Relação entre temperatura, espessura, carga e velocidade .....</i>	<b>75</b>
<b>4.4. Conclusões .....</b>	<b>78</b>
<b>REFERÊNCIAS.....</b>	<b>79</b>
<b>5. EFEITO DA REOLOGIA E DA ADESIVIDADE DE LIGANTES ASFÁLTICOS A DIFERENTES SUBSTRATOS NA RESISTÊNCIA AO CONDICIONAMENTO POR UMIDADE .....</b>	<b>82</b>
<b>5.1. Introduction .....</b>	<b>82</b>
<b>5.2. Experiments description .....</b>	<b>84</b>

<b>5.2.1. Materials .....</b>	<b>84</b>
<b>5.2.2. Moisture conditioning procedure for the rheological tests .....</b>	<b>85</b>
<b>5.2.3. Tests with the Dynamic Shear Rheometer .....</b>	<b>86</b>
<b>5.2.4. Digital image processing (DIP) .....</b>	<b>87</b>
<b>5.2.5. Asphalt Bond Strength (ABS) .....</b>	<b>88</b>
<b>5.3. Results and discussion .....</b>	<b>90</b>
<b>5.3.1. Linear viscoelastic characterization .....</b>	<b>90</b>
<b>5.3.2. Multiple Stress Creep Recovery (MSCR) .....</b>	<b>91</b>
<b>5.3.3. Digital Image Processing of HMA substrates .....</b>	<b>91</b>
<b>5.3.4. Asphalt Bond Strength (ABS) test .....</b>	<b>93</b>
<b>5.3.4.1. Mineral Aggregate used as Substrate.....</b>	<b>93</b>
<b>5.3.4.2. HMAs used as Substrate .....</b>	<b>94</b>
<b>5.3.5. Correlation Between POTS and ADIP<sub>AGG</sub> in dry and moisture conditions.....</b>	<b>95</b>
<b>5.4. Conclusions.....</b>	<b>96</b>
<b>REFERENCES .....</b>	<b>97</b>
<b>6. CONCLUSÕES E RECOMENDAÇÕES PARA TRABALHOS FUTUROS .....</b>	<b>100</b>
<b>6.1. Considerações iniciais.....</b>	<b>100</b>
<b>6.2. Principais Contribuições da Tese .....</b>	<b>100</b>
<b>6.3. Principais Conclusões Oriundas do Programa Experimental.....</b>	<b>101</b>
<b>6.3.1. Quanto às análises realizadas no artigo 1 .....</b>	<b>101</b>
<b>6.3.2. Quanto às análises realizadas no artigo 2 .....</b>	<b>101</b>
<b>6.3.3. Quanto às análises realizadas no artigo 3 .....</b>	<b>102</b>
<b>6.3.1. Quanto às análises realizadas no artigo 4 .....</b>	<b>102</b>
<b>6.4. Recomendações para Trabalhos Futuros .....</b>	<b>103</b>
<b>REFERÊNCIAS BIBLIOGRÁFICAS .....</b>	<b>104</b>

## 1. INTRODUÇÃO

### 1.1. Considerações iniciais

A adesividade agregado-ligante é um tema amplamente estudado tanto nacional quanto internacionalmente. A literatura aponta quatro teorias para descrever a interação entre esses dois materiais, a saber: (i) teoria da adesão mecânica (Terrel e Al-Swailmi, 1994); (ii) teoria da orientação molecular (Majidzadeh e Brovold, 1968); (iii) teoria da energia de superfície (Terrel e Shute, 1989); e (iv) teoria da reação química (Hicks, 1991). Devido à complexidade do tema, ainda hoje não há uma teoria unificada que explique a adesão entre agregados e ligantes asfálticos. Os principais mecanismos de perda de adesividade descritos na literatura (Kiggundu e Roberts, 1988; Johnson e Freeman, 2002) são o deslocamento, o desprendimento, a pressão no poros ou pressão neutra, o polimento hidráulico e a emulsificação espontânea. Há uma grande variedade de ensaios laboratoriais para avaliação da adesividade ou dos efeitos da umidade, tais quais os ensaios de deslocamento da película asfáltica quando em contato com a água, como o ensaio tradicional de adesividade usado no Brasil (ABNT 12583, 2017) ou ainda o ensaio internacionalmente utilizado conhecido como *Water Boiling Test* (ASTM D3625, 2020), ou, alternativamente os ensaios de energia de superfície e os ensaios de arrancamento como o *Asphalt Bond Strength* (ABS) (AASHTO TP 91, 2013) e o *Pell Test* etc. Existem ainda ensaios que avaliam o efeito da umidade na mistura asfáltica como o Dano por Umidade Induzida (ABNT 15617, 2015) ou o *Hamburg Wheel-Tracking Test* (AASHTO T324, 2019). Os estudos sobre adesividade a nível nacional e internacional têm avançado consideravelmente o conhecimento nos últimos anos (Aguiar-Moya *et al.*, 2015; Lucas Júnior *et al.*, 2019), devido às novas tecnologias e ao desenvolvimento de novos ensaios (Kanitpong e Bahia, 2003; Santagata *et al.*, 2009; Dong *et al.*, 2020). O avanço do conhecimento sobre a adesividade será fundamental para uma melhor previsão de desempenho e para um dimensionamento de pavimentos mais racional, de forma a otimizar os recursos e aumentar a vida útil dos pavimentos.

### 1.2. Justificativa

A literatura especializada em materiais betuminosos já identificou que o uso de ligante asfáltico puro pode reduzir a qualidade da mistura asfáltica, quando esta é submetida a condições severas de temperatura, de frequência de carregamento, de tráfego e de umidade, especialmente quando utilizada com agregados de natureza ácida. A mistura com tais características, quando aplicada em campo, pode comprometer o comportamento mecânico do

pavimento asfáltico, o que leva ao aparecimento precoce de defeitos, ocasionando uma redução da vida útil do pavimento e, por conseguinte, um aumento dos custos com manutenção, restauração e/ou reconstrução. Ao se utilizar ligantes com adesividade insatisfatória é necessário usar algum aditivo para prevenir os danos por umidade.

Segundo a Secretaria da Infraestrutura do Estado do Ceará (SEINFRA-CE, 2021), o custo da tonelada de Cimento Asfáltico de Petróleo (CAP 50/70) é de R\$ 3.249,60 e o custo do kg de aditivo melhorador de adesividade à base de amina (DOPE) é de R\$ 38,80. Como exemplo, se o teor desse aditivo em uma obra de pavimentação for de 0,25% em relação a massa de CAP, cada tonelada de CAP utilizada requererá 2,5 kg de aditivo, ocasionando um aumento de R\$ 97,00 reais e uma elevação do custo em relação ao ligante de 3%. Se o teor necessário de DOPE for de 0,5% esse custo será aumentado em aproximadamente 6%.

Por isso, o presente trabalho se destina a investigar como a seleção de agregados minerais e do ligante asfáltico pode afetar a adesividade, com o correspondente impacto nas misturas asfálticas, utilizando diferentes técnicas experimentais, e por consequência seus efeitos nos pavimentos asfálticos.

### **1.3. Problema de pesquisa**

Em relação à umidade, uma alternativa para combater seus efeitos é utilizar um aditivo melhorador de adesividade à base de aminas. A literatura tem reportado que a adesividade está intimamente ligada ao dano por umidade, porém seu impacto em outros defeitos como o trincamento por fadiga e a deformação permanente ainda tem sido pouco estudado. Além disso, não há procedimentos experimentais consagrados e há pouca variabilidade de técnicas experimentais propostas. O fato de a adesividade não ser amplamente estudada em relação a esses defeitos está ligado a complexidade do fenômeno e a confiabilidade dos meios de medição em laboratório dessa propriedade.

O problema de pesquisa desse estudo está amparado no fato de que, tanto nacional quanto internacionalmente, não avançamos cientificamente o suficiente para entender os mecanismos que governam a adesividade agregado-ligante e não desenvolvemos técnicas que nos permitam medir diretamente essa propriedade. Entender a adesividade já é um problema complexo e, quando associado à compreensão de seus impactos em outros defeitos, torna essa busca bastante desafiadora. De toda forma, podemos usar diferentes técnicas experimentais que indicam indiretamente a força adesiva dos diferentes materiais que se deseja combinar e, com isso, prever o efeito de sua escolha nos defeitos dos pavimentos asfálticos.

## **1.4. Objetivo geral**

O objetivo geral desta tese de doutorado foi investigar os efeitos e as inter-relações da adesividade agregado-ligante nas misturas asfálticas utilizando diferentes técnicas experimentais e o impacto desta adesividade na previsão de desempenho dos pavimentos por meio de métodos mecanístico-empíricos.

### ***1.4.1. Objetivos específicos***

- (i) Estudar o efeito das propriedades de forma dos agregados e da adesividade agregado-ligante em diferentes ensaios utilizados para avaliar o comportamento mecânico de misturas asfálticas, tanto por tração-compressão quanto por compressão simples.
- (ii) Avaliar o impacto de um aditivo melhorador de adesividade à base de amina na vida de fadiga dos pavimentos asfálticos.
- (iii) Determinar o efeito da temperatura, da espessura, da carga e da velocidade na previsão de área trincada de pavimentos asfálticos com diferentes adesividades agregado-ligante.
- (iv) Investigar o efeito da reologia e da adesividade de ligantes asfálticos em diferentes substratos na resistência ao condicionamento por umidade.

## **1.5. Estrutura do trabalho**

A presente tese de doutorado foi escrita no formato de artigos. Cada artigo trata diretamente de um dos objetivos específicos da tese e é reproduzido, na sua forma aceita ou na sua forma submetida a uma revista científica, em um capítulo deste documento, sendo publicado ou submetido a um periódico científico da área. Uma introdução geral é apresentada antes do primeiro artigo, enquanto uma conclusão geral da tese com recomendações para trabalhos futuros é apresentada após o último. Este documento foi então dividido em 6 tópicos e por fim são apresentadas as referências bibliográficas, a saber:

- (i) INTRODUÇÃO: as considerações iniciais e a estrutura do trabalho são descritas, além de serem expostos a justificativa, o problema de pesquisa, o objetivo geral e os objetivos específicos da tese como um todo. É apresentada uma síntese dos resultados obtidos em cada artigo. Essa síntese, além de ter por finalidade situar o leitor sobre as diferenças entre cada artigo, também se destina a estimular o leitor a se aprofundar melhor no artigo que tenha resultados mais instigantes, na sua visão particular. Por fim, são apresentadas algumas informações sobre resultados importantes de outros trabalhos publicados pelo autor e seus orientadores, que serviram como base para o desenvolvimento da tese.

- (ii) ARTIGO 1: abordou os efeitos das propriedades de forma dos agregados e da adesividade do ligante ao agregado nos resultados dos ensaios à compressão e à tração/compressão em misturas asfálticas a quente. Foram investigados os ensaios de módulo complexo à compressão (AASHTO T342, 2011), módulo complexo à tração-compressão, fadiga (AASHTO TP107, 2020), *Flow Number* (DNIT 184, 2018), resistência à tração por compressão diametral (DNIT 136, 2018). Esse artigo foi publicado no periódico *Materials and Structures* em abril de 2020.
- (iii) ARTIGO 2: avaliou o efeito do aditivo melhorador de adesividade à base de amina na vida de fadiga prevista de pavimentos asfálticos utilizando o ensaio de fadiga à tração compressão associada ao modelo S-VECD como entradas para a ferramenta computacional FlexPAVE. Esse artigo foi publicado no periódico *International Journal of Pavement Engineering* em janeiro de 2021.
- (iv) ARTIGO 3: destinou-se a determinar o efeito da temperatura, da espessura, da carga e da respectiva velocidade na previsão de área trincada de pavimentos asfálticos com diferentes adesividades agregado-ligante. Foi usada a ferramenta CAP3D-D desenvolvida no LMP. Este artigo foi submetido à Revista Transportes em janeiro de 2021.
- (v) ARTIGO 4: tratou do efeito da reologia e da adesividade de ligantes asfálticos a diferentes substratos na resistência ao condicionamento por umidade. Foram usados os ensaios *Frequency Sweep* (ASTM D 7175, 2015) e *Multiple Stress Creep and Recovery* (ASTM D7405) para ligantes asfálticos e o ensaio *Asphalt Bond Strength* (AASHTO TP91, 2013) para avaliar a adesividade e também o processamento digital de imagem. Este artigo foi submetido ao periódico *The Journal of Adhesion* em fevereiro de 2021.
- (vi) CONCLUSÕES E RECOMENDAÇÕES PARA TRABALHOS FUTUROS: apresentou-se as considerações finais desta Tese de Doutorado, bem como as recomendações propostas para trabalhos futuros.

## 1.6. Síntese dos resultados

- **Efeito das propriedades de forma dos agregados e da adesividade do ligante ao agregado nos resultados dos ensaios à compressão e à tração/compressão em misturas asfálticas a quente.**

O artigo correspondente foi publicado em 04 de abril de 2020 no periódico *Materials and Structures* (Fator de Impacto 2,901) com o seguinte título: “*Effect of aggregate shape properties and binder's adhesiveness to aggregate on results of compression and*

*tension/compression tests on hot mix asphalt”.*

O objetivo deste trabalho foi investigar o efeito das propriedades de forma e textura das partículas dos agregados, bem como a adesividade agregado-ligante, em diferentes ensaios de resistência mecânica das misturas asfálticas: resistência à tração por compressão axial; dano por umidade induzida; deformação permanente uniaxial de carga repetida; módulo dinâmico, tanto por compressão quanto por tração/compressão; e vida de fadiga por tração/compressão. O *Aggregate Image Measurement System* foi usado para analisar as propriedades de forma das partículas de agregados. Os resultados do ensaio *Asphalt Bond Strength* foram usados como um indicador da adesão agregado-ligante.

**SÍNTESE:** Os principais resultados desse capítulo mostram que as propriedades de forma dos agregados influenciaram mais fortemente os valores de ensaios mecânicos à compressão. Enquanto isso, o ligante asfáltico que produziu melhor adesividade com os agregados minerais influenciou mais fortemente os resultados do ensaio de vida de fadiga à tração/compressão de misturas asfálticas. Agregados mais esféricos e rugosos melhoraram o intertravamento das misturas analisadas, enquanto que misturas com agregados mais lamelares e mais polidos tiveram menores diferenças entre os resultados dos ensaios de módulo dinâmico à compressão em comparação ao módulo dinâmico à tração/compressão, devido à melhor adesividade agregado-ligante.

- **Avaliação do efeito do aditivo melhorador de adesividade a base de amina na vida de fadiga de pavimentos asfálticos.**

Este artigo foi publicado em 12 de janeiro de 2021 no periódico *International Journal of Pavement Engineering* (Fator de Impacto 2,646) com o seguinte título: “***Evaluating the effect of amine-based anti-stripping agent on the fatigue life of asphalt pavements***”.

O objetivo do trabalho foi avaliar o impacto do uso de um aditivo melhorador de adesividade à base de amina na vida de fadiga dos pavimentos asfálticos. Foram utilizados um CAP 50/70 puro e modificado por 0,2% deste aditivo em massa de ligante. As misturas investigadas incluem 2 fontes de agregados, granítica e fonolítica, perfazendo um total de 4 misturas asfálticas. Foram utilizados a caracterização da rigidez, o modelo Viscoelástico de Dano Contínuo Simplificado e o software FlexPAVE™.

**SÍNTESE:** As misturas com ligante modificado por aditivo melhorador de adesividade à base de amina apresentaram menores danos por fadiga previstos em estruturas de pavimentos quando comparadas às misturas com ligante puro. As misturas com agregado

granítico também apresentam dano previsto inferior às misturas com agregado fonolítico. Todas as estruturas analisadas mostraram trincas de baixo para cima (*bottom-up cracking*) no revestimento asfáltico. Do ponto de vista da modelagem de dano por fadiga, a investigação das diferentes combinações de misturas mostrou que é mais recomendado o uso de misturas com melhorador de adesividade à base de amina nas camadas superiores e misturas com ligante puro na parte inferior. No caso em questão essa análise foi realizada sem o condicionamento à umidade. Ressalta-se que as misturas com ligante puro não poderiam ser utilizadas devido a não atingirem requisitos mínimos de aceitação dos órgãos rodoviários nacionais, pois apresentaram adesividade insatisfatória e dano por umidade induzida menor que 70%.

- **Efeito da temperatura, da espessura, da carga e da velocidade na previsão de área trincada de pavimentos asfálticos com diferentes adesividade agregado-ligante.**

O artigo em questão foi submetido em 09 de janeiro de 2021 à Revista Transportes com o seguinte título: *“Previsão de área trincada em pavimentos asfálticos: quais as principais variáveis a considerar?”*

O objetivo deste artigo foi avaliar como a temperatura, a espessura do revestimento asfáltico, a carga aplicada e a velocidade do tráfego afetam o comportamento à fadiga dos pavimentos asfálticos com um revestimento contendo um CAP 50/70 puro e o mesmo CAP, porém modificado por 0,2% de aditivo orgânico melhorador de adesividade à base de amina. Para isso, utilizou-se a caracterização viscoelástica linear (AASHTO T342), a caracterização de fadiga por meio do ensaio à tração-compressão (AASHTO TP107), bem como o modelo S-VECD como entradas para simulação no CAP3D-D.

**SÍNTESE:** Os pavimentos com aditivo melhorador de adesividade à base de amina apresentaram menores valores de área de trincada quando comparadas aos pavimentos com CAP 50/70 puro. Assim como os pavimentos revestidos com misturas com agregado granítico apresentaram menores valores de área trincada quando comparados aos pavimentos revestidos com misturas com agregado fonolítico. Para as misturas analisadas neste trabalho, cada variação de  $\pm 1\text{cm}$  de espessura do revestimento asfáltico produziu na área trincada um efeito semelhante a, aproximadamente, variações de  $\pm 1,1^\circ\text{C}$ ,  $\pm 5,6\text{km/h}$  ou  $\pm 16,6\text{kN}$  de carga por roda em um eixo simples. Esses resultados sugerem a ordem de grandeza dos custos com sobrecargas e sublinha as importâncias dos efeitos das velocidades de tráfego e da temperatura do pavimento no seu desempenho.

- **Efeito da reologia e da adesividade de ligantes asfálticos a diferentes substratos na resistência ao condicionamento por umidade.**

O respectivo artigo foi submetido em 19 de fevereiro de 2021 ao periódico *The Journal of Adhesion* (Fator de Impacto 2,576) com o seguinte título: “*Effects of rheology and adhesiveness of asphalt binders to different substrates on the resistance to moisture conditioning*”.

O objetivo deste artigo foi investigar os efeitos da reologia e da adesividade de ligantes asfálticos em diferentes substratos na resistência ao condicionamento por umidade. Para isso, ensaios de módulo complexo e de deformação permanente foram realizados nos ligantes asfálticos, tanto em condição seca quanto em condição após tratamento com umidade.

A adesão foi medida pelo teste ABS e a área de contato do aglutinante de asfalto com o percentual de agregado da superfície dos substratos foi obtida por processamento digital de imagem (PDI) antes de todos os testes ABS. O objetivo da análise PDI foi determinar se a área de agregado em contato com o aglutinante afeta a adesão e como esses resultados podem ajudar compreender o fenômeno da adesividade agregado-ligante.

**SÍNTESE:** O condicionamento à umidade reduziu a rigidez média em 15,2% tanto para o ligante puro e quanto para o modificado. A adição do melhorador de adesividade à base de amina reduziu a rigidez do aglutinante puro 9,5% na condição seca e 8,7% nas amostras condicionadas à umidade. Até a temperatura de 76°C, os resultados do  $J_{nr}$  foram semelhantes, mas a 82°C o ligante puro apresentou maior resistência à deformação permanente quando comparado ao ligante modificado. A área de agregado nos substratos em contato com o ligante asfáltico não apresentou uma boa correlação com a  $R_{POTS}$  na condição seca, mas mostrou boas correlações nas amostras condicionadas à umidade. Isso sugere que a força de adesão em si pode não ser influenciada pelo contato adequado entre o agregado e o ligante, mas este contato evita danos por umidade na interface.

## 1.7. Informações de trabalhos anteriores do autor que embasaram a tese

No trabalho publicado na Revista Transportes (Lucas Júnior e Soares, 2019) foi desenvolvida uma metodologia capaz de determinar os percentuais de área de agregado recoberto pelo ligante asfáltico após o ensaio tradicional de adesividade (ABNT 12583, 2017), empregando uma técnica de processamento digital de imagens (PDI). Isso possibilitou um avanço na análise do ensaio empírico, partindo de uma análise qualitativa (satisfatório ou insatisfatório) para uma análise quantitativa cujos resultados se correlacionaram muito bem aos

de ensaios quantitativos, como o de Lottman modificado.

O trabalho apresentado no 8<sup>th</sup> EATA (*European Asphalt Technology Association International Conference* em Granada, Espanha e publicado na edição especial do periódico *Road Material and Pavement Design* (Lucas Júnior *et al.*, 2019a) buscou identificar as principais propriedades que afetam a adesividade. As propriedades físicas (angularidade, esfericidade, textura e porosidade medida indiretamente pela absorção) não foram capazes de prever a adesividade medida pelo deslocamento da película asfáltica com uso do PDI. Por outro lado, a composição química dos agregados afetou consideravelmente a adesividade medida por PDI. Agregados com maior teor de óxido de cálcio e de óxido de ferro apresentaram melhor adesividade, enquanto que agregados com maiores teores de sílica e de óxido de potássio apresentaram pior adesividade.

No trabalho publicado no periódico *Construction and Building Materials* (Lucas Júnior *et al.*, 2019b), a adesividade (medida por meio de PDI e do ensaio de Lottman modificado que busca mensurar o dano por umidade induzida com procedimento padronizado) pareceu retardar a formação e a propagação das microtrincas quando as amplitudes de deformações usadas em ensaios de fadiga foram menores. Para amplitudes maiores, esse efeito de retardação não foi observado. É possível que grandes cargas, que resultem em maiores amplitudes de deformação, excedam o limite que a força de adesão agregado-ligante oferece para prevenir a formação e a propagação das microtrincas, tornando a adesão menos importante no caso de maiores amplitudes de deformação.

O trabalho publicado no periódico *Journal of Testing and Evaluation* (Lucas Júnior *et al.*, 2020) avaliou o efeito da adesividade medida pelo ensaio *Asphalt Bond Strength* (ABS) na vida de fadiga de misturas asfálticas. As misturas com ligante com aditivo melhorador de adesividade apresentaram maior vida de fadiga do que as misturas com ligante puro. O aditivo proporcionou vida de fadiga ( $N_f$ ) mais de três vezes maior quando comparado às misturas com ligante puro.

## **2. EFEITO DAS PROPRIEDADES DE FORMA DOS AGREGADOS E DA ADESIVIDADE DO LIGANTE AO AGREGADO NOS RESULTADOS DOS ENSAIOS À COMPRESSÃO E À TRAÇÃO/COMPRESSÃO EM MISTURAS ASFÁLTICAS A QUENTE**

Publicado em *Materials and Structures*

### **Effect of aggregate shape properties and binder's adhesiveness to aggregate on results of compression and tension/compression tests on hot mix asphalt**

Jorge L. O. Lucas Júnior<sup>a,b\*</sup>, Lucas F. A. L. Babadopoulos<sup>c</sup> & Jorge B. Soares<sup>a</sup>

<sup>a</sup> Department of Transportation Engineering, Federal University of Ceará at Fortaleza, Brazil

<sup>b</sup> Department of Civil Engineering, College Ari de Sá, Fortaleza, Brazil

<sup>c</sup> Department of Structural Engineering and Civil Construction, Federal University of Ceará at Fortaleza, Brazil

\* Corresponding author.

E-mail addresses: [j.lucas.j@det.ufc.br](mailto:j.lucas.j@det.ufc.br) (Jorge L.O. Lucas Júnior), [babadopoulos@ufc.br](mailto:babadopoulos@ufc.br) (Lucas F.A.L. Babadopoulos), [jsoares@det.ufc.br](mailto:jsoares@det.ufc.br) (Jorge B. Soares).

#### **ABSTRACT**

The mechanical behavior of hot mix asphalt is affected by their constituent properties, i.e., aggregate and asphalt binder properties. The loading path used in laboratory testing is also a factor that may influence results. The objective of this work was to investigate the effect of aggregate particle shape properties and texture, as well as of the aggregate-binder adhesion, on different tests used to evaluate mixture resistance: indirect tensile strength in axial compression (ITS); moisture-induced damage – modified Lottman; uniaxial repeated load permanent deformation – Flow number (FN); dynamic modulus, both at compression and at tension/compression; and tension/compression fatigue life. The Aggregate Image Measurement System (AIMS2) was used for analyzing aggregate particle shape properties. Asphalt Bond Strength test results were used as an indicator of aggregate-binder adhesion. The results indicate that the binder is relatively more important for tension/compression tests, while aggregate properties are relatively more important for compression tests. For the latter, the higher the load applied in the test, the greater the importance of the aggregate to the mixture result, which is expected since this favor interlocking. ITS and FN results appear to be strongly affected by aggregate sphericity and texture. Dynamic modulus at compression depends more on aggregate shape properties, while fatigue life is more influenced by aggregate-binder adhesion.

**Keywords:** Aggregate shape properties, adhesion, moisture damage, anti-stripping agent.

#### **2.1. Introduction**

The mechanical behavior of an asphalt mixture is affected by properties of its constituents, such as aggregate shape and aggregate-binder adhesion. The loading path (e.g. compression or tension/compression) used in mechanical tests also influences the measured properties. Nguyen et al. (2016) investigated complex modulus on cylindrical samples, for three different kinds of sinusoidal loading: only tension, only compression and tension/compression. Those authors concluded that the selected loading path could significantly influence the measured properties depending on temperature and loading frequency. While values obtained

from tests on compression only, tension only, and tension/compression, may be similar for average and low temperatures (approximately 0.1Hz at 11.1°C for a classical asphalt mixture), at higher temperatures differences of up to 40% in stiffness and 7° (degrees) in phase angle may be observed. Forough et al. (2014) mention that the loading path (tension or compression) is an important factor that also affects the relaxation modulus of mixtures. Lytton et al. (2017) point that the undamaged properties of an asphalt mixture may be different when it is loaded in tension or in compression.

Several authors (Al-Rousan, 2004; Mahmoud et al., 2010; Diógenes et al., 2018) have used the Aggregate Image Measurement System (AIMS) to investigate aggregate shape properties and their impact on asphalt mixtures behavior. Al-Rousan (2004) developed a classification system based on the distribution of aggregate shape characteristics. Ibiapina et al. (2018) developed the same kind of system focusing on Brazilian aggregate sources, such as the ones investigated in this paper. Bessa et al. (2015) investigated aggregate shape properties and their effect on the behavior of hot-mix asphalt (HMA), based on several laboratorial tests such as resilient modulus, indirect tensile strength (ITS), fatigue under controlled diametral compression load, and uniaxial repeated load. They concluded that despite differences in mineralogical composition of the investigated aggregates, because they had similar shape properties resulted in HMA samples with similar mechanical behavior.

Liu et al. (2017) examined the effects of morphological characteristics of coarse aggregate on the rutting and fatigue performance of stone matrix asphalt (SMA). More spherical, angular and rougher aggregate particles provided improved rutting performance of the investigated mixtures. Spherical coarse aggregate resulted in improved fatigue performance.

Lucas Júnior et al. (2019a) evaluated the correlation between angularity and texture in the stripping of the asphalt film from coated aggregate, a property closely related to moisture damage in asphalt pavements. The authors concluded that neither of the investigated morphological properties were able to predict stripping. Valdés-Vidal et al. (2015) measured stiffness and cracking resistance of asphalt mixtures and concluded that morphology and surface texture of both coarse and fine aggregate influenced results.

Most adhesiveness studies are focused on investigating failure in asphalt pavements from the point of view of the physico-chemical and morphological properties of the materials (Hicks, 1991; Kanitpong and Bahia, 2003; Bhasin et al., 2006; Lucas Júnior et al., 2019a, 2019b, 2019c). Since asphalt mixtures have several other variables impacting their behavior, the understanding of failure mechanisms could benefit from studies in which a great number of

variables are fixed and the effect of just a few of them are investigated. With that in mind, the objective of this work was to investigate the effect of aggregate shape properties and aggregate-binder adhesiveness in different tests used to evaluate HMA: indirect tensile strength (ITS); uniaxial repeated load permanent deformation – Flow number (FN); dynamic modulus at compression and at tension/compression; and tension/compression fatigue life.

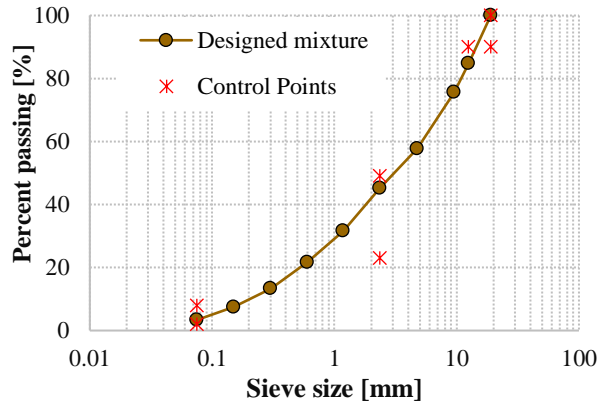
## 2.2. Materials and tests

Aggregate from two different sources (a phonolitic and a granitic) were considered on the research. According to Alexander and Mindess (2005), acid aggregate contains at least 65% of SiO<sub>2</sub> (silicon oxide) in its composition, while intermediate acidity aggregate has between 55 and 65% SiO<sub>2</sub>, and, finally, basic aggregate contains less than 55% of the referred oxide. Both the phonolitic and granitic aggregate sources used in this research present 49% of SiO<sub>2</sub>, being classified as basic in nature with respect to their silicon oxide content. However, in practice, they are considered to present the behavior of acidic aggregates used in paving applications, since they have poor adhesiveness to the asphalt binder utilized in the same region, making the corresponding mixes susceptible to moisture damage.

Two asphalt binders were investigated. The first one is a 50/70 penetration grade neat binder commonly used in Northeastern Brazil, while the second one is obtained from the modification of the 50/70 penetration grade binder by an amine-based anti-stripping agent. Combinations of these materials produced 4 HMAs in the Superpave Gyratory Compactor (SGC) with 5.0% binder content, and 4.0 ± 0.4% air voids. The aggregate particles were sieved prior to weighting and mixture fabrication to ensure equal gradation for all mixtures. The sieves used are between 19.0 and 0.075mm, as presented in Figure 1. Mixing and compaction temperatures were 160°C and 150°C, respectively, for all mixtures. The mixture terminology in this paper is used according to the characteristics of the aggregate and the binders, i.e., Ph for phonolite, G for granite, N for neat binder, and A for anti-stripping agent. Therefore, the 4 HMAs are designated as follows: Ph-N, Ph-A, G-N and G-A. In total, 62 specimens were used to carry out all tests. Two considerations are important for the analysis of the results herein:

- The only difference between Ph-N and Ph-A mixtures is the anti-stripping of the Ph-A mixture. The same occurs with G-N and G-A mixtures.
- The only difference between Ph-N and G-N mixtures is the aggregate type. The same occurs with Ph-A and G-A mixtures.

Figure 1 – Aggregate gradation for both granite and phonolite



### 2.2.1. Shape properties of coarse aggregate

Aggregate particle shape properties were investigated with AIMS2: this system consists of a camera and two lighting schemes, with two modes of use, each depending on the particle size to be characterized. Coarse particles (retained on the 4.75-mm sieve) are analyzed by means of black and white (angularity) and grey scale (texture) images. Three aggregate shape properties were analyzed: sphericity, texture, and angularity. Before AIMS2 scanning, the aggregate was separated by size in the following sieves: 12.5, 9.5 and 4.75 mm (minimum number of 50 aggregate particles). The parameters measured are briefly described here and more details can be found in Masad (2004). Equations 1 to 3 are used by AIMS2. The classification system used for aggregate morphological parameters was the one by Ibiapina et al. (2018).

- Sphericity: establishes a relation between the three dimensions of the particle.

Classification: Elongated (< 0.5), Low (0.5 – 0.7), Moderate (0.7 – 0.9), and High (> 0.9);

$$\text{Sphericity} = \sqrt[3]{\frac{d_s d_I}{d_L^2}} \quad (1)$$

where  $d_s$  is the particle's shortest dimension;  $d_I$  is the particle's intermediate dimension and  $d_L$  is the particle's longest dimension.

- Texture: defines the relative roughness of aggregate surface by means of wavelet analysis.

Classification: Polished (< 260), Smooth (260 – 440), Low (440 – 600), Moderate (600 – 825), and High (> 0.9);

$$\text{Texture} = \frac{1}{3N} \sum_{i=1}^3 \sum_{j=1}^N D_{i,j}(x, y)^2 \quad (2)$$

where  $D$  is the decomposition function;  $N$  is the total number of coefficients in the image;  $i$  is

the considered direction of texture (1, 2 or 3), and  $j$  is the wavelet coefficient index.

- Angularity: measured by means of the gradient method, which uses black and white images to calculate the changes in gradient along the particle outline.

Classification: Rounded (< 1260), Sub rounded (1260 – 4080), Sub angular (4080 – 7180), and Angular (> 7180);

$$\text{Angularity} = \frac{1}{(N/3) - 1} \sum_{i=1}^{n-3} |\theta_i - \theta_{i+3}| \quad (3)$$

where  $\theta$  is the angle of orientation of the edge points;  $n$  is the total number of points analyzed, and  $i$  is the  $i$ th point on the boundary of a particle.

The reader is referred to the works by Masad (2004) and Al-Rousan (2004) for further details on the equations used by AIMS2.

### 2.2.2. Aggregate-binder adhesion

The Asphalt Bond Strength test was used to characterize aggregate-binder adhesion. The specimens of sawed aggregate and the asphalt binder were placed in the oven at 150°C for 30min. After this time, the aggregate was heated to 60°C for 30min, the binder (0.4±0.05 g) was placed in a circular silicone mold at room temperature for 30min and the metal stubs (20mm diameter) were oven-heated at 150°C for 30 min. The binder was added to the part of the metal stub designed to accommodate the fixed film thickness. The pull-off tensile strength (POTS), which is the maximum applied pull-off stress, was then determined. The ABS equipment is similar to the Pneumatic Adhesion Tensile Testing Instrument (PATTI) (which uses a pneumatic device), but with a hydraulic pressure system which reports POTS automatically. The loading rate was 0.2MPa/s. Two conditioning procedures were analyzed: 24h dry (POTS<sub>DRY</sub>) and 12h wet (POTS<sub>WET</sub>). The Bond Strength Ratio (R<sub>POTS</sub>) is determined by Equation (4).

$$R_{POTS} = \frac{POTS_{WET}}{POTS_{DRY}} \cdot 100\% \quad (4)$$

### 2.2.3. Indirect tensile strength for axial compression and moisture induced damage

The indirect tensile strength (ITS) test was conducted on unconditioned (ITS<sub>U</sub>) and moisture conditioned (ITS<sub>C</sub>) specimens with 7.0 ± 0.5% air voids. The three tested moisture conditioned specimens were subjected to the following steps indicated by NBR 15617 (similar to AASTHO T283): 55-80% saturation; cooling to -18 ± 3°C for 16h; water bath at 60 ± 1°C

for  $24 \pm 1$ h; water bath at  $25 \pm 1^\circ\text{C}$  for 2 to 3h. Then, moisture conditioned ITS was obtained from the average result of three specimens.  $\text{ITS}_U$  is obtained from the average result of ITS from specimens without the conditioning procedure. ITS is obtained by diametral compression according to ABNT 15087 using 100-mm diameter and approximately 63.5-mm height specimens, with a deformation rate of  $0.8 \pm 0.1\text{mm/s}$ . For analyzing the HMA resistance to moisture-induced damage the indirect tensile strength ratio (TSR), in percentage, is determined by Equation (5):

$$\text{TSR} = \frac{\text{ITS}_C}{\text{ITS}_U} \cdot 100\% \quad (5)$$

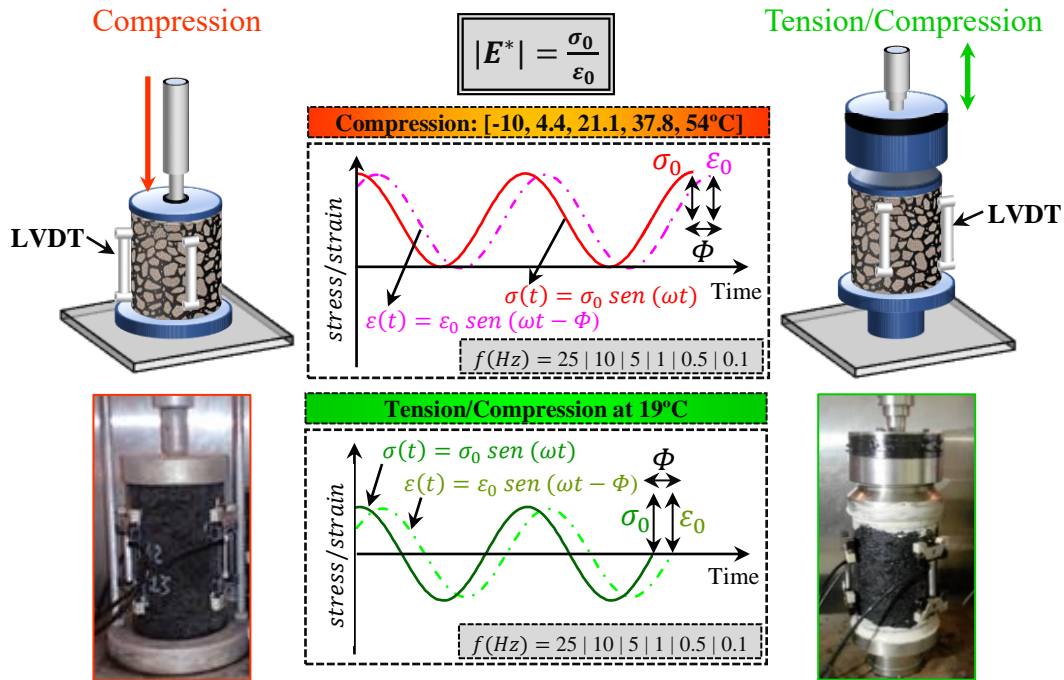
#### **2.2.4. Uniaxial repeated load**

The Uniaxial Repeated Load Permanent Deformation test (also known as the Flow Number test) was used in this research. The 150-mm height and 100-mm diameter cylindrical specimens were submitted to compressive stress with a haversine pulse load of 0.1s followed by 0.9s of rest, during which a contact load is still applied. The peak stress value is 204kPa during loading, and 10.2kPa (5% of peak load) is applied during the rest period, at  $60^\circ\text{C}$ . Test results include the accumulated permanent strain ( $\varepsilon_p$ ) *versus* number of cycles (N) curve, which is divided in three zones. In the primary zone, specimen densification occurs at an elevated rate; the secondary zone contains smaller and approximately constant strain rates; and the tertiary zone indicates the specimen failure. The number of cycles in which the tertiary zone starts is known as the Flow Number (FN), and it is where plastic deformation rate is minimal. In this research, tested specimens presented  $4.0 \pm 0.4\%$  air voids.

#### **2.2.5. Stiffness characterization**

The Dynamic Modulus ( $|E^*|$ ) of the four investigated HMA was determined using two loading paths: (i) axial compression, and (ii) axial tension/compression. The specimens had  $4.0 \pm 0.4\%$  air voids. Three specimens were used for each mixture for both the compression and the tension-compression tests, in a total of twenty-four specimens. The results reported are always the average for each mixture. The dynamic modulus at compression ( $|E^*|_{\text{COMPRESSION}}$ ) followed AASHTO T 342 (frequencies of 25; 10; 5; 1; 0.5 and 0.1Hz and temperatures of -10; 4.4; 21.1; 37.8 and  $54^\circ\text{C}$ ). The dynamic modulus at tension/compression ( $|E^*|_{\text{TENSION/COMPRESSION}}$ ) followed the procedure of the fingerprint test proposed by AASHTO TP 107. Loading amplitudes were selected to apply  $68 \pm 8\mu\text{m/m}$  (peak to peak strain amplitude). Figure 2 shows the basic testing scheme.

Figure 2 – Dynamic moduli at compression and tension/compression



### 2.2.6. Damage characterization & fatigue simulation

Controlled crosshead tension-compression sinusoidal loading was used to analyze fatigue life of HMA according to AASHTO TP 107. For each mixture, three 130-mm height by 100-mm diameter specimens ( $4.0 \pm 0.4\%$  air voids) were tested.

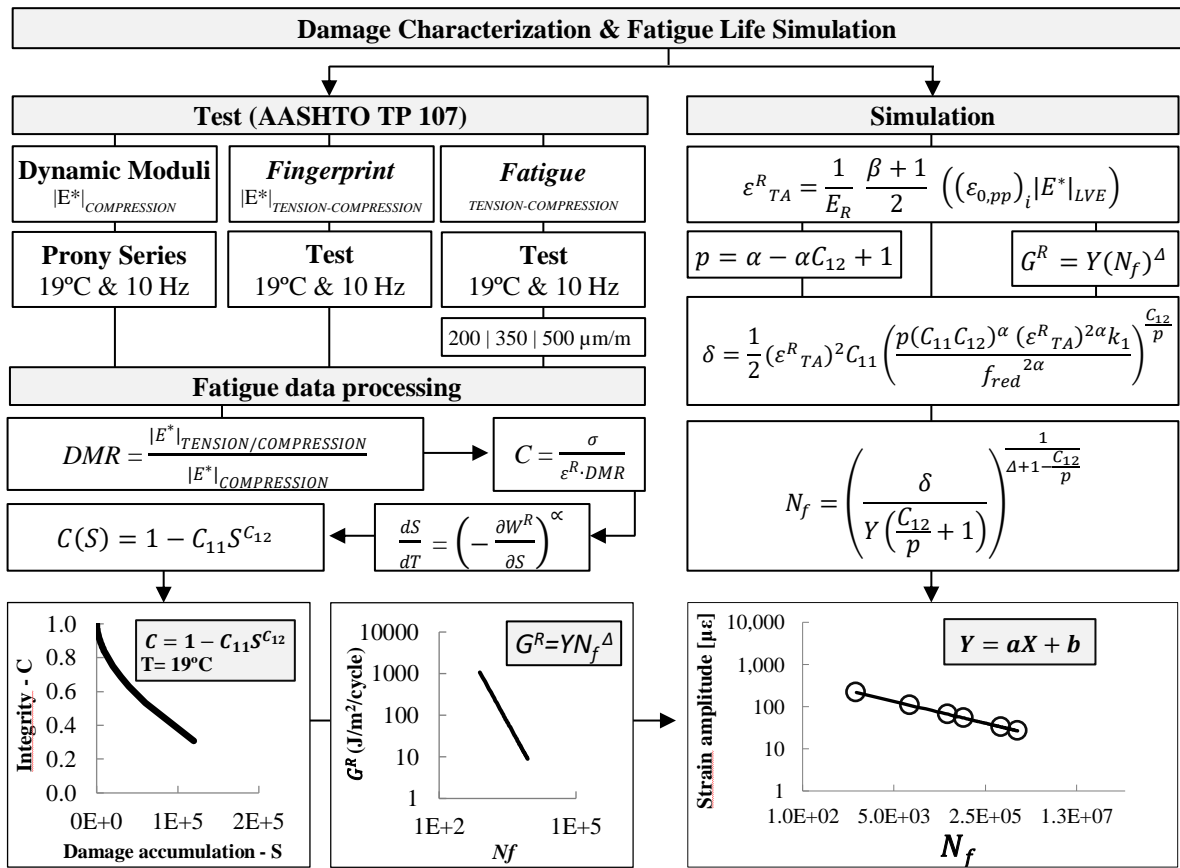
The S-VECD model is based on three main concepts: pseudo strain ( $\varepsilon^R$ ) from the elastic-viscoelastic correspondence principle (Schapery, 1984), continuum damage mechanics-based work potential theory (Park *et al.*, 1996) and time-temperature superposition (t-TS) principle with growing damage (Chehab *et al.*, 2002).

The damage characteristic curves ( $C$  vs  $S$ ) were fitted by Power Law equation ( $C = 1 - C_{11}S^{C_{12}}$ ) and the  $G^R$  failure criterion ( $G^R = YN_f^\Delta$ ) was used to determine failure in the damage simulations ( $C_{11}$ ,  $C_{12}$ ,  $Y$  and  $\Delta$  are the material parameters obtained from the damage characterization and used for damage simulation). The simulation to obtain fatigue life ( $N_f$ ) is performed using the Equations presented by Nascimento (2016), presented in the flowchart in Figure 3.

Loading is shown in Figure 2, and analysis procedures and simulation for damage characterization is summarized in the flowchart in Figure 3, where the different variables are: dynamic modulus ratio ( $DMR$ ); pseudo stiffness ( $C$ ); measured maximum stress ( $\sigma$ ); correspondent pseudo strain ( $\varepsilon^R$ ); pseudo strain energy density ( $W^R$ ); damage parameter ( $\alpha = 1 + 1/m$ ); relaxation modulus maximum absolute time derivative ( $m$ ); damage characteristic

curve ( $C$  vs.  $S$ ) fitting coefficients ( $C_{11}$  and  $C_{12}$ ); material integrity ( $C(S)$ ); number of cycles at failure ( $N_f$ ); rate of change of the averaged released pseudo strain energy (per cycle) throughout the entire history of the test ( $G^R$ ); failure criterion envelope ( $G^R$  vs.  $N_f$ ) fitting coefficients ( $\Delta$  and  $Y$ ); reduced frequency ( $f_{red}$ ) considering time-temperature superposition (t-TS) principle; tension part of the pseudo strain amplitude ( $\varepsilon^R_{TA}$ ); load form factor ( $k_1$ ); portion of the cycle in which tensile stress occurs ( $\beta$ ) and peak-to-peak strain amplitude ( $\varepsilon_{0,pp}$ ). Details about the tests used for fatigue characterization and the variables in the simulation can be found in Lucas Júnior et al. (2019).

Figure 3 – Summary of fatigue testing and analysis



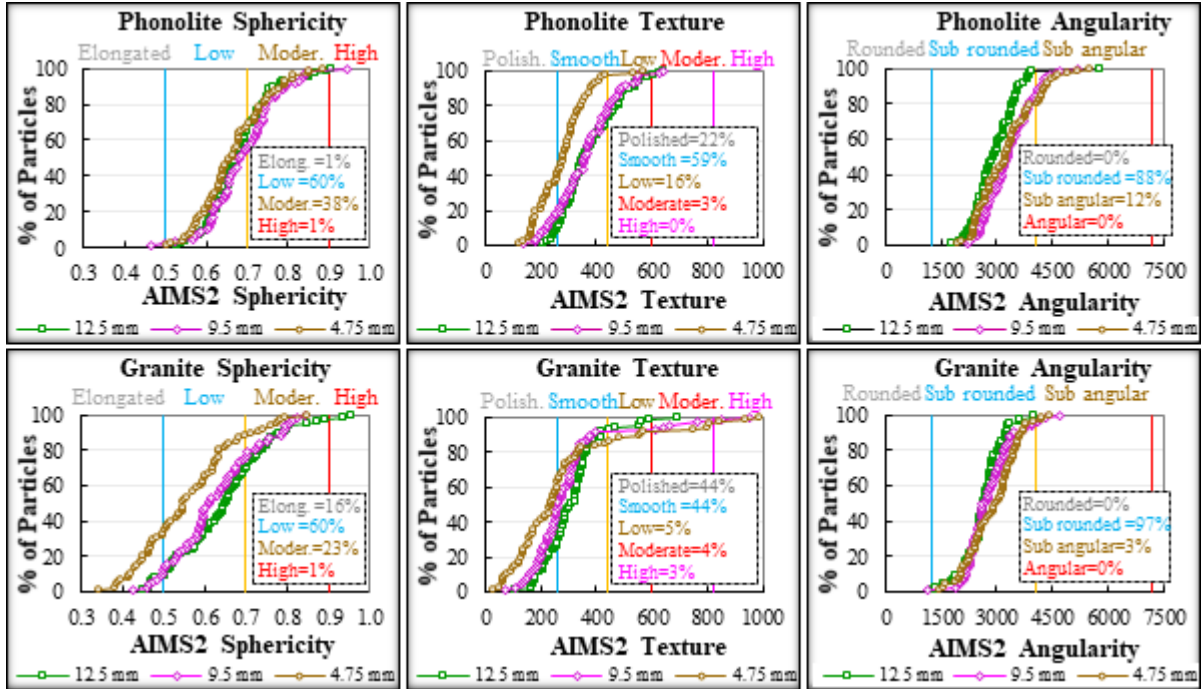
## 2.3. Results and discussions

### 2.3.1. Shape properties of the investigated aggregate sources

On average, the phonolitic aggregate presented 15% more particles classified as having moderate sphericity than the granitic aggregate. Meanwhile, the granitic aggregate presented 15% less particles classified as elongated than the phonolitic aggregate. With respect to texture, the phonolitic is less polished than the granite. The angularity of the two aggregate sources presented undistinguishable values (Figures 4). It is concluded for this research that the studied

phonolitic aggregate should provide better interlocking than the studied granitic aggregate due to morphological properties when used in asphalt mixtures.

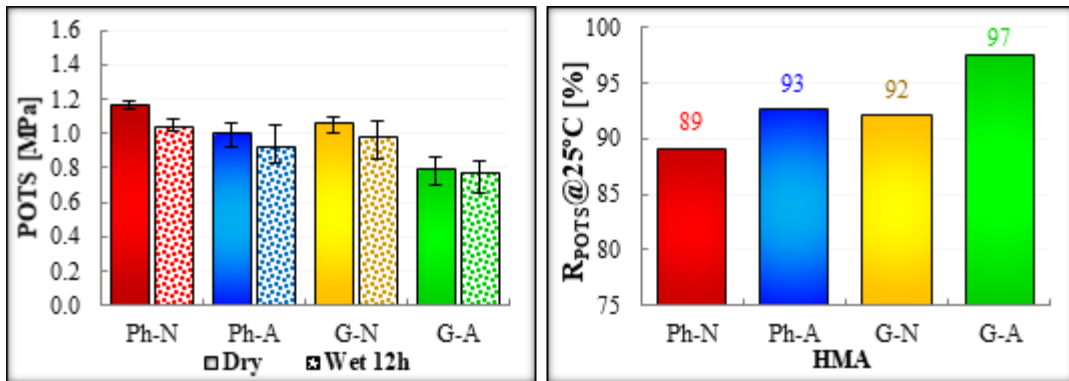
Figure 4 – Morphological properties of the aggregates



### 2.3.2. Adhesion properties of the investigated different combinations

From Figure 5 it is noted that the neat binder provided higher POTS values than the binder modified with the anti-stripping agent. It is speculated that this additive may decrease the stiffness of the binder, which could explain the observed difference. This happened in the dry test and wet conditioned to 12 hours of moisture. On the other hand, when analyzing the loss of POTS by moisture (Figure 5), the anti-stripping additive lead to better results when compared to the neat binder. The combinations with greater resistance to moisture damage were in the following order: G-A > Ph-A > G-N > Ph-N. These results showed that the anti-stripping amine-based and the granitic aggregate presented better results than the neat binder and the phonolitic aggregate. Most of the failures were of the cohesive (7 failures) type and very few of them were adhesive-cohesive (1 failure - G-N at 12h wet), without any observable trend on the POTS results. The addition of the anti-stripping agent changed the viscoelastic properties of the binder (the modified binder tends to flow more than the unmodified one). Since this pullout test is strongly dependent on viscoelasticity (viscoelastic flow properties affect the pullout test), it is possible that the binder stiffness was slightly reduced by the additive because the additive viscosity is considerably lower than the neat binder viscosity, resulting in lower POTS.

Figure 5 – Aggregate-binder adhesion properties

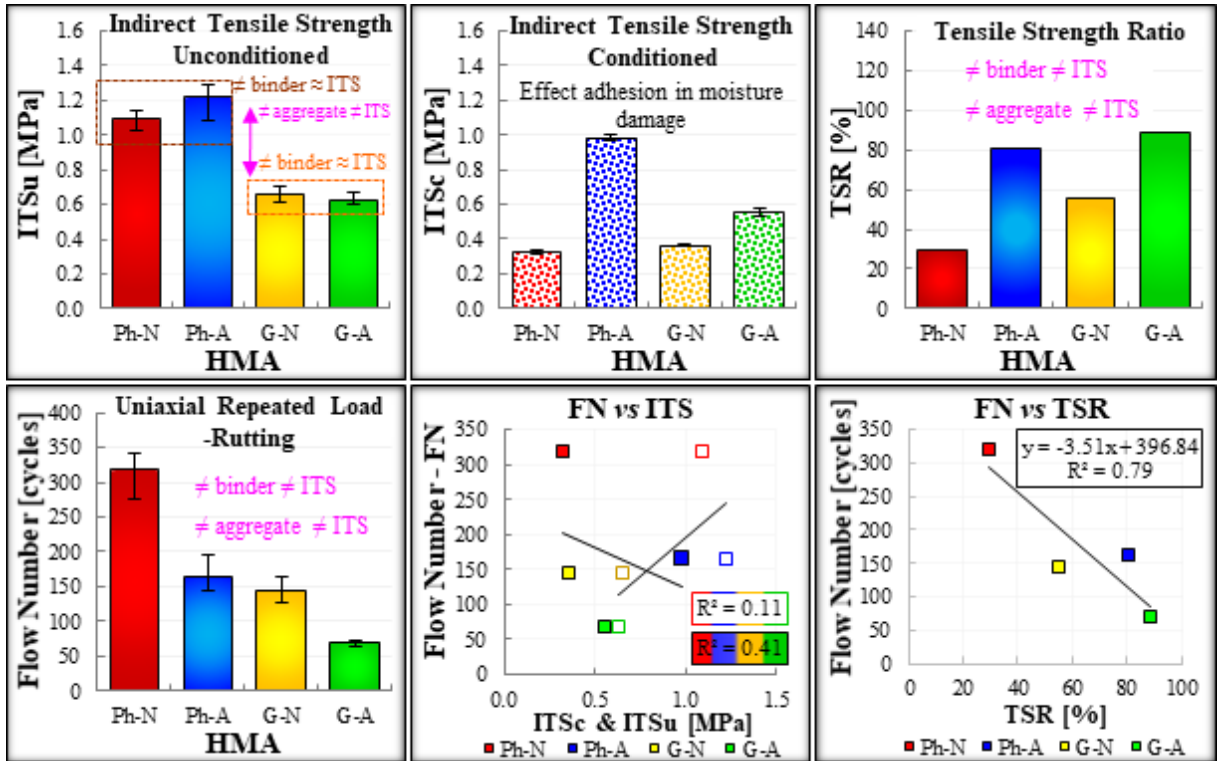


### 2.3.3. Effect of aggregate and asphalt binder on its and rutting of HMA

Figure 6 presents results from ITS and FN tests, as well as relationships between the obtained results. The  $ITS_U$  test captures the differences in shape properties between the two aggregate sources, since mixtures with phonolitic aggregate have reached much higher  $ITS_U$  than mixtures with granitic aggregate (Figure 6). However, this test does not seem to be able to capture the change between the neat binder and the binder modified with the anti-stripping agent, since no significant increase in  $ITS_U$  was observed. Previous work by the authors (Lucas Júnior et al., 2019b) indicated improvements in properties such as fatigue life when the anti-stripping agent was added, possibly because of an enhancement in adhesiveness (as suggested by the increase in  $R_{POTS}$ ), which was not noticed in the  $ITS_U$  results. When test specimens are conditioned to moisture,  $ITSC$  continues to capture the differences between the shape properties in the case of the comparison between Ph-A and G-A in Figure 6 (but not in the case of Ph-N and G-N). It captures more pronouncedly the influence of the binder (confirmed by the lowest values of Ph-N and G-N). The importance of the anti-stripping agent is highlighted by the TSR (Figure 6). Lucas junior et al. (2019a) reported that the texture and the angularity did not present high correlation with the stripping resistance, i.e. these aggregate morphological properties do not influence stripping or resistance to moisture damage. Therefore, it is speculated that the sphericity has a more important role in the interlocking of the analyzed mixtures, consequently in the ITS values. The FN is influenced by aggregate and binder in a more balanced manner, as indicated in Figure 6. Although not correlated with ITS directly (Figure 6), a negative correlation was observed between resistance to moisture damage and resistance to permanent deformation. As the permanent deformation (FN) test uses a severe load (204kPa), associated to large deformations in the specimen, the anti-stripping additive reduced the resistance to viscoplastic flow, and therefore the permanent deformation. Lucas Júnior et al. (2019b) reported

that the anti-stripping agent was able to reduce fatigue cracking for small amplitude strains. For small deformations, a better aggregate-binder adhesiveness seems to improve the fatigue life, while for large deformations this property does not seem to have the same capacity, as in the case of permanent deformation.

Figure 6 – ITS and Flow Number for the investigated HMA



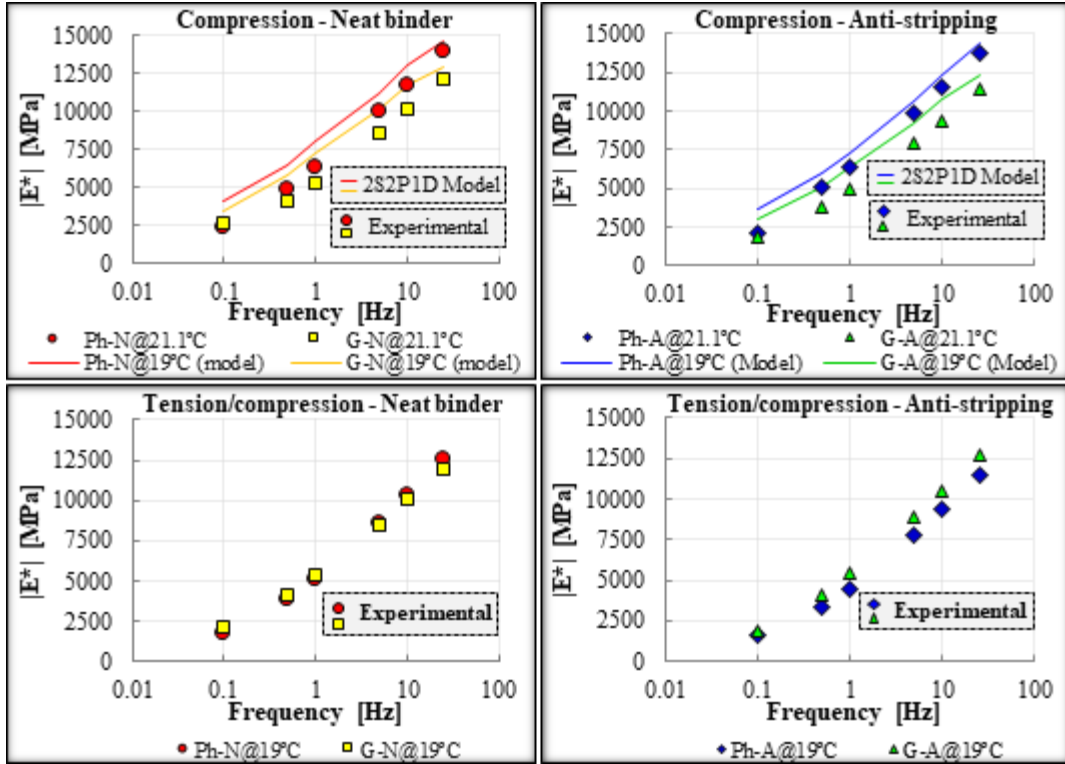
### 2.3.4. Effect of aggregate and asphalt binder on the dynamic moduli of HMA

In the HMA with neat binder, the phonolitic aggregate led to higher stiffness than the granite aggregate in the compression test, while in the lower frequencies (0.1, 0.5 and 1Hz) in the tension/compression test, the granite aggregate resulted in stiffer mixes than the phonolitic aggregate. In the HMA with anti-stripping additive, the phonolitic aggregate let to greater stiffness than the granitic aggregate in the compression test, whereas in the tension/compression test this trend is reversed. Mixtures Ph-N, Ph-A and G-N were, respectively, 21%, 32% and 4% higher for compression than for tension/compression. The G-A mixture behaved differently from the others, resulting in 7% greater tension/compression stiffness when compared to compression stiffness.

The 2S2P1D (Olard and Di Benedetto, 2003) model, with a Williams-Landel-Ferry (WLF) Equation representing change in characteristic time, was fitted to complex modulus experimental data (frequencies of 25; 10; 5; 1; 0.5 and 0.1Hz and temperatures of -10; 4.4; 21.1;

37.8 and 54°C) and then used to determine the axial compression stiffness of the mixtures at 19°C. The results showed that even after modeling the same trend was maintained, i.e. higher modulus values for HMA with phonolitic aggregate (cf. Figure 7). Moreover, this modeling procedure was necessary to compare results from tension-compression tests and from compressive tests, as indicated ahead.

Figure 7 – Dynamic moduli at compression and tension/compression

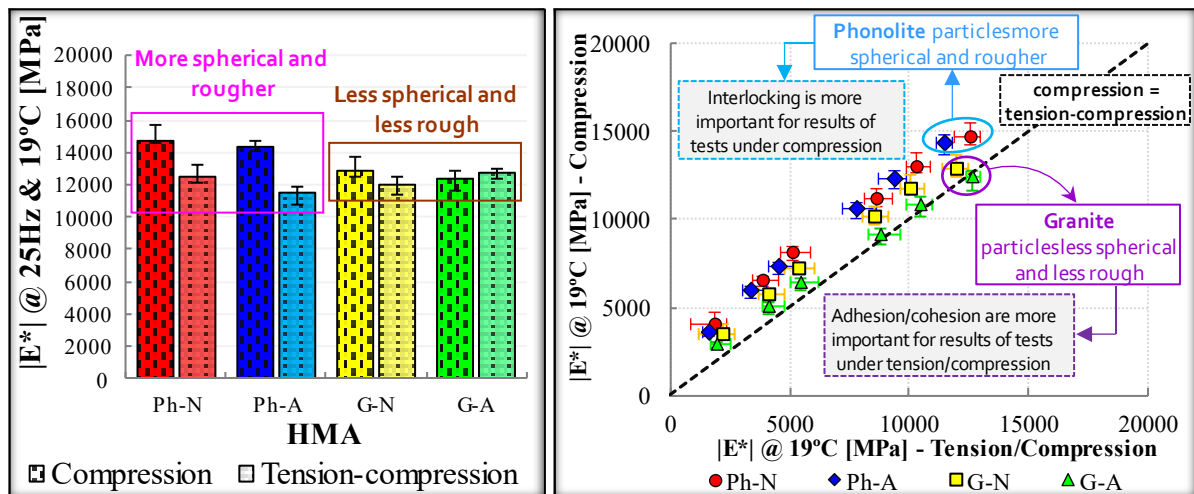


When the mixture has a good interlocking due to the aggregate shape properties, such as the mixtures with the phonolitic aggregate (Ph-N and Ph-A), the dynamic modulus at compression (21.1°C) has higher values than the dynamic modulus at tension-compression at 19°C (17% and 27%, respectively). When this comparison is made at a slightly lower temperature, 19°C, the dynamic modulus at compression surpasses the values at tension-compression by 56% and 60%, respectively, for Ph-N and Ph-A.

On the other hand, when the interlocking of the mixture is poorer (because the aggregate is more elongated and polished, cf. Figure 4), as in the case of mixtures with the granitic aggregate (G-N), the dynamic modulus at compression (21.1°C) has similar values when compared to the dynamic modulus at tension-compression and 19°C (2%), despite the difference in temperature. Meanwhile, for the mixture with granitic aggregate and anti-stripping agent (G-A), the dynamic modulus at compression and 21.1°C has lower values than the

dynamic modulus at tension/compression and 19°C (8%), i.e. the effect of compression was even more important than the 2.1°C decrease in temperature. When the comparison is made at the same temperature (19°C), the dynamic modulus at compression for G-N and G-A is 29% and 16% higher than at tension/compression, respectively. These data suggested the following hypothesis to the authors: the mechanical interlocking of the mixture due to aggregate sphericity and texture (more spherical and rougher) increases the dynamic modulus at compression; whereas in mixtures with poor interlocking, the dynamic modulus at tension-compression approaches or it is superior when compared to the modulus at compression, because the aggregate-binder adhesiveness has a greater power to interfere in the result, as presented in Figure 8. The left-hand part of Figure 8 presents average values of dynamic modulus at 19°C and 25 Hz analyzed for each mixture, considering the temperatures of 19°C for compression and tension-compression tests. Since the values of compressive dynamic modulus at compression are obtained from simulation at 19°C (with the fitted 2S2P1D model to the experimental results, representing the average expected material behavior), the represented statistical errors are obtained from the experimental values at 21.1°C (nearest temperature tested, 2.1°C from the simulated temperature).

Figure 8 – Dynamic moduli at compression and at tension/compression



### 2.3.5. Effect of aggregate and asphalt binder on the fatigue life of HMA

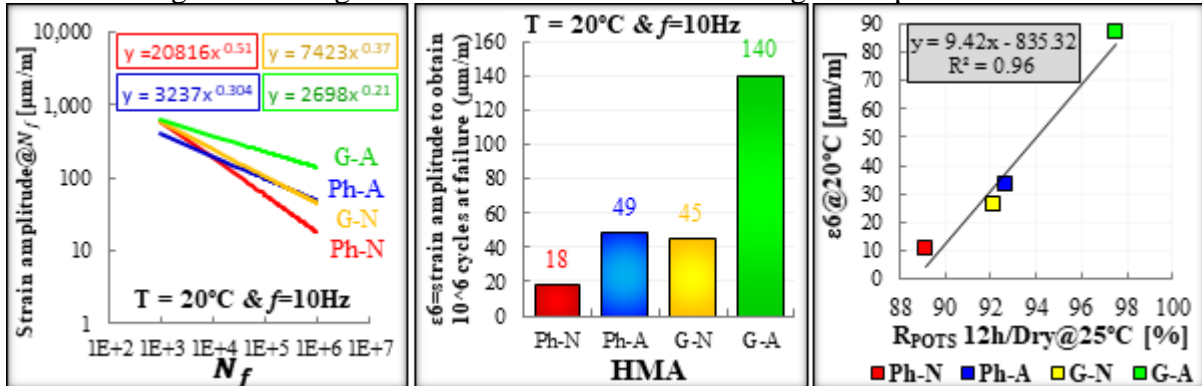
Table 1 presents the estimated Power Law coefficients  $C_{11}$  and  $C_{12}$  for the damage characteristic curve, the measured average material integrity at failure ( $C_f$ ), and the measured average damage accumulation at failure ( $S_f$ ) obtained for the investigated HMA. It also shows the values of the fitting coefficients ( $Y$  and  $\Delta$ ) for the  $G^R vs N_f$  failure envelope criterion, the mean dynamic modulus ratio ( $DMR$ ) and the damage parameter ( $\alpha$ ) value for each mixture.

Table 1 – Results of fitted parameters used in simulated fatigue life of the HMA

HMA	Damage characteristic curves				$G^R vs N_f$		$/E^*/$	Damage Parameter $\alpha$
	$C_{11}$	$C_{12}$	Mean $C_f$	Mean $S_f$	$Y(20^\circ\text{C})$	$A(20^\circ\text{C})$	Mean DMR	
Ph-N	3.29E-04	6.37E-01	0.38	144,013	4.59E+11	-2.687	0.89	3.191
Ph-A	1.37E-04	7.37E-01	0.53	75,305	5.82E+08	-1.983	0.80	3.197
G-N	8.68E-04	5.71E-01	0.31	124,809	3.41E+09	-2.068	0.87	3.088
G-A	4.50E-04	6.33E-01	0.35	101,565	8.07E+07	-1.535	0.95	2.971

Figure 9 shows the simulated Whöler curves for the four investigated HMA at  $20^\circ\text{C}$  in different simulated number of cycles at failure ( $N_f$ ). The investigated mixtures show a different trend when considering the ranking before and after  $N_f = 1.0\text{E}+04$ . After  $N_f = 1.0\text{E}+04$ , the HMA with amine-based anti-stripping agent showed tolerance to significantly greater strain amplitude than neat binder HMA for a fixed  $N_f$ . The presence of the anti-stripping agent seemed more important for the fatigue life than the aggregate shape properties (sphericity, texture and angularity). Figure 9 presents the simulated strain amplitudes to obtain fatigue failure with  $10^6$  loading cycles at 10Hz at a given temperature ( $\varepsilon_6$ ). The results represent the average expected material behavior from the fitted material model parameters. From Figure 9, it is noticed that the anti-stripping agent produced an average increase of 233% in the strain amplitudes supported by the HMA. On the other hand, the granitic aggregate (with less spherical and rough particles) increased, on average, 176% the strain amplitudes supported by the HMA. It is speculated that the higher fatigue life results of the mixture with granitic aggregate when compared to the mixture with phonolitic aggregate is linked to the better aggregate-binder adhesiveness. This information is based on the result contained in Figure 5, since this same trend was noticed in the analysis of the moisture damage resistance of HMA that is strongly related to the aggregate-binder adhesion (Lucas Júnior et al., 2019b). Figure 9 shows that there is a tendency of HMA with amine-based anti-stripping agent had better adhesion results and present greater resistance at higher strain amplitude.

Figure 9 – Fatigue simulation results of the investigated asphalt mixtures



### ***2.3.6. Summary of test results and their relationships***

From Figures 6 and 9 it is noticed that the main characteristic that increased the resistance to rutting was the shape properties of the phonolitic aggregate (sphericity and texture), while the main characteristic that increased the fatigue life was the addition of anti-stripping agent that improved adhesion or moisture damage. It is frequently found in the literature the association of adhesion to water sensitivity (Terrel and Al-Swailmi, 1994; Kanitpong and Bahia, 2003). This is due to the fact that when more adhesion exists between the binder and the aggregate, there is more energy in the bond to be overcome by the affinity between water and aggregate. Then, aggregate-binder adhesion is intimately related to water sensitivity.

To analyze the effect that the aggregate and the binder had on the results of the different tests investigated, the mixtures with a different variable were compared, i.e., between Ph-N and G-N the different variables are the shape properties, since particle size curve, air voids, and binder content are equal. Between Ph-P and Ph-A, the only different variable is the aggregate-binder adhesion. For each test, the highest value of the mixture was divided by the lowest value in an attempt to perceive how much change the aggregate or the binder increased the test result. As it was possible to have two comparisons for aggregate and two for binder, the average was performed. After this step, the weighted average was determined to evaluate the effect of aggregate and asphalt binder, according to Figure 10.

Figure 10 – Scheme of determination of the relative effects of aggregate and asphalt binder properties on HMA behavior

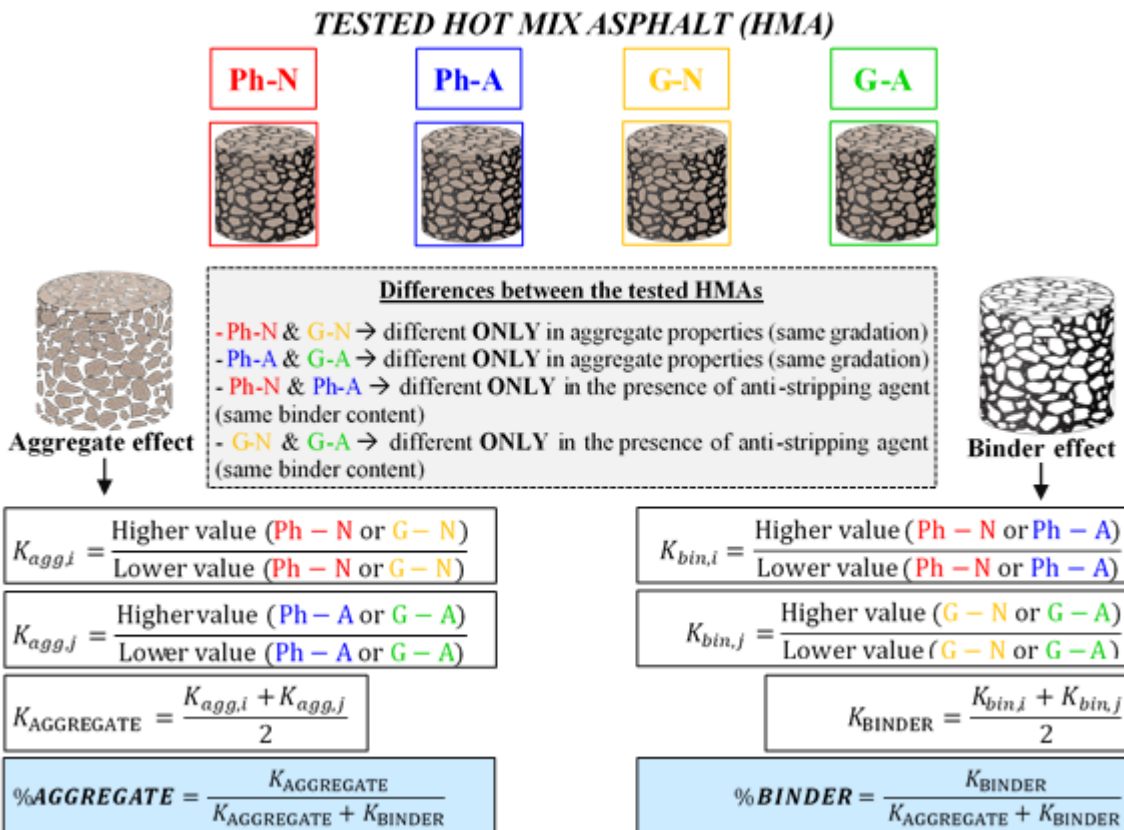


Figure 11 shows the effect the aggregate and asphalt binder in the results of different tests used for HMA characterization. For the compression tests, the aggregate was of greater importance, whereas for the tension-compression tests the type of the binder was found to be more important. The applied load intensity seems to be affected by the type of aggregate and binder. The higher the load amplitude, the greater the effect of some characteristics of the aggregates as sphericity and texture, while for smaller loads the effect of the aggregate on the test result decreases. The better adhesion provided by the anti-stripping agent seems to have a positive effect on the tension-compression results in both the dynamic modulus and the fatigue life.

Figure 11 – Effect of aggregate and asphalt binder in different tests

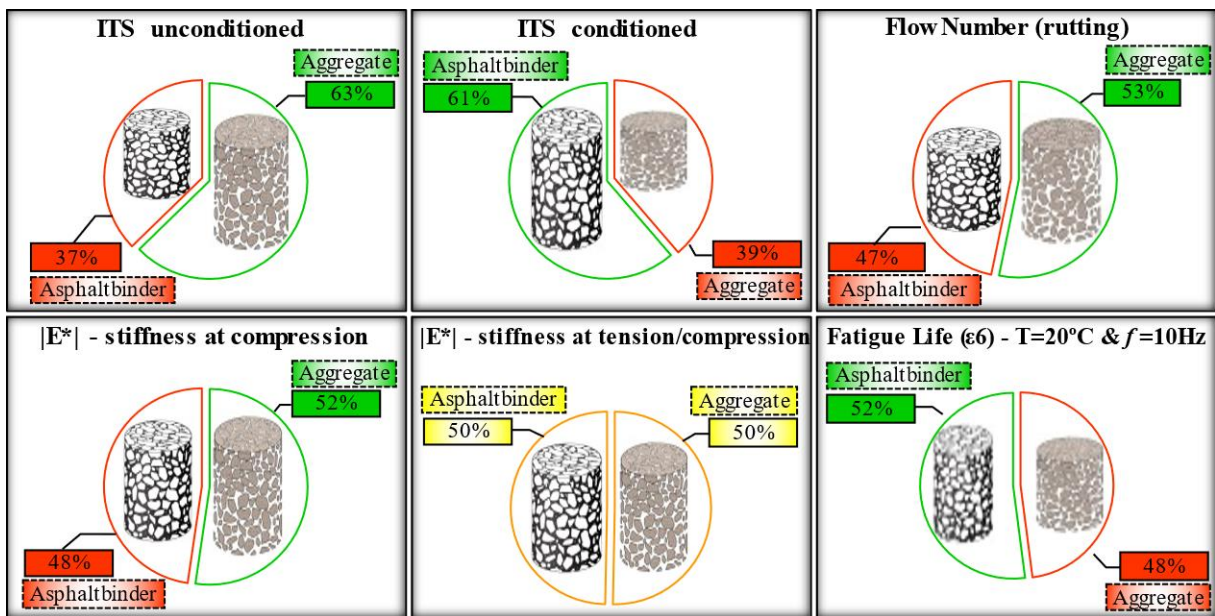
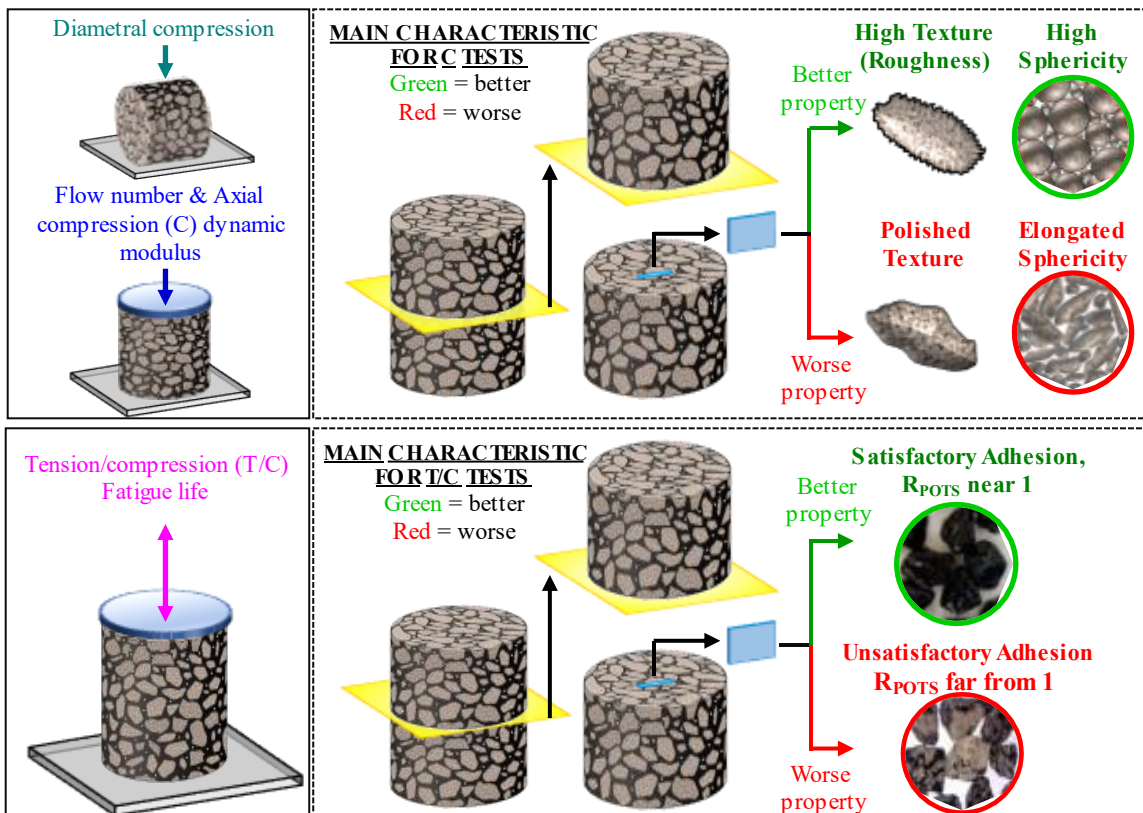


Figure 12 presents which component is relatively more important for each of the tests investigated. Higher aggregate texture and higher sphericity are more important for compression tests, while adhesion is more important for tension/compression tests.

Figure 12 – Important characteristics of the materials for each of the tests investigated



The method proposed may be used for different sets of aggregate and binder. In this paper, two different aggregate sources and two binders differing only by the presence of amine-based anti-stripping agent were investigated. It should be noted that depending on the modifier or the investigated materials, the relative effect of the aggregate and of the asphalt binder is expected to be different. In other words, two mixtures containing binders with inadequate compatibility with the utilized aggregate may have a greater relative effect by the type of the aggregate. Meanwhile, a strong polymer modification can have such an impact that the result of the relative effect of the binder can be very high.

## 2.4. Conclusions

The objective of this research was to investigate the effects that the aggregate morphological characteristics (shape properties) and aggregate-binder adhesion have on the results of different tests used to characterize HMA. In this paper, all other variables were fixed in the comparisons to make it possible to determine the influence of aggregate shape properties and aggregate-binder adhesiveness. Future work should account for aspects such as a change in the air voids, as higher values than 4% could prevent interlocking to produce measurable effects such as observed in the present paper. A methodology to determine the effects of aggregate and aggregate-binder adhesiveness on HMA behavior was proposed. The following conclusions were drawn in the light of the materials, methodology and tests considered:

- Aggregate-binder adhesiveness seems to be relatively more important than aggregate morphology for fatigue tension-compression test, while aggregate proved to be more important for compression tests;
- For the compression tests, the higher the load applied, the greater is the importance of the aggregate to the mixture;
- Indirect Tensile Strength and Flow Number appear to be strongly influenced by aggregate sphericity and texture;
- Dynamic modulus at compression depends relatively more on the aggregate shape properties than at tension-compression;
- For a fixed aggregate gradation, fatigue life is more influenced by aggregate-binder adhesion than by aggregate morphology.

### **Conflict of Interest**

The authors declare that they have no conflict of interest.

## Acknowledgement

This work was financially supported by Foundation for Scientific and Technological Development from State of Ceará (FUNCAP), Brazilian Federal Agency for Support and Evaluation of Graduate Education (CAPES) & National Council for Scientific and Technological Development (CNPq).

## REFERENCES

- [1] AASHTO T 283 (2014) American Association of State and Highway Transportation Officials - Standard Method of Test for Resistance of Compacted Asphalt Mixtures to Moisture Induced Damage.
- [2] AASHTO T 342 (2011) Standard Method of test for Determining Dynamic Modulus of Hot-Mix Asphalt Concrete Mixtures, American Association of State Highway and Transportation Officials, Washington, DC.
- [3] AASHTO TP 107-14 (2018) Standard Method of Test for Determining the Damage Characteristic Curve of Asphalt Mixtures from Direct Tension Cyclic Fatigue Tests, American Association of State Highway and Transportation Officials, Washington, DC.
- [4] ABNT NBR 15087 (2012) Misturas asfálticas – Determinação da resistência à tração por compressão diametral, Associação Brasileira de Normas Técnicas (*in Portuguese*).
- [5] ABNT NBR 15617 (2015) Misturas Asfálticas – Determinação do dano por Umidade Induzida, Associação Brasileira de Normas Técnicas (*in Portuguese*).
- [6] Alexander M., Mindess S. (2005) Aggregates in concrete. New York: Taylor and Francis, p. 439.
- [7] Al-Rousan T.M. (2004) Characterization of aggregate shape properties using a computer automated system (Doctoral dissertation). Department of Civil Engineering. Texas A&M University, College Station, TX.
- [8] Bessa I.S., Branco V.T.F.C., Soares J.B., Neto J.A.N. (2015) Aggregate Shape Properties and Their Influence on the Behavior of Hot-Mix Asphalt. Journal of Materials in Civil Engineering 27(7), 04014212. [https://doi:10.1061/\(asce\)mt.1943-5533.0001181](https://doi:10.1061/(asce)mt.1943-5533.0001181)
- [9] Bhasin A., Masad E., Little D., Lytton R. (2006) Limits on adhesive bond energy for improved resistance of hot mix asphalt to moisture damage. Transportation Research Record 1970: 3-13. <https://doi:10.3141/1970-03>
- [10] Chehab G.R., Kim Y.R., Schapery R.A., Witzczak M.W., Bonaquist R. (2002) Time-Temperature Superposition Principle for Asphalt Concrete Mixtures with Growing Damage in Tension State. Journal of the Association of Asphalt Paving Technologists, AAPT 71: 559-593.
- [11] Diógenes L.M., Bessa I.S., Branco V.T.F.C., Mahmoud E. (2018) The influence of stone crushing processes on aggregate shape properties. Road Materials and Pavement Design, 1-18. <https://doi:10.1080/14680629.2017.1422792>
- [12] Forough S.A., Moghadas Nejad F., Khodaii A. (2014) Comparison of tensile and compressive relaxation modulus of asphalt mixes under various testing conditions. Materials and Structures 49(1-2): 207-223. <https://doi:10.1617/s11527-014-0489-y>
- [13] Hicks R.G. (1991) Moisture damage in asphalt concrete. National Cooperative Highway Research Program. Synthesis of Highway Practice 175, Transportation Research Board, Washington.
- [14] Ibiapina D.S., Castelo Branco V.T.F., Diógenes L.M., Motta L.M.G., Freitas S.M. (2018) Proposição de um sistema de classificação das propriedades de forma de agregados caracterizados com o uso do processamento digital de imagens a partir de materiais oriundos do Brasil. Transportes 26(4). <https://doi:10.14295/transportes.v26i4.1510> (*in Portuguese*).

- [15] Kanitpong K., Bahia H.U. (2003) Role of adhesion and thin film thickness of asphalt binders in moisture damage of HMA. Journal of the association of asphalt paving technologists 72: 502-528.
- [16] Liu Y., Huang Y., Sun W., Nair H., Lane D.S., Wang L. (2017) Effect of coarse aggregate morphology on the mechanical properties of stone matrix asphalt. Construction and Building Materials 152: 48–56. <https://doi:10.1016/j.conbuildmat.2017.06.062>
- [17] Lucas Júnior J.L.O., Babadopoulos L.F.A.L., Soares J.B. (2019a) Aggregate–binder adhesiveness assessment and investigation of the influence of morphological and physico-chemical properties of mineral aggregates. Road Materials and Pavement Design, 1–16. <https://doi:10.1080/14680629.2019.1588773>
- [18] Lucas Júnior J.L.O., Babadopoulos L.F.A.L., Soares J.B. (2019b) Moisture-induced damage resistance, stiffness and fatigue life of asphalt mixtures with different aggregate–binder adhesion properties. Construction and Building Material 216: 166-175. <https://doi.org/10.1016/j.conbuildmat.2019.04.241>
- [19] Lucas Júnior J.L.O., Soares J.B. (2019c) Desenvolvimento de metodologia para avaliação da adesividade agregado-ligante com o uso de processamento digital de imagem. Transportes (*in Portuguese*). <https://doi.org/10.14295/transportes.v27i1.1552>
- [20] Lytton R.L., Gu F., Zhang Y., Luo X. (2017) Characteristics of undamaged asphalt mixtures in tension and compression. International Journal of Pavement Engineering 19(3): 192-204. <https://doi:10.1080/10298436.2017.1279489>
- [21] Mahmoud E., Gates L., Masad E., Erdogan S., Garboczi E. (2010) Comprehensive evaluation of AIMS texture, angularity, and dimension measurements. Journal of Materials in Civil Engineering 22(4): 369-379. [https://doi:10.1061/\(asce\)mt.1943-5533.0000033](https://doi:10.1061/(asce)mt.1943-5533.0000033)
- [22] Masad E. (2004) Aggregate imaging system (AIMS): basics and applications (Report nº FHWA/TX-05/5- 1707-01-1). College Station, TX: Texas Transportation Institute. Retrieved from <http://tti.tamu.edu/documents/5-1707-01-1.pdf>
- [23] Nascimento L.A.H. (2016) Apresentação realizada no Departamento de Engenharia de Transportes na Universidade Federal do Ceará. Data: 21/12/2016, Fortaleza-CE.
- [24] Nguyen Q.T., Di Benedetto H., Sauzéat C., Nguyen M.L., Hoang T.T.N. (2016) 3D complex modulus tests on bituminous mixture with sinusoidal loadings in tension and/or compression. Materials and Structures 50(1). <https://doi:10.1617/s11527-016-0970-x>
- [25] Olard F., Di Benedetto H. (2003) General “2S2P1D” model and relation between the linear viscoelastic behaviours of bituminous binders and mixes, Road Material and Pavement Design 4 (2). <https://doi.org/10.1080/14680629.2003.9689946>.
- [26] Park S.W., Kim Y.R., Schapery R.A. (1996) A viscoelastic continuum damage model and its application to uniaxial behavior of asphalt concrete. Mechanics of Materials 24: 241-255. [https://doi.org/10.1016/S0167-6636\(96\)00042-7](https://doi.org/10.1016/S0167-6636(96)00042-7)
- [27] Schapery R.A. (1984) Correspondence Principles and a Generalized J-integral for Large Deformation and Fracture Analysis of Viscoelastic Media. International Journal of Fracture 25: 195-223. <https://doi.org/10.1007/BF01140837>
- [28] Terrel R.L., Al-Swailmi S. (1994) Water sensitivity of asphalt-aggregate mixes: Test selection. SHRPA-403, strategic highway research program. Washington, DC: National Research Council.
- [29] Valdés-Vidal G., Calabi-Floody A., Miró-Recasens R., Norambuena-Contreras J. (2015) Mechanical behavior of asphalt mixtures with different aggregate type. Construction and Building Materials 101: 474–481. <https://doi:10.1016/j.conbuildmat.2015.10.050>

### **3. AVALIAÇÃO DO EFEITO DO ADITIVO MELHORADOR DE ADESIVIDADE A BASE DE AMINA NA VIDA DE FADIGA DE PAVIMENTOS ASFÁLTICOS**

Publicado em *International Journal of Pavement Engineering*

#### **Evaluating the effect of amine-based anti-stripping agent on the fatigue life of asphalt pavements**

Jorge L.O. Lucas Júnior <sup>a,b\*</sup>, Lucas F.A.L. Babadopoulos<sup>c</sup>, Jorge B. Soares<sup>a</sup>, Leonardo T. Souza<sup>b</sup>

<sup>a</sup> Department of Transportation Engineering, Federal University of Ceará at Fortaleza, Brazil

<sup>b</sup> Department of Civil Engineering, College Ari de Sá, Fortaleza, Brazil

<sup>c</sup> Engineering and Civil Construction, Federal University of Ceará at Fortaleza, Brazil

\* Corresponding author.

E-mail addresses: [j.lucas.j@det.ufc.br](mailto:j.lucas.j@det.ufc.br) (Jorge L.O. Lucas Júnior), [babadopoulos@ufc.br](mailto:babadopoulos@ufc.br) (Lucas F.A.L. Babadopoulos), [jsoares@det.ufc.br](mailto:jsoares@det.ufc.br) (Jorge B. Soares), [leonardo.tavares@aridesa.com.br](mailto:leonardo.tavares@aridesa.com.br) (Leonardo T. Souza).

#### **ABSTRACT**

Aggregate-binder adhesiveness is a property that can affect the service life of asphalt pavements. In order to reduce the effects of the loss of adhesion between aggregates and binders over time, lime or amine-based anti-stripping agents are commonly used. The objective of this paper is to evaluate the impact of using an amine-based anti-stripping agent on the fatigue life of asphaltic pavements. Besides the two binders, the investigated mixtures include 2 aggregate sources, granitic and phonolitic, making a total of 4 asphalt mixtures. Stiffness characterization, the Simplified Viscoelastic Continuum Damage model, and the software FlexPAVE™ were used. Two different layered structures were analyzed: one with a 0.10m asphalt layer thickness, and another with a combination of two 0.05m asphalt layers, with the same 0.10m total asphalt layers thickness. The 10 years fatigue simulation was considered with 1,000,100 total ESALs traffic volume, single wheel loading of 40 kN, traffic speed of 60km/h, and constant temperature of 20°C. The effect of the position of the asphalt layers was also investigated, i.e., using the most damage-resistant mixture on top or bottom of the surface course. It was concluded that mixtures with anti-stripping agent and/or granitic aggregate showed better fatigue behavior than mixtures with neat binder and/or phonolitic aggregate. All investigated pavements showed bottom-up predicted crack initiation. It is more recommended to use the mixtures with amine-based anti-stripping agent on the bottom asphalt layer and mixtures with neat binder on the top layer.

**Keywords:** Fatigue cracking, amine-based anti-stripping agent, adhesion, performance prediction, FlexPAVE™.

#### **3.1. Introduction**

Moisture damage (Bagampadde et al., 2005; Kringos et al., 2008) and aggregate-binder adhesiveness can affect the life cycle of asphalt pavements (Aguiar-Moya et al., 2016; Lucas Júnior et al., 2020a). In order to reduce the effects of the loss of adhesion between aggregates and binders, lime or amine-based anti-stripping agents are commonly used by the pavement industry. Numerous studies on amine-based anti-stripping agents have investigated how this additive prevents moisture damage (Chen and Huang, 2008; Arabani et al., 2012; Cui et al., 2014; Hesami and Mehdizadeh, 2017).

Caro et al. (2008) mentioned that common distresses in asphalt pavements, such as

stripping, raveling, and hydraulic scour, are a direct consequence of moisture damage within asphalt mixtures. Additionally, rutting, potholes and alligator cracking can be accelerated because of the action of moisture.

Kanitpong and Bahia (2008) concluded that pavements with mixtures containing the most common liquid anti-stripping additive in the state of Wisconsin, USA, showed lower severity in rutting than those without additives. Hicks (1991) explained that stripping failures could take the form of potholes or cracking and surface raveling of the pavement.

It is noted that amine-based anti-stripping agents are widely used to improve aggregate-binder adhesion and to reduce moisture damage. In Brazil and in the open literature, the effects of moisture on distresses such as fatigue life and rutting still attracts and requires further research. If additives are used to reduce moisture damage, their impact on other distresses should also be investigated. It is becoming increasingly necessary to use new tests and analyzes to predict how the use of such additives affects asphalt mixtures. The work presented herein is part of a broader research project which aims to investigate the effect of aggregate-binder adhesiveness on asphalt mixtures. Then, the problem addressed in this paper is the lack of clarity that the effects of anti-stripping modification within asphalt mixtures have on pavement fatigue behavior.

With the purpose of investigating the formation, location and progression of cracking in asphalt pavement simulations, several authors (Park et al., 2014; Norouzi and Kim, 2015; Nascimento, 2015; Wang et al., 2016; Babadopoulos et al., 2018; Etheridge et al., 2019; Sabouri, 2020) have used FlexPAVE™, formerly known as LVECD (Layered Viscoelastic Pavement Analysis for Critical Distresses) according to Table 1. This software incorporates the Simplified Viscoelastic Continuum Damage (S-VECD) model to predict asphalt layer fatigue damage and predict pavement fatigue cracking. The base layers and the subgrade are modeled as linear elastic materials.

Table 1. Studies about fatigue analysis using the LVECD/FlexPAVE™

Authors	Conclusion
Park et al. (2014)	Overall, the agreement rate between the field core observations and field condition survey and the predicted LVECD simulation results is about 78% in terms of cracking direction and severity.
Norouzi and Kim (2015)	This study found reasonable agreement in trends between the damage growth throughout the pavement cross sections as predicted by the LVECD software and the surface crack growth as evidenced by field observations.
Nascimento (2015)	Based on the prediction errors determined for all 44 pavement test sections (Fundao and National MEPDG test sections), it was concluded that the proposed LVECD program framework has very good fatigue cracking prediction capability.
Wang et al. (2016)	For the multilayer pavement sections, not only does the LVECD program take into account the stiffness and fatigue properties of all asphalt layers.

---

Babadospolous et al. (2018)	The effect of aging seems to improve service life. It was also observed that simulating the asphalt layer as composed by two half-layers (aged at the top and unaged at the bottom) did not lead to significantly different results with respect to fatigue performance of an evenly aged layer.
Etheridge et al. (2019)	Reasonable correlations were found between Pavement ME and FlexPAVE™ analyses for the top-down and bottom-up cracking predictions for a 10.2cm.
Sabouri (2020)	Increasing the RAP content and/or reducing the binder content deteriorates the fatigue resistance while improves the rutting performance. The study indicated that it is possible to produce an economical well-performing asphalt mixture by balancing fatigue and rutting performances.

---

FlexPAVE™ is a pavement performance analysis tool based on an efficient framework developed by combining time-scale separation and layered viscoelastic analysis. It captures the effects of the viscoelasticity of the pavement material, the temperature (thermal stress and changes in the viscoelastic properties), and the moving nature of the traffic load. FlexPAVE™ is a fast Fourier transform-based three-dimensional viscoelastic finite element analysis tool that can simulate moving loads and climatic conditions, predicting fatigue damage throughout the pavement design life (Eslaminia et al., 2012; Kim, 2018). It makes use of the S-VECD model to represent fatigue damage behavior of the asphalt layer.

Etheridge et al. (2019) mention that the damage contours (a heat map of damage) of cross-sections of the asphalt layers are generated from the analysis and plotted to indicate the location of damage (e.g., top-down *versus* bottom-up cracking) as well as the level of damage.

The objective of this paper is to evaluate the impact of using amine-based anti-stripping agent on the fatigue life of asphaltic pavements. FlexPAVE™ 1.1<sup>Alpha</sup> performance simulation tool is used. Linear viscoelastic characterization with respect to complex modulus (AASHTO T342), associated to the S-VECD model (Underwood et al., 2012; AASHTO TP 107, 2018) were used to obtain basic material parameters (dynamic modulus, damage parameter  $\alpha$ ,  $C_{11}$  and  $C_{12}$  fitting coefficients for  $C$  vs.  $S$  curves,  $Y$  and  $\Delta$  fitting coefficients  $G^R$  vs.  $N_f$  curves). These parameters are inputs to predict fatigue cracking performance in FlexPAVE™. Some simulations were performed on structures containing two asphalt layers. Their analyses are based on the influence of the use of the aggregate-binder adhesiveness additive, which is not to be confused with the adherence between the asphalt layers, which is not an object of the present study.

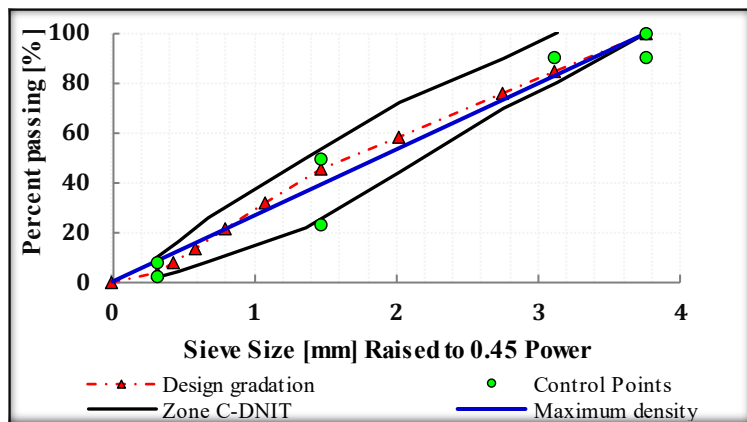
### 3.2. Materials characterization and performance prediction method

The asphalt mixtures' terminology used in the paper hereon is as follows: Ph-N, Ph-A, G-N and G-A (Ph for phonolite, G for granite, N for neat binder, and A for amine-based anti-

stripping agent). The only difference between Ph-N and Ph-A is that Ph-N uses neat binder while Ph-A incorporates 0.2% (w/w of asphalt binder) of an amine-based anti-stripping agent. In Brazil, it is only mandatory according to national standards to use lime or additive if the mixture does not have good adhesion (ABNT 12583) or if the Indirect Tensile Strength Ratio is less than 70% (ABNT 15617 – similar to modified Lottman test described in AASHTO T283).

The same difference holds for G-N and G-A. The only difference between Ph-N and G-N is that Ph-N uses phonolitic aggregate, while G-N uses granitic aggregate, equivalently with Ph-A and G-A. The remaining mixture composition parameters, such as volumetric properties and aggregate gradation were fixed using an aggregate sieving process before preparing the mixtures, and a gyratory compaction control. The following sieves were used to keep the same gradation for all mixtures: 19.0, 12.5, 9.5, 4.75, 2.36, 1.18, 0.60, 0.30, 0.15 and 0.075mm. The phonolitic aggregate is an intrusive igneous rock, while the granitic aggregate is an extrusive igneous rock. The granitic aggregate had a specific gravity of 2.394g/cm<sup>3</sup> and Los Angeles abrasion of 20.2%, while the granitic aggregate had a specific gravity of 2.656g/cm<sup>3</sup> and Los Angeles abrasion of 31.7%. The design gradation and control points are shown in Figure 1. Binder content and air voids were 5% and 4%, respectively, for all mixtures. Mixing and compaction temperatures were 160°C and 150°C, respectively, for the investigated mixtures.

Figure 1 – Aggregate gradation of the asphalt mixtures



The results of the aggregate-binder adhesiveness are not direct inputs for the prediction of fatigue cracking using FlexPAVE™. However, the difference on adhesiveness is carried out to the linear viscoelastic and damage properties (Lucas Júnior et al., 2019a) of the mixtures. These properties are briefly presented in the next section.

### 3.2.1. Adhesiveness test, linear viscoelastic and fatigue damage characterization

The adhesiveness test used in this paper was ABNT 12583 (similar to Static Immersion tests). In this test, 500g of coarse aggregate (passing through 19.0mm sieve and retained in the 12.5mm sieve) are heated at 100°C, and mixed with 17.5g of asphalt binder at 120°C until full coating. The mixture is, then, placed in a glass beaker with distilled water at 40°C for 72h, time after which the water is removed, and visual analysis of the aggregate coating is carried out to detect stripping.

Linear viscoelastic characterization was performed according to AASHTO T342. The compressive dynamic modulus was obtained at different frequencies (25, 10, 5, 1, 0.5 and 0.1Hz) and temperatures (-10, 4.4, 21.1, 37.8 and 54°C). The required inputs for the stiffness characterization in the FlexPAVE™ are the Poisson's ratio (assumed constant, 0.30), adopted reference temperature, number of frequencies used in the tests, and dynamic modulus ( $|E^*|$ ).

Fatigue characterization was performed according to AASHTO TP 107 (2018), which describes the testing and analysis procedure to obtain S-VECD model parameters. The damage characteristic curves ( $C_{vs.S}$ ) were fitted using Power Law equations (cf. Equation 1) and the  $G^R$  failure criterion (Sabouri and Kim, 2014) were used (cf. Equation 2).

$$C(S) = 1 - C_{11}S^{C_{12}} \quad (1)$$

where  $C(S)$  is the material integrity,  $C_{11}$  and  $C_{12}$  are fitting coefficients, and  $S$  is damage accumulation internal state variable.

$$G^R = Y(N_f)^\Delta \quad (2)$$

where  $G^R$  is the rate of change of the average released pseudo strain energy (per cycle) throughout the entire history of the test,  $Y$  and  $\Delta$  are fitting coefficients, and  $N_f$  is the number of cycles at fatigue failure, determined in the test from the perception of the phase angle drop. Figure 2(a) shows photographs of the obtained coated aggregates after the aggregate-binder adhesiveness test for the four asphalt mixtures analyzed. Ph-N and G-N (neat binder) mixtures had unsatisfactory adhesiveness, while Ph-A and G-A (amine-based anti-stripping agent) mixtures had satisfactory adhesiveness. A total of 24 specimens of four asphalt mixtures were used in this work, without moisture conditioning. The dynamic modulus master curves are presented in Figure 2(b). At -10°C the mixtures with neat binder had higher stiffness than the mixture with anti-stripping agent. At 27.7°C and 54.4°C the mixture with granite and anti-stripping agent produced the mixture with the highest stiffness. The characteristic damage curves fitting is presented in Figure 2(c). Analyzing Figure 2(c) it is noticed that the mixtures with granitic aggregate and neat asphalt binder had greater integrity for the same accumulated

damage. However, C vs. S curve by itself is not able to give a direct indication about the fatigue resistance of the asphalt mixtures, it should be used as a material property to model behavior under other specific conditions. The stiffness characterization and fatigue modeling coefficients are presented in Table 2. Those results are thoroughly discussed in Lucas Júnior et al. (2019a, 2020a and 2020b). Figure 2a indicates visually the effect of the use of the investigated amine-based anti-stripping agent. It is analyzed more in-depth and with proposition of quantitative results from digital image processing elsewhere (Lucas Júnior et al, 2019b).

Figure 2 – Adhesiveness test, stiffness characterization and damage characteristic curves

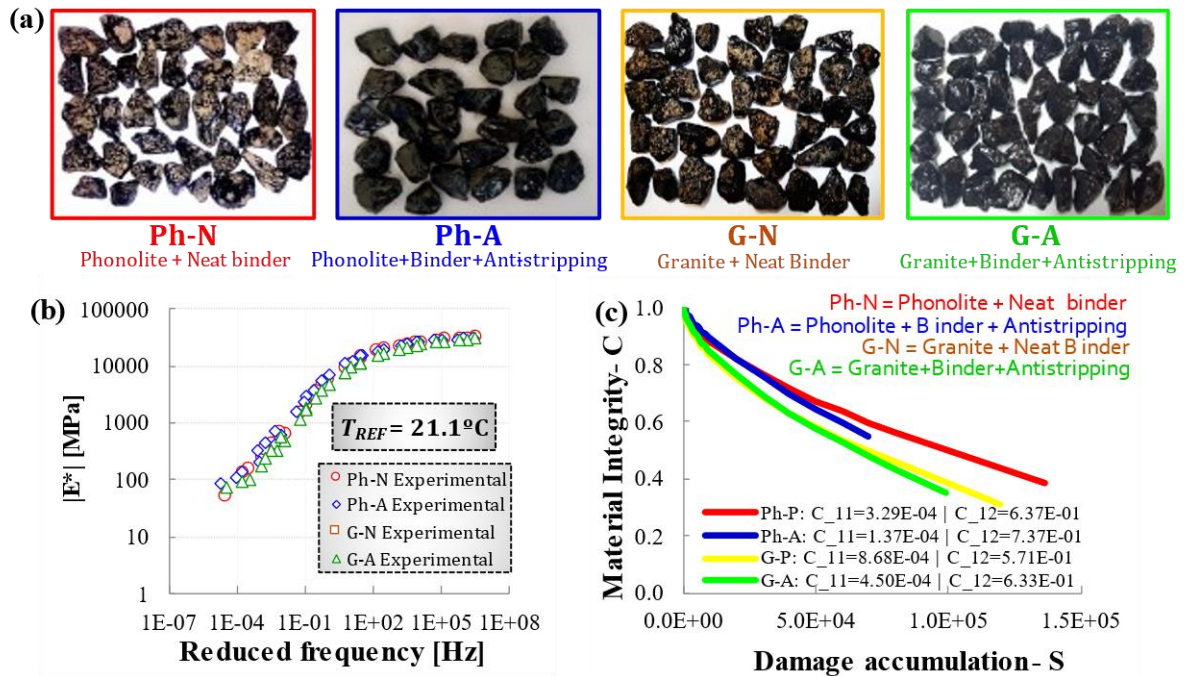


Table 2. Stiffness characterization and fatigue coefficients used in FlexPAVE™ simulation

Asphalt mixtures	Temperature (°C)	Dynamic Modulus (kPa)							Fatigue	
		25	10	Frequency (Hz)			0.5	0.1		
Ph-N Phonolite + Neat binder	-10.1	32,767,000	32,093,330	31,513,660	30,028,660	29,242,660	27,171,660	Alpha ( $\alpha$ )	3.191	
	4.4	26,307,000	24,805,330	23,544,330	20,335,000	18,813,660	15,151,000	$C_{11}$	3.29E-04	
	21.2	13,742,000	11,024,000	9,413,330	6,011,660	4,720,660	2,328,000	$C_{12}$	0.637	
	37.8	3,628,330	2,251,330	1,548,330	655,000	471,000	261,330	Gama ( $\gamma$ )	4.60E+11	
	54.4	683,330	449,660	337,000	150,330	132,000	66,000	Delta ( $\Delta$ )	-2.687	
Ph-A Phonolite + Neat binder + Anti-stripping	-10.1	30,839,000	30,284,000	29,739,000	28,463,000	27,794,000	25,912,000	Alpha ( $\alpha$ )	3.197	
	4.4	25,636,000	24,192,000	23,015,000	19,952,000	18,503,000	14,961,000	$C_{11}$	1.37E-04	
	21.2	14,842,000	12,561,000	10,850,000	7,113,700	5,634,700	2,960,300	$C_{12}$	0.737	
	37.8	3,620,000	2,259,000	1,536,300	612,670	419,670	213,330	Gama ( $\gamma$ )	5.83E+08	
	54.40	697,000	462,670	323,670	136,330	110,670	85,667	Delta ( $\Delta$ )	-1.983	
G-N Granite + Neat binder	-10.1	32,968,000	32,119,000	31,475,000	29,508,000	28,572,000	26,129,000	Alpha ( $\alpha$ )	3.088	
	4.4	24,775,000	22,987,000	21,551,000	18,075,000	16,498,000	12,950,000	$C_{11}$	8.68E-04	
	21.2	12,576,000	10,519,000	8,939,300	5,596,300	4,320,700	2,122,700	$C_{12}$	0.571	
	37.8	3,323,700	2,122,300	1,497,300	603,330	440,000	274,330	Gama ( $\gamma$ )	3.42E+09	
	54.4	726,330	477,670	377,330	145,670	94,667	60,000	Delta ( $\Delta$ )	-2.068	
G-A Granite	-10.2	30,362,000	29,570,000	28,927,000	27,162,000	26,273,000	23,941,000	Alpha ( $\alpha$ )	2.971	
	4.4	22,962,000	21,232,000	19,893,000	16,514,000	15,028,000	11,588,000	$C_{11}$	4.50E-04	

+	21.2	11,332,000	9,331,700	7,890,300	4,844,300	3,729,000	1,806,700	$C_{12}$	0.633
Neat binder	37.8	2,781,700	1,726,300	1,175,700	471,330	330,330	173,000	Gama ( $Y$ )	8.07E+07
+	54.4	577,330	340,000	243,000	99,333	91,333	73,667	Delta ( $\Delta$ )	-1.535

Mixtures with amine-based anti-stripping agent showed greater inclinations in the  $G^R$  vs.  $N_f$  curves than those with neat binder. This shows that mixtures with amine-based anti-stripping require more cycles to release the same pseudo strain energy (per cycle) throughout the entire history of the test, and this energy dissipation can be indicative of the asphalt mixture fatigue life.

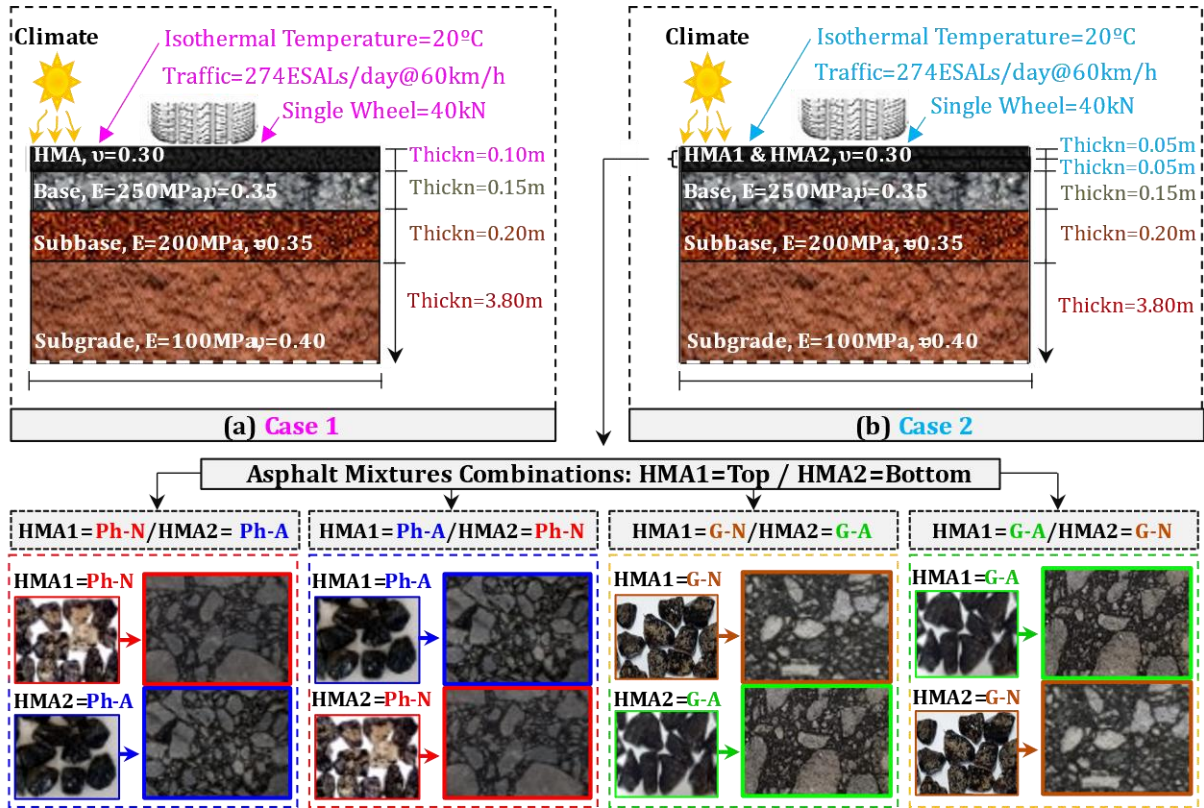
### 3.2.2. FlexPAVE™ 1.1<sup>Alpha</sup> simulation

Two different layer configuration were simulated. The thickness, modulus and Poisson's ratio of the granular layers were considered fixed values (indicated on Figure 2). The climate consideration was a constant temperature of 20°C. In asphalt mixtures many variables are involved in the analysis. In this study, the authors have decided to fix variables external to the pavement, such as temperature. The temperature of 20°C was used in accordance to the following premises: (i) in Brazil, it is the average acceptable temperature associated to pavement cracking, (ii) AASHTO TP107 mentions that the test must be between 18°C and 21°C, and (iii) the purpose herein is not investigate the temperature as a variable, and therefore it was fixed at 20°C.

The traffic level was considered as 274 ESALs/day, and the simulation time used for project analysis is 10 years (i.e., a 1,000,100 total ESALs traffic volume). Healing and aging models were not used in this simulation. A single wheel load of 40kN and traffic speed of 60km/h were used. As for the state-of-practice in Brazil, surface courses in pavements do not exceed a thickness of 12.5cm under heavy traffic. A significant portion of pavement surface layers is constructed with 5, 7.5 and 10cm of asphalt mixtures.

Two different pavement structures were considered, differing in the asphalt layers: either a single layer or a double layer with half of the thickness in each (total thickness kept the same in both cases). In Case 1, cf. Figure 3(a), a 0.10m single asphalt layer was analyzed, while in Case 2, cf. Figure 3(b), two 0.05m double asphalt layers were considered.

Figure 3 – Scheme of the investigated variables in FlexPAVE™



The  $G^R$  failure criterion was used in this paper (Sabouri and Kim, 2014). Moreover, the Damage Factor as defined in Equation 3, using Miner's law, and assuming values from 0 (undamaged) to 1 (damaged). According to FlexPAVE™ 1.1<sup>Alpha</sup> User Guide (2018), when the damage factor becomes 1.0, the asphalt element is considered to be completely cracked.

$$\text{Damage Factor} = \frac{N}{N_f} \quad (3)$$

According to Wang et al. (2018), the percentage of damage (referred to as 'percent damage') is defined as the ratio of the sum of the damage factors within the reference cross-section area to the reference cross-section area, as shown in Equation 4.

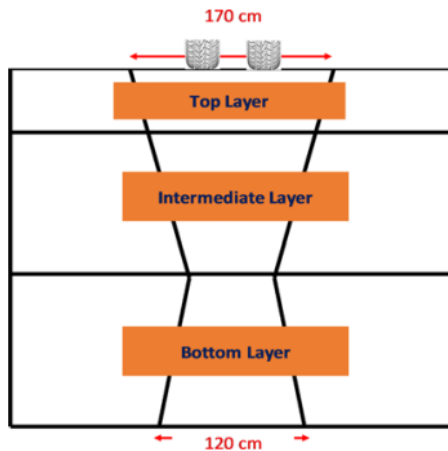
$$\text{Percent Damage} = \frac{\sum_i^M (\text{Damage factor})_i \cdot A_i}{\sum_i^M A_i} \quad (4)$$

where  $i$  is the nodal point number in finite element mesh,  $M$  is the total number of nodal points in finite element mesh,  $A_i$  is the area represented by the nodal point  $i$  in the finite element mesh, and  $\sum A_i$  is the reference area.

Figure 4 illustrates the area in which it is calculated the percent damage. FlexPAVE™

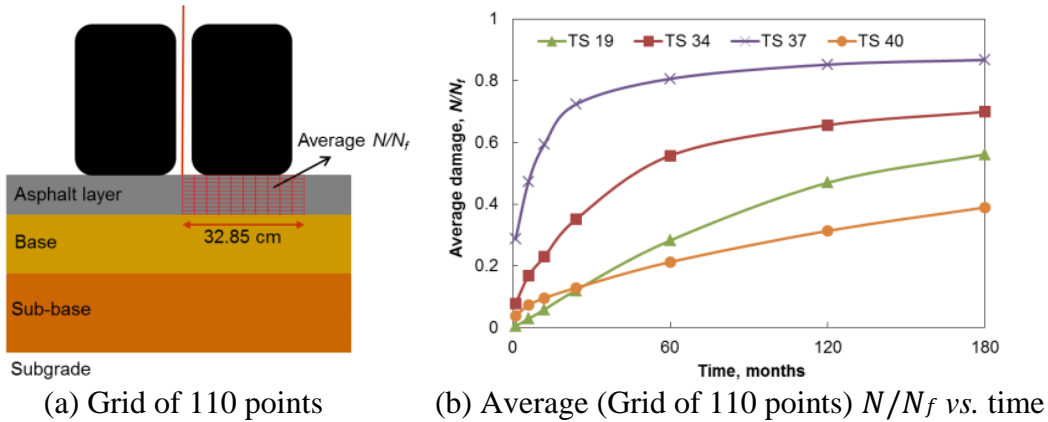
uses two overlapping triangles to form the reference cross-section area within which the level of damage is calculated. The top inverted triangle has a 170-cm wide base located at the top of the surface layer, and a vertex located at the bottom of the lower asphalt layer. The 120-cm wide base of the second triangle is located at the bottom of the lower asphalt layer and its vertex is positioned at the surface layer (Wang et al., 2018). The dual tires spacing used was 0.3047m, the contact area shape was rectangular, and the aspect ratio is defined as length/width (length is measured along the traffic direction whereas width is perpendicular to the length). The value used was 1.5714.

Figure 4 – Reference area for Percent Damage definition in FlexPAVE™ (Wang et al., 2018)



Nascimento (2015) proposed to use as an indicator of the global severity of fatigue damage within the asphalt layer a spatial average of  $N/Nf$  ratio values underneath the loaded area. The average damage is computed for a grid of 110 points ( $N/Nf$  evaluated at 110 different points). Ten points are homogeneously distributed in the horizontal direction from the center of the loading (0 cm) to 32.85cm distant from this center, and 11 points are homogeneously distributed in the vertical direction, from the bottom of the asphalt layer to the surface, as shown in Figure 5(a). The advantage of using this averaging approach for damage computation is the direct consideration of the stress distribution throughout the asphalt layer during the damage analysis, which includes the tire-pavement contact stresses. Figure 5(b) presents examples of the evolution of the average damage for different test sections, suggesting that the proposed indicator may differ considerably between pavement structures. Numbered TS stand for different test sections analyzed by Nascimento (2015).

Figure 5 – Grid of 110 points considered in the average  $N/N_f$  and averaged  $N/N_f$  vs. time data simulated in the LVECD (former version of FlexPAVE™) (Nascimento, 2015)



Based in field observations (44 pavement sections), percent cracked area vs. averaged damage curves were shifted horizontally, using a damage growth rate variable, in order to obtain a unique relationship between the field-observed cracked area and the shifted damage (reduced damage –  $N/N_f red_s$ ). A damage growth rate variable ( $T_{0.35}$ ) has been defined as the time in the simulation, in months, when the averaged damage is 0.35, and the best damage shift function is presented in Equation 5. The averaged reduced damage ( $N/N_f red_s$ ) was calculated using Equation 6. The reduced averaged damage-to-cracked area transfer function is the power form presented in Equation 7, where  $C_1$  and  $C_2$  are the fitting coefficients from the field calibration. The percent cracked area prediction using the LVECD framework presented a standard error of the mean of 1.27% and  $R^2$  of 0.72 (Nascimento, 2015).

$$S_{T_{0.35}} = A \cdot T_{0.35} + B \quad (5)$$

$$N/N_f red_s = N/N_f \cdot S_{T_{0.35}} \quad (6)$$

$$CA = C_1 \cdot (N/N_f red_s)^{C_2} \quad (7)$$

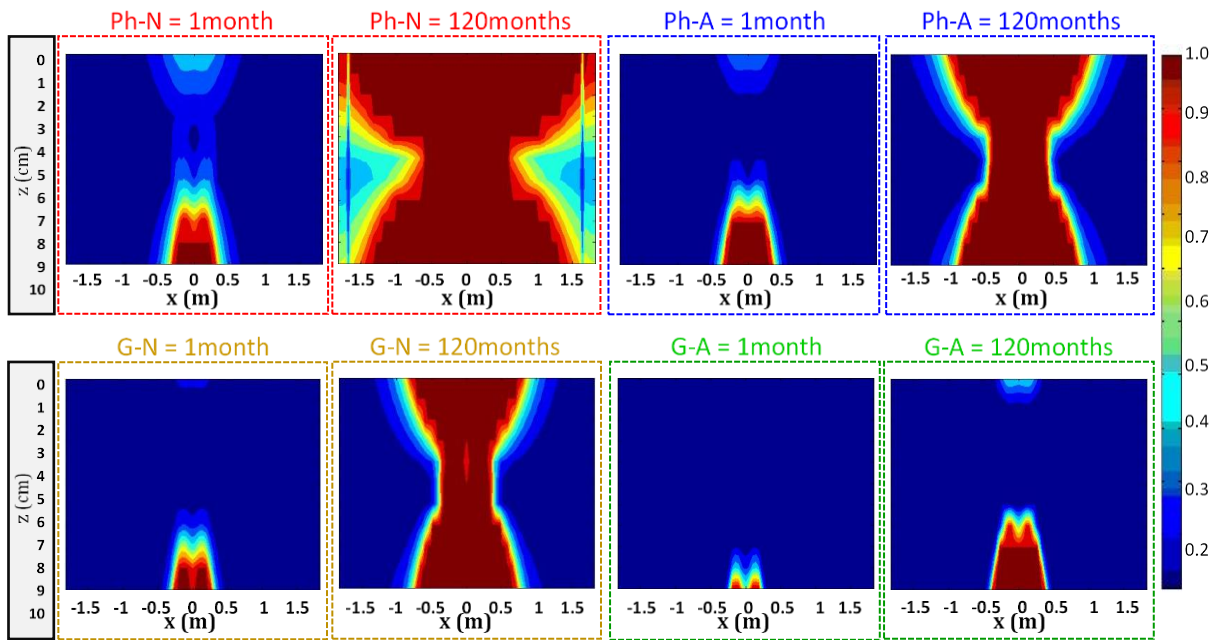
where  $S_{T_{0.35}}$  is the damage shift factor,  $A=0.00872$  and  $B=0.635237$  are the linear function fitting coefficients from the field calibration procedure,  $N/N_f red_s$  is the average reduced damage based on the multiplicative shift factor ( $S$ ),  $C_1=7272.68$  and  $C_2=8.6629$  are the fitting coefficients from the field calibration, and  $CA$  is the predicted cracked area, in percentage.

### 3.3. Results and discussion

#### 3.3.1. Fatigue cracking spatial distribution (damage contours) and percent damage

Figure 6 shows the damage contours obtained from the simulation of the pavement behavior for the four investigated mixtures, at month 1 and month 120, for Case 1 (single 0.10m asphalt layer). Only bottom-up cracking was noted. The mixtures with amine-based anti-stripping agent presented a smaller area of damage contours than the mixtures with neat binder (Ph-N vs. Ph-A, and G-N vs. G-A). The granitic aggregate also had a larger area of damage contours in comparison to the phonolitic aggregate (Ph-N vs. G-N, and Ph-A vs. G-A). Although the addition of anti-stripping agent has been shown to decrease fatigue cracking, simple modification of the aggregate used in the mixture has also proved to be effective.

Figure 6 – Damage contours for the four investigated asphalt mixtures in one single 0.10m layer at the beginning (1 month) and at the end (120 months) of the pavement simulation



The results presented in Figure 7 show the simulation performed for Case 2 (cf. Figure 3), i.e. double 0.05m asphalt layers (top/bottom), with a different mixture in each layer. Cracks start at the bottom and go up for the investigated structures. If the mixtures with better fatigue behavior (with amine-based anti-stripping agent) are placed in the bottom layer, damage contour results are smaller, indicating a more resistant structure. Comparing single layer structures with double layer structures (Figure 6 vs. Figure 7), it was noticed that when analyzing a structure only with mixtures with neat binder it was better to change to a double layer structure using mixture with anti-stripping agent in one of them (Ph-N vs. Ph-N/Ph-A).

and/or G-N vs. G-N/G-A). When analyzing a structure only with mixtures with the binder containing anti-stripping agent, it was better to keep the single layer than to change to a double layer structure with one of the asphalt layers with neat binder (Ph-A vs. Ph-A/Ph-N, and/or G-A vs. G-A/G-N), since damage contours had a larger area in the latter case.

Figure 7 – Damage contours for the four investigated asphalt mixtures in double 0.05m layers (0.10m total thickness) at the beginning (1 month) and at the end (120 months) of the pavement simulation

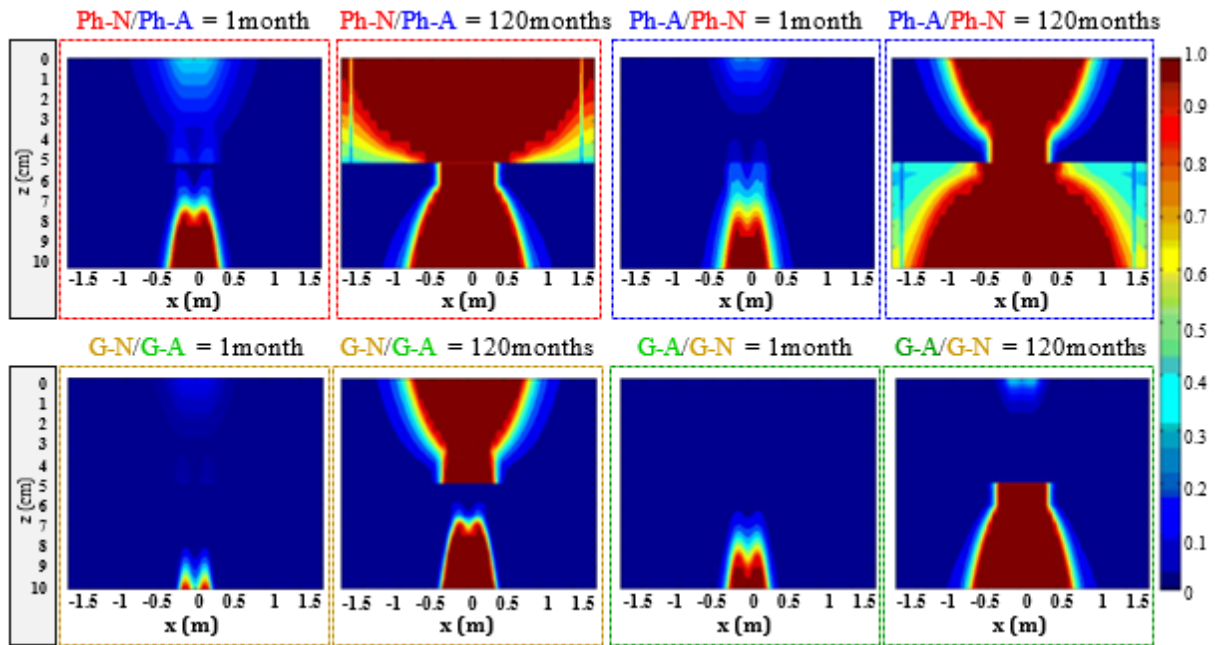
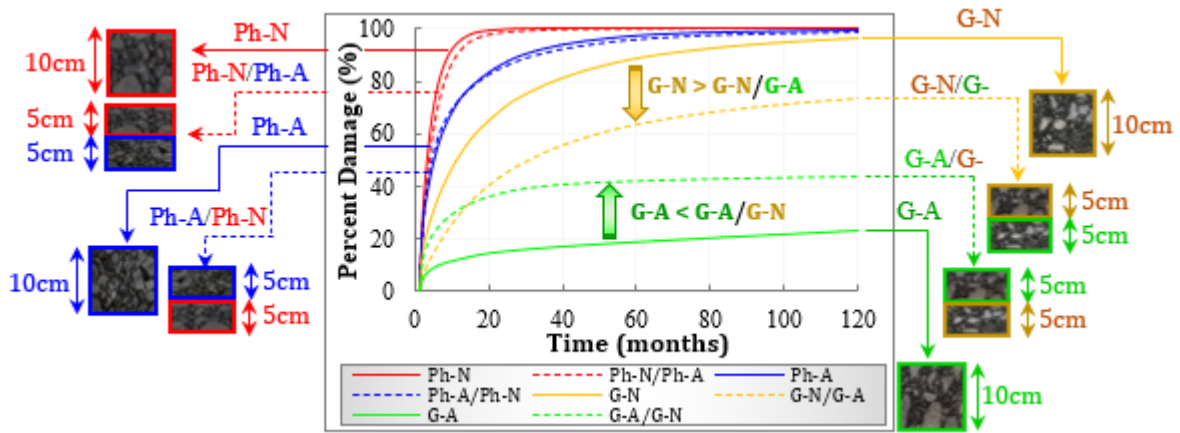


Figure 8 shows the percent damage, determined by Equation (4), to the single layer and double asphalt layer structures, a total thickness of 0.10m in both cases. The Ph-N mixture had 100% percent damage at 39 months, while Ph-A, G-N and G-A mixtures at 39 months presented 92, 79 and 16% of percent damage. Asphalt mixtures Ph-A, G-N and G-A mixtures showed 99, 96 and 23% of percent damage at 120 months. At 120 months the same mixtures combinations presented 99, 98, 73 and 44% of average damage, according to Figure 8.

Figure 8 – Percent damage distribution as a function of time

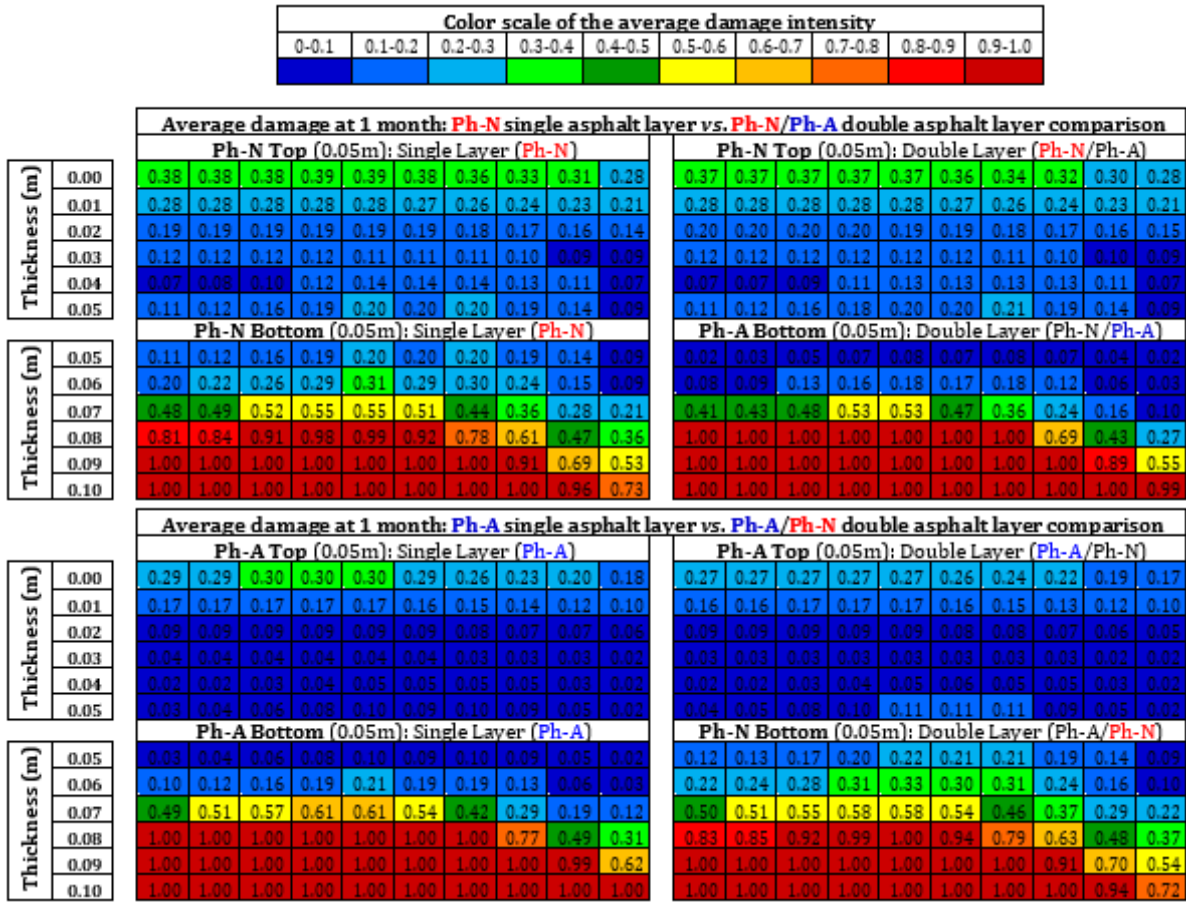


The comparison between the percent damage of the structure composed by a 0.10m single layer surface course with Ph-N mixture, and the structure composed by a 0.05m double layer containing Ph-N on the top and Ph-A on the bottom showed a slight improvement with the use of the double-layer. The same occurred in the comparison between Ph-A single layer and Ph-A/Ph-N double layer. The G-N/G-A structure showed considerable improvement when compared to G-N. On the other hand, the G-A (single layer) presents higher percent damage when compared G-A/G-N. The analyzed results show that the combination of asphalt layers must be considered with caution. The choice of the position of the mixtures (top or bottom layer) is discussed in the next item.

### 3.3.2 Average damage ( $N/N_f$ of 110 points) vs. time

The average damage is determined according to Nascimento (2015), as described in Figure 5. Figure 9 shows the results of the average damage of each of the 110 points analyzed, comparing the 8 structures analyzed, for 1 month of simulation. The Ph-N (single layer) structure showed average damage of 0.41, while the Ph-N/Ph-A structure presented average damage of 0.37, for 1 month of simulation, according to Figure 9. On the average of the 120 months average damage was 0.90 for Ph-N and 0.88 for the Ph-N/Ph-A. The Ph-A (single layer) structure showed average damage of 0.37 and Ph-A/Ph-N structure had 0.35 for 1 month of simulation, but on the average of 120 months the average damage was the same. This is probably due to the fact that the calculation of  $N/N_f$  is limited to 1 and cannot evolve beyond that value.

Figure 9 – Average damage ( $N/N_f$  of 110 points) at 1 month: phonolitic aggregate



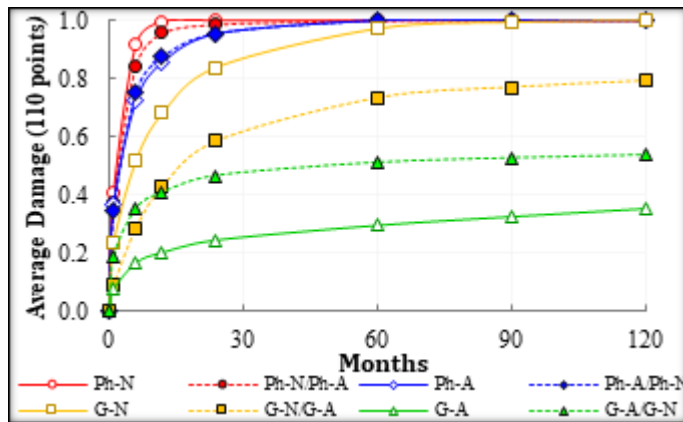
The G-N (single layer) structure showed average damage of 0.23, while G-N/G-A (double layer) structure presented average damage of 0.09 for 1 month of simulation, according to Figure 10. Considering the average of the 120 months, the average damage was 0.75 for G-N structure, while the G-N/G-A structure had average damage of 0.53. The G-A (single layer) structure showed average damage of 0.07, and G-A/G-N structure had 0.19 for 1 month of simulation. For the 120 months, the average damage was 0.24 for G-A structure, and 0.43 for G-A/G-N structure.

Figure 10 – Average damage ( $N/N_f$  of 110 points) at 1 month: granitic aggregate

Color scale of the average damage intensity											
	0-0.1	0.1-0.2	0.2-0.3	0.3-0.4	0.4-0.5	0.5-0.6	0.6-0.7	0.7-0.8	0.8-0.9	0.9-1.0	
<b>Average damage at 1 month: G-N single asphalt layer vs. G-N/G-A double asphalt layer comparison</b>											
	<b>G-N Top (0.05m): Single Layer (G-N)</b>						<b>G-N Top (0.05m): Double Layer (G-N/G-A)</b>				
Thickness (m)	0.00	0.12	0.12	0.12	0.12	0.11	0.10	0.08	0.07		
	0.01	0.07	0.07	0.07	0.07	0.06	0.06	0.05	0.04		
	0.02	0.04	0.04	0.04	0.04	0.04	0.03	0.03	0.02		
	0.03	0.02	0.02	0.02	0.02	0.02	0.01	0.01	0.01		
	0.04	0.01	0.01	0.02	0.02	0.02	0.02	0.01	0.01		
	0.05	0.02	0.03	0.04	0.04	0.04	0.04	0.02	0.01		
Thickness (m)	0.05	0.02	0.03	0.04	0.04	0.04	0.04	0.02	0.01		
	0.06	0.04	0.05	0.06	0.07	0.08	0.08	0.05	0.03	0.01	
	0.07	0.16	0.17	0.19	0.21	0.21	0.15	0.10	0.07	0.04	
	0.08	0.44	0.46	0.54	0.61	0.63	0.55	0.40	0.26	0.16	0.10
	0.09	0.89	0.94	1.00	1.00	1.00	0.85	0.54	0.33	0.20	
	0.10	1.00	1.00	1.00	1.00	1.00	1.00	1.00	0.60	0.36	
<b>Average damage at 1 month: G-A single asphalt layer vs. G-A/G-N double asphalt layer comparison</b>											
	<b>G-A Top (0.05m): Single Layer (G-A)</b>						<b>G-A Top (0.05m): Double Layer (G-A/G-N)</b>				
Thickness (m)	0.00	0.00	0.00	0.00	0.00	0.00	0.00	0.00	0.00		
	0.01	0.00	0.00	0.00	0.00	0.00	0.00	0.00	0.00		
	0.02	0.00	0.00	0.00	0.00	0.00	0.00	0.00	0.00		
	0.03	0.00	0.00	0.00	0.00	0.00	0.00	0.00	0.00		
	0.04	0.00	0.00	0.00	0.00	0.00	0.00	0.00	0.00		
	0.05	0.00	0.00	0.00	0.00	0.00	0.00	0.00	0.00		
Thickness (m)	0.05	0.00	0.00	0.00	0.00	0.00	0.00	0.00	0.00		
	0.06	0.00	0.00	0.00	0.00	0.00	0.00	0.00	0.00		
	0.07	0.00	0.01	0.01	0.01	0.01	0.00	0.00	0.00		
	0.08	0.04	0.04	0.06	0.08	0.09	0.06	0.03	0.01		
	0.09	0.17	0.19	0.26	0.35	0.39	0.30	0.16	0.06		
	0.10	0.50	0.57	0.82	1.00	1.00	0.52	0.21	0.07	0.02	
<b>G-A Bottom (0.05m): Single Layer (G-A)</b>											
Thickness (m)	0.00	0.00	0.00	0.00	0.00	0.00	0.00	0.00	0.00		
	0.05	0.00	0.00	0.00	0.00	0.00	0.00	0.00	0.00		
	0.06	0.00	0.00	0.00	0.00	0.00	0.00	0.00	0.00		
	0.07	0.00	0.00	0.01	0.01	0.01	0.00	0.00	0.00		
	0.08	0.04	0.04	0.06	0.08	0.09	0.06	0.03	0.01		
	0.09	0.17	0.19	0.26	0.35	0.39	0.30	0.16	0.06		
	0.10	0.50	0.57	0.82	1.00	1.00	0.52	0.21	0.07	0.02	
<b>G-N Bottom (0.05m): Double Layer (G-A/G-N)</b>											
	0.01	0.02	0.03	0.03	0.04	0.04	0.04	0.03	0.02	0.01	
	0.04	0.04	0.06	0.07	0.08	0.07	0.06	0.05	0.03	0.01	
	0.16	0.17	0.19	0.20	0.21	0.18	0.14	0.10	0.06	0.04	
	0.42	0.45	0.52	0.60	0.63	0.54	0.39	0.25	0.16	0.10	
	0.86	0.92	1.00	1.00	1.00	1.00	0.84	0.52	0.32	0.20	
	1.00	1.00	1.00	1.00	1.00	1.00	1.00	0.95	0.57	0.34	

It is important to notice that the average damage ( $N/N_f$  of 110 points) vs. time simulated curves whose results are shown in Figure 11 are displayed for the comparison between the damage behavior of single asphalt layer (0.10m) and double asphalt layer of 0.05m asphalt layers each (0.10m total thickness). The analysis of average damage showed that for structures with neat binder the combination of two half-layers performed well, but for structures with neat binder modified by amine-based anti-stripping agent, the combination was not beneficial.

Figure 11 – Average damage ( $N/N_f$  of 110 points) vs. simulated time

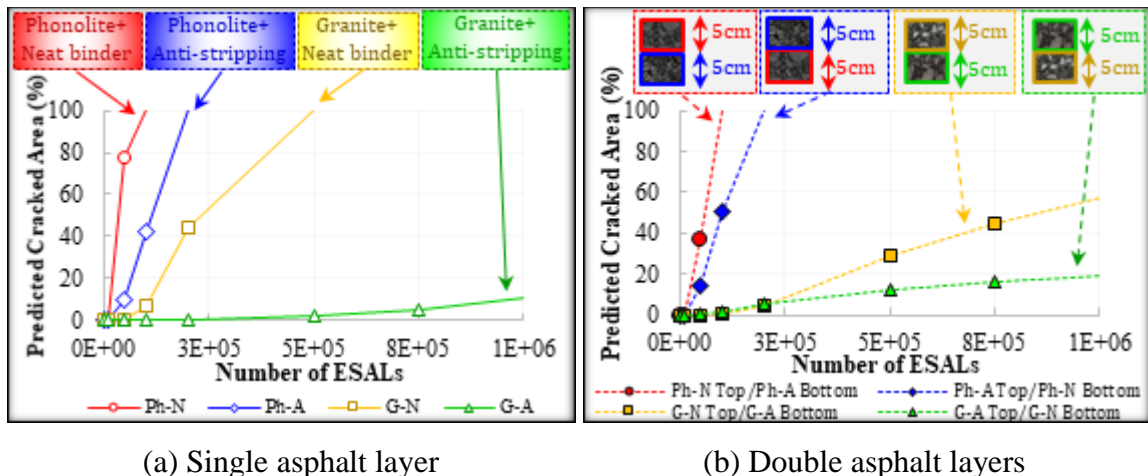


### 3.3.3 Predicted cracked area of the pavement with the different combinations of asphalt mixtures

Figure 12(a) presents the predicted cracked area (according to Equation 7) of the four analyzed 0.10m single asphalt layer structures. Figure 12(b) presents the predicted cracked area for the four analyzed double 0.05m asphalt layers (0.10m total thickness) with different positioning of the asphalt mixtures. Mixtures with the granitic aggregate (G-A and G-N) had smaller cracked areas than the phonolitic aggregate (Ph-A and Ph-N) in a single asphalt layer structure. The amine-based anti-striping agent produced mixtures with better fatigue behavior, having a smaller predicted cracked area than mixtures with neat asphalt binder (Ph-A vs. Ph-N and G-A vs. G-N). Figure 12(b) shows that when the mixtures with neat binder (Ph-N or G-N) are placed on the top of the structure and mixtures with amine-based modified binder (Ph-A or G-A) in the bottom, this structure had smaller cracked areas than to structures with a single layer with neat binder.

On the other hand, structures with amine-based anti-striping agent (a single asphalt layer) had a smaller cracked area than structures with double asphalt layers. Analyzing Figure 12(b), the choice of using two asphalt layers is not trivial and, in some cases, it may be more advantageous to maintain just one asphalt layer, as is the case with the structures with the Ph-A and G-A mixtures. This is a function on the investigated materials. A mixture with bad fatigue behavior tends to improve its behavior if combined with a mixture of better behavior. In addition, the positioning of the mixtures in the top and in the bottom layers must be analyzed case-by-case, so that the choice of which mixture should be placed on top and which mixture should be placed on bottom translates into a longer pavement life. The mixtures with better predicted fatigue behavior in field were G-A, G-N, Ph-A and Ph-N, respectively.

Figure 12 – Comparisons of predicted cracked area *vs.* number ESALs (single asphalt layers *vs.* double asphalt layers)



Based on the trend observed using 0.2% amine-based anti-stripping agent, higher contents, as it is common in some countries, would not necessarily be helpful for the investigated asphalt mixtures, since fatigue life (see Figure 12a) was higher for asphalt mixtures with only 0.2% amine-based anti-stripping agent than asphalt mixtures with neat binder, while for moisture damage the employed content was already sufficient (see Figure 2a).

In addition to the effect of the additive, the results show that the aggregate type may also produce mixtures more resistant to fatigue. This change of aggregate introduces numerous variables that affect mixture performance. The better adhesion of the granite aggregate to the binder may have been one of the factors, but properties such as shape (Monismith, 1970), angularity (Baladi, 1989), may also have influenced the results. Bessa et al. (2015) investigated the fatigue life of asphalt mixtures containing fine phonolytic and granitic aggregate. The mixture with fine granitic aggregate had a longer fatigue life than the mixture with fine phonolytic aggregate, with results similar to this research. The variation in the thickness of the asphalt film depending on the binder used and/or the aggregate may also have affected the fatigue life (Khodary, 2010). It seems that it is becoming increasingly relevant to research the isolation of each of the variables that may affect adhesion and fatigue in order to gain confidence on the effect of each variable.

### **3.4. Conclusions**

This paper evaluates the impact of using an amine-based anti-stripping agent on the fatigue life of asphaltic pavements. It employs stiffness and fatigue damage characterizations of asphalt mixtures and uses FlexPAVE™ 1.1<sup>Alpha</sup> to compute damage in the asphalt layers. Then, predicted cracked area is obtained from calibrated models found in the literature for the employed prediction system. Two different structures were analyzed: one with a single 0.10m asphalt layer and a second with a combination of double 0.05m asphalt layers (0.10m total thickness). Considering the differences in aggregate-binder adhesiveness of the investigated mixtures and the methodology employed, it was possible to formulate the following conclusions:

- Mixtures containing the binder with amine-based anti-stripping agent showed a smaller area damage contour when compared to the control mixtures (with neat binder).
- Mixtures with granitic aggregate present a smaller area damage contour than mixtures with phonolitic aggregate.

- All the asphalt layers showed crack initiation from bottom-up cracking in the investigated pavements.
- From a point of view of the damage modeling, the investigation of the different combinations of mixtures showed that it is more recommended to use mixtures with amine-based anti-stripping agent on the bottom layers and mixtures with neat binder on the top.

Finally, the importance of assessing material properties and using them for subsequent performance predictions to help decision-making during pavement design should be underlined. This is presented in this paper by the simulation results of pavement structures using different materials considering several arrangements of asphalt layers.

The major limitation of this study was that the various asphalt mixtures evaluated using the FlexPAVE platform were not moisture-conditioned. This work is part of an effort to understand the phenomenon of fatigue of asphalt mixtures from the point of view of the adhesion between the materials and its effects on pavement performance. Research is still scarce on this topic. In this paper, mixtures with better aggregate-binder adhesiveness were observed to be less susceptible to fatigue cracking even in dry conditions, which may be of use for future materials' selection. Those results suggest that this topic should be further investigated. Furthermore, healing and aging models were not employed in the 120-month analyses and simulations. It should be noted that further research is needed before such complex simulations can be performed. Finally, the authors would like to mention that the results presented in this manuscript are part of a broader project on adhesiveness and there is current ongoing work to assess the fatigue life of moisture-conditioned specimens.

### **Acknowledgements**

This research was financially supported by Foundation for Scientific and Technological Development from State of Ceara (FUNCAP), Brazilian Federal Agency for Support and Evaluation of Graduate Education (CAPES), National Council for Scientific and Technological Development (CNPq) & Brazilian National Agency for Petroleum, Natural Gas and Biofuels (ANP).

### **Conflict of interest**

The authors declare that they have no conflict of interest

## REFERENCES

- [1] AASHTO T 342 (2011) Standard Method of test for Determining Dynamic Modulus of Hot-Mix Asphalt Concrete Mixtures, American Association of State Highway and Transportation Officials, Washington, DC.
- [2] AASHTO TP 107-18 (2018) Standard Method of Test for Determining the Damage Characteristic Curve of Asphalt Mixtures from Direct Tension Cyclic Fatigue Tests, American Association of State Highway and Transportation Officials, Washington, DC.
- [3] ABNT (2017) NBR 12583: Agregado Graúdo - Determinação da adesividade ao ligante betuminoso. Associação Brasileira de Normas Técnicas. (*in Portuguese*).
- [4] Aguiar-Moya J.P., Baldi-Sevilla A., Salazar-Delgado J., Pacheco-Fallas, J.F., Loria-Salazar L., Reyes-Lizcano F., & Cely-Leal N. (2016). Adhesive properties of asphalts and aggregates in tropical climates. International Journal of Pavement Engineering, 19(8), 738–747. <https://doi:10.1080/10298436.2016.1199884>
- [5] Arabani M., Roshani H., Hamed G.H. (2012) Estimating Moisture Sensitivity of Warm Mix Asphalt Modified with Zycosoil as an Antistrip Agent Using Surface Free Energy Method. Journal of Materials in Civil Engineering, 24(7), 889–897. [https://doi:10.1061/\(asce\)mt.1943-5533.0000455](https://doi:10.1061/(asce)mt.1943-5533.0000455)
- [6] Babadopoulos L.F.A.L., Soares J.B., Ferreira J.L.S., Nascimento L.A.H. (2018) Fatigue cracking simulation of aged asphalt pavements using a viscoelastic continuum damage model. Road Materials and Pavement Design, 19(3), 546–560. <https://doi:10.1080/14680629.2018.1418715>
- [7] Bagampadde U., Isacsson U., Kiggundu B.M. (2005) Influence of aggregate chemical and mineralogical composition on stripping in bituminous mixtures. International Journal of Pavement Engineering, 6(4), 229–239. <https://doi:10.1080/10298430500440796>
- [8] Baladi G. (1989). Fatigue life and permanent deformation characteristics of asphalt concrete mixes. Transportation Research Record 1227. Washington, DC: Transportation Research Board.
- [9] Bessa I.S., Branco V.T.F.C., Soares J.B., Neto J.A.N. (2015) Aggregate Shape Properties and Their Influence on the Behavior of Hot-Mix Asphalt. Journal of Materials in Civil Engineering, 27(7), 04014212. [https://doi:10.1061/\(asce\)mt.1943-5533.0001181](https://doi:10.1061/(asce)mt.1943-5533.0001181)
- [10] Caro S., Masad E., Airey G., Bhasin A., Little D. (2008) Probabilistic analysis of fracture in asphalt mixtures caused by moisture damage. Transportation Research Record 2057, Transportation Research Board, Washington, DC, 28–36.
- [11] Chen X., Huang B. (2008) Evaluation of moisture damage in hot mix asphalt using simple performance and superpave indirect tensile tests. Construction and Building Materials, 22(9), 1950-1962. <https://doi:10.1016/j.conbuildmat.2007.07.014>
- [12] Cui S., Blackman B.R.K., Kinloch A.J., Taylor A.C. (2014) Durability of asphalt mixtures: Effect of aggregate type and adhesion promoters. International Journal of Adhesion and Adhesives, 54, 100–111. <https://doi:10.1016/j.ijadhadh.2014.05.009>
- [13] Eslamnia M.S., Thirunavukkarasu S., Guddati M.N., Kim Y.R. (2012) Accelerated pavement performance modeling using layered viscoelastic analysis. 7th RILEM International Conference on Cracking in Pavements, 4, 497–506. [https://doi:10.1007/978-94-007-4566-7\\_48](https://doi:10.1007/978-94-007-4566-7_48)
- [14] Etheridge R.A., Wang Y.D., Kim S.S., Kim Y.R. (2019) Evaluation of Fatigue Cracking Resistance of Asphalt Mixtures Using Apparent Damage Capacity. Journal of Materials in Civil Engineering, 31(11), 04019257. [https://doi:10.1061/\(asce\)mt.1943-5533.0002870](https://doi:10.1061/(asce)mt.1943-5533.0002870)
- [15] Hesami E., Mehdizadeh G. (2017) Study of the amine-based liquid anti-stripping agents by simulating hot mix asphalt plant production process. Construction and Building Materials, 157, 1011–1017. <https://doi:10.1016/j.conbuildmat.2017.09.168>

- [16] Hicks R.G. (1991) Moisture damage in asphalt concrete. National Cooperative Highway Research Program. Synthesis of Highway Practice 175, Transportation Research Board, Washington.
- [17] Kanitpong K., Bahia H.U. (2008) Evaluation of HMA moisture damage in Wisconsin as it relates to pavement performance. International Journal of Pavement Engineering, 9(1), 9–17. <https://doi:10.1080/10298430600965122>
- [18] Kim Y.R. (2018) Advances in Materials and Pavement Performance Prediction: Proceedings of the International AM3P Conference. Edited by Masad E., Bhasin A., Scarpas T., Menapace I., Kumar A. Taylor & Francis Group, London, ISBN 978-1-338-313095
- [19] Khodary F. (2010) Evaluation of fatigue resistance for modified asphalt concrete mixtures based on dissipated energy concepts. PhD Thesis, Technische Universität Darmstadt, Darmstadt.
- [20] Kringos N., Scarpas T., Kasbergen C., Selvadurai P. (2008) Modelling of combined physical–mechanical moisture-induced damage in asphaltic mixes, Part 1: governing processes and formulations. International Journal of Pavement Engineering, 9(2), 115–128. <https://doi:10.1080/10298430701792185>
- [21] Lucas Júnior J.L.O., Babadopoulos L.F.A.L., Soares J.B. (2019a) Moisture-induced damage resistance, stiffness and fatigue life of asphalt mixtures with different aggregate–binder adhesion properties. Construction and Building Material 216: 166–175. <https://doi.org/10.1016/j.conbuildmat.2019.04.241>
- [22] Lucas Júnior J.L.O., Soares J.B. (2019b) Desenvolvimento de metodologia para avaliação da adesividade agregado-ligante com o uso de processamento digital de imagem. Transportes. <https://doi.org/10.14295/transportes.v27i1.1552> (*in Portuguese*)
- [23] Lucas Júnior J.L.O., Babadopoulos L.F.A.L., Soares J.B (2020a) Influence of Aggregate–Binder Adhesion on Fatigue Life of Asphalt Mixtures. Journal of Testing and Evaluation 48: 1, 150–160. <https://doi:10.1520/JTE20190109>
- [24] Lucas Júnior J.L.O., Babadopoulos L.F.A.L., Soares J.B. (2020b) Effect of aggregate shape properties and binder’s adhesiveness to aggregate on results of compression and tension/compression tests on hot mix asphalt. Materials and Structures 53, 1–15. <https://doi.org/10.1617/s11527-020-01472-1>
- [25] Monismith C.L. (1970) Influence of shape, size, and surface texture on the stiffness and fatigue response of asphalt mixtures. Technical Report 109, Transportation Research Record, National Research Council.
- [26] Nascimento L.A.H. (2015) Implementation and validation of the viscoelastic continuum damage theory for asphalt mixture and pavement analysis in Brazil (Ph.D., dissertation). North Carolina State Univ., Raleigh, NC.
- [27] Norouzi A., Kim Y.R. (2015) Mechanistic evaluation of fatigue cracking in asphalt pavements. International Journal of Pavement Engineering, 18(6), 530–546. doi:10.1080/10298436.2015.1095909
- [28] Park H.J., Eslaminia M., Kim Y.R. (2014) Mechanistic evaluation of cracking in in-service asphalt pavements. Materials and Structures, 47(8), 1339–1358. <https://doi:10.1617/s11527-014-0307-6>
- [29] Sabouri M., Kim Y.R. (2014) Development of a failure criterion for asphalt mixtures under different modes of fatigue loading. Transportation Research Record: Journal of the Transportation Research Board, 2447(4), 117–125. <https://doi:10.3141/2447-13>
- [30] Sabouri M. (2020) Evaluation of performance-based mix design for asphalt mixtures containing Reclaimed Asphalt Pavement (RAP). Construction and Building Materials, 235, 117545. <https://doi:10.1016/j.conbuildmat.2019.117545>
- [31] Underwood B.S., Baek C., Kim Y.R. (2012) Simplified viscoelastic continuum damage

- model as platform for asphalt concrete fatigue analysis. *Transportation Research Record* 2296, 36–45.
- [32] User Guide (2018) Layered viscoelastic pavement analysis for critical distresses FlexPAVE 1.1<sup>Alpha</sup>. Department of Civil, Construction, and Environmental Engineering North Carolina State University. Accessed in: [http://onlinepubs.trb.org/Onlinepubs/nchrp/docs/FlexPAVE1.1Standalone\\_UserManual.ocx](http://onlinepubs.trb.org/Onlinepubs/nchrp/docs/FlexPAVE1.1Standalone_UserManual.ocx).
- [33] Wang Y., Norouzi A., Kim Y.R. (2016) Comparison of Fatigue Cracking Performance of Asphalt Pavements Predicted by Pavement ME and LVECD Programs. *Transportation Research Record: Journal of the Transportation Research Board*, 2590, 44–55. <https://doi:10.3141/2590-06>
- [34] Wang Y.D., Keshavarzi B., Kim Y.R. (2018) Fatigue Performance Analysis of Pavements with RAP Using Viscoelastic Continuum Damage Theory. *KSCE Journal of Civil Engineering*, 22(6), 2118–2125. <https://doi:10.1007/s12205-018-2648-0>

## 4. EFEITO DA TEMPERATURA, DA ESPESSURA, DA CARGA E DA VELOCIDADE NA PREVISÃO DE ÁREA TRINCADA DE PAVIMENTOS ASFÁLTICOS

Submetido à Revista Transportes

### Previsão de área trincada em pavimentos asfálticos: quais as principais variáveis a considerar?

Jorge L.O. Lucas Júnior<sup>a,b\*</sup>, Lucas F.A.L. Babadopulos<sup>c</sup>, Jorge B. Soares<sup>a</sup>

<sup>a</sup> Departamento de Engenharia de Transportes, Universidade Federal do Ceará, Fortaleza, Brasil

<sup>b</sup> Departamento de Engenharia Civil, Faculdade Ari de Sá, Fortaleza, Brasil

<sup>c</sup> Departamento de Engenharia e Construção Civil, Universidade Federal do Ceará, Fortaleza, Brasil

\* Autor correspondente.

E-mail addresses: [j.lucas.j@det.ufc.br](mailto:j.lucas.j@det.ufc.br) (Jorge L.O. Lucas Júnior), [babadopulos@ufc.br](mailto:babadopulos@ufc.br) (Lucas F.A.L. Babadopulos), [jsoares@det.ufc.br](mailto:jsoares@det.ufc.br) (Jorge B. Soares).

#### RESUMO

O desempenho em campo dos pavimentos asfálticos pode ser afetado por diversas variáveis, dentre elas as variáveis controláveis, como materiais usados, espessura e volume de vazios do revestimento compactado, teor de ligante, e as variáveis não-controláveis, como temperatura do ambiente, carga e velocidade de passagem de veículos. O objetivo desse trabalho foi avaliar como a temperatura, a espessura do revestimento, a carga aplicada por roda e a velocidade do tráfego afetam o comportamento à fadiga dos pavimentos asfálticos com um CAP 50/70 puro e com outro constituído pelo mesmo CAP modificado por 0,2% de aditivo orgânico melhorador de adesividade à base de amina, além de agregados de origens distintas. As avaliações foram feitas em termos de variação unitária do percentual previsto de área trincada. Utilizou-se a caracterização viscoelástica linear por meio do módulo complexo à compressão axial simples, a caracterização de fadiga por meio do ensaio à tração-compressão, o modelo *Simplified Viscoelastic Continuum Damage* e a simulação no software CAP3D-D, calibrado para previsão de trincamento em pistas experimentais nacionais. Concluiu-se que pavimentos com aditivo melhorador de adesividade à base de amina apresentaram menores valores de área de trincada quando comparadas aos pavimentos com CAP 50/70 puro, além de que atendem aos requisitos de resistência ao dano por umidade. Os pavimentos com agregado granítico apresentaram menores valores previstos de área trincada quando comparados aos pavimentos com agregado fonolítico. A maioria dos pavimentos teve mais variações unitárias de área trincada devido à variação de espessura do revestimento e de temperatura. Cada variação de  $\pm 1\text{cm}$  de espessura do revestimento asfáltico produziu aproximadamente o mesmo efeito na área trincada que as variações de  $\pm 1,1^\circ\text{C}$ ,  $\pm 5,6\text{km/h}$  ou  $\pm 16,6\text{kN}$  de carga por roda.

**Palavras chave:** vida de fadiga, área trincada, adesividade, CAP3D-D.

#### ABSTRACT

The field performance asphalt pavements can be affected by several variables, including controllable variables, such as materials used, surface course thickness and compacted air voids, binder content, and non-controllable variables, such as temperature, or load and speed of traffic of vehicles. The objective of this work was to evaluate how the temperature, asphalt layer thickness, wheel load and traffic speed affect the fatigue behavior of asphalt pavements with a neat CAP 50/70 and with another binder consisting of the same CAP 50/70 modified by 0.2% of amine-based anti-stripping agent, in addition to aggregates of different origins. The proposed evaluations were made in terms of unit variation of the predicted percentage of cracked area. As a step in obtaining material parameters, it was used linear viscoelastic characterization through the complex modulus to axial compression, the characterization of fatigue through the tension-compression test, the Simplified Viscoelastic Continuum Damage model, and simulation using the CAP3D-D software, calibrated to predict cracking in national experimental test sections. It was concluded that pavements with amine-based anti-stripping agent showed lower crack area values when compared to pavements with neat CAP 50/70, in addition to meeting the requirements for

resistance to moisture damage. Pavements with granitic aggregate had lower predicted values of cracked area when compared to pavements with phonolytic aggregate. Most pavements had more unitary variations in cracked area due to the variation in the thickness of the asphalt layer and the temperature. Each variation of  $\pm 1\text{cm}$  in thickness of the asphalt layer produced the same effect in the cracked area as, approximately, the variations of  $\pm 1.1^\circ\text{C}$ ,  $\pm 5.6\text{km/h}$  or  $\pm 16.6\text{kN}$  of load per wheel.

**Keywords:** fatigue life, cracked area, adhesiveness, CAP3D-D.

#### 4.1. Introdução

O desempenho em campo dos pavimentos asfálticos pode ser afetado por diversas variáveis, dentre elas as variáveis controláveis, como materiais usados, espessura e volume de vazios compactado do revestimento, teor de ligante, entre outras, e as variáveis não-controláveis, como temperatura, ou carga e velocidade de passagem de veículos. Estas duas últimas podem ter controle de limites máximos regulamentados, mas há alta variabilidade em seus valores. A união de todas essas variáveis e outras deveria ser determinante para o dimensionamento dos pavimentos asfálticos. Pelo menos as variáveis que produzem maior efeito no desempenho do pavimento deveriam ser levadas em conta no processo de determinação das espessuras das camadas do pavimento.

Uma das propriedades que interferem na vida útil dos pavimentos é a adesividade agregado-ligante. Alguns estudos têm demonstrado a importância da adesividade no trincamento por fadiga de misturas asfálticas (Hou *et al.*, 2018; Cheng *et al.*, 2002; Azarhoosh *et al.*, 2016; Lucas Júnior *et al.* 2019, 2020a, 2020b). Entender o efeito dessa propriedade em associação a variações de temperatura, espessura do revestimento, carga e velocidade de passagem dos veículos na vida de fadiga pode ser fundamental na escolha dos materiais e no dimensionamento dos pavimentos.

Al-Qadi *et al.* (2008) estudaram o efeito das cargas dos veículos na distribuição de tensões e deformações no pavimento. Concluíram que a tensão de tração na parte inferior do revestimento asfáltico diminuiu significativamente à medida que a espessura dessa camada aumenta. Pais *et al.* (2013) também concluíram que o aumento da espessura do revestimento asfáltico fez com que o efeito das cargas no pavimento seja reduzido. Rys *et al.* (2015) mencionaram que o aumento da porcentagem de veículos com sobrecarga de 0 para 20% pode reduzir a vida de fadiga do pavimento asfáltico em até 50%.

Santos *et al.* (2020) investigaram a influência da temperatura e da velocidade do tráfego na previsão de área trincada de pavimentos asfálticos. Concluiu-se que a temperatura e a velocidade do tráfego são relevantes na previsão de percentual de área trincada (%AT) em pavimentos asfálticos, com o nível de influência dependendo da rigidez e da resistência à fadiga

da mistura asfáltica investigada.

Diversos pesquisadores (Rocha Segundo *et al.*, 2016; Santiago *et al.*, 2018; Santos *et al.*, 2020) têm investigado o trincamento por fadiga nos pavimentos asfálticos por meio do programa computacional CAP3D-D, que é uma evolução do software desenvolvido por Holanda *et al.* (2006) como um programa de análise pavimentos usando o método dos elementos finitos denominado CAP3D (*Computational Analysis of Pavements-3D*). Conforme Araújo *et al.* (2010), o CAP3D é capaz de tratar modelos planos, axissimétricos e tridimensionais, utilizando elementos de diferentes formas e ordens de interpolação (linear e quadrática). O sistema ainda é capaz de realizar análises lineares e não lineares, estáticas e dinâmicas. A adição da letra D significou um avanço do programa para aplicação de previsão de desempenho e dimensionamento, mas fixando para este fim o modelo de análise de tensões (axissimétrico, elástico linear equivalente viscoelástico, ou seja, considerando as propriedades viscoelásticas das misturas asfálticas). Além disso, o CAP3D-D incorpora o modelo *Simplified Viscoelastic Continuum Damage* (S-VECD) para prever dano por fadiga no revestimento asfáltico. Para a previsão de dano por fadiga, as camadas granulares são modeladas como materiais elásticos lineares.

O principal objetivo deste trabalho foi avaliar como a temperatura, a espessura do revestimento asfáltico, a carga aplicada e a velocidade do tráfego afetam o comportamento à fadiga de pavimentos asfálticos com um CAP 50/70 puro e modificado por 0,2% de aditivo orgânico melhorador de adesividade à base de amina (conhecido como DOPE no meio técnico).

#### **4.2. Materiais e métodos**

As misturas foram nomeadas conforme o tipo de agregado e de ligante utilizado. A terminologia das quatro misturas são Ph-N, Ph-A, G-N e G-A. Agregado fonolítico (F), agregado granítico (G), CAP 50/70 puro (P) e modificado com aditivo melhorador de adesividade (A) a base de amina. A única diferença entre as misturas Ph-N e Ph-A é que Ph-N usa ligante puro e Ph-A tem a adição de 0,2% (em relação à massa de ligante) de melhorador de adesividade à base de amina. O mesmo ocorre entre G-N e G-A. A única diferença entre Ph-N e G-N é que a primeira mistura usa agregado fonolítico e a segunda usa agregado granítico. O mesmo ocorre entre Ph-N e G-N.

Os agregados usados nas misturas foram fracionados em 10 peneiras (AASHTO) variando entre 19,0 e 0,075mm. Isso foi realizado para evitar que variações da curva granulométrica afetassem o comportamento das misturas. Todas as misturas foram dosadas pela

metodologia *Superpave* e tiveram 5,0% de ligante, volume de vazios médio de 4,0%, temperatura de usinagem de 160°C e de compactação de 150°C.

A caracterização viscoelástica linear foi realizada com ensaios de módulo complexo por compressão axial simples (AASHTO T342, enquanto a caracterização de fadiga por meio do ensaio de fadiga à tração-compressão (AASHTO TP107), com resultados analisados com uso do *Simplified Viscoelastic Continuum Damage model* (S-VECD, Underwood *et al.*, 2012). Para a etapa de previsão de desempenho, utilizou-se simulação no software CAP3D-D, calibrado para previsão de trincamento em pistas experimentais nacionais através dos parâmetros de viscoelasticidade linear dos materiais e dano em meio contínuo viscoelástico (Santos *et al.*, 2020). Os resultados da caracterização viscoelástica linear através dos parâmetros das funções polinomial e sigmoidal e os parâmetros de fadiga do modelo S-VECD foram usados como entradas para a previsão do %AT com o CAP3D-D. Como esses dados foram utilizados como entradas para a simulação e o resultado da adesividade servirá como base para discussão dos resultados, eles são apresentados na seção de caracterização de materiais.

#### 4.2.1. Ensaio de Adesividade Agregado-Ligante

A adesividade foi avaliada por meio da norma ABNT 12583. A Figura 1 mostra o resultado do ensaio de adesividade dos agregados graúdos das quatro misturas asfálticas analisadas. As misturas Ph-N e G-N (ligante puro) apresentaram adesividade insatisfatória, enquanto as misturas de Ph-A e G-A (ligante puro com aditivo melhorador de adesividade à base de amina) apresentaram adesividade satisfatória.

Figura 1 – Ensaio de adesividade das misturas asfálticas investigadas



#### 4.2.2. Caracterização viscoelástica linear e de fadiga

Para a caracterização linear viscoelástica, foi utilizado o procedimento da norma AASHTO T342. Para obtenção do valor absoluto do módulo complexo  $E^*$  (módulo dinâmico,  $|E^*|$ ) à compressão foram realizadas varreduras de frequência (25; 10; 5; 1; 0,5 e 0,1Hz) e de temperatura (-10; 4,4; 21,1; 37,8 e 54°C). As curvas mestras de  $|E^*|$  para as misturas testadas foram obtidas a partir de translação de isotermas (multiplicação da frequência real pelo fator de translação  $a_T$  para obtenção da frequência equivalente ou frequência reduzida) usando a função polinomial, de acordo com a Equação (1), com a aplicação do princípio de superposição tempo-temperatura (t-TS) para uma temperatura de referência arbitrária, adotada como 21,1°C nesta pesquisa. Então, os dados de  $|E^*|$  em função da frequência reduzida foram ajustados por uma função sigmoidal (Equação 2).

$$\log(a_T) = \alpha_1 T^2 + \alpha_2 T + \alpha_3 \quad (1)$$

em que,  $a_T$  é o *shift factor*,  $T$  é a temperatura em que é observado o valor de módulo e  $\alpha_1$ ,  $\alpha_2$  and  $\alpha_3$  são os coeficientes da função polinomial.

$$\log|E^*| = \alpha + \frac{b}{1 + \frac{1}{e^{d+g \cdot \log f_{red}}}} \quad (2)$$

em que,  $E^*$  é o modulo complexo,  $\delta$ ,  $\alpha$ ,  $\beta$ ,  $\gamma$  são os coeficientes da função sigmoidal e  $f_{red} = a_T \cdot f$  é a frequência reduzida.

A caracterização da fadiga foi realizada segundo o modelo S-VECD e a norma AASHTO TP 107. As curvas características de dano ( $C$  vs.  $S$ ), consideradas uma propriedade do material, foram ajustadas por uma lei de potência, de acordo com a Equação 3, e o critério de falha  $G^R$  vs  $N_f$  (Equação 4).

$$C(S) = 1 - C_{11} S^{C_{12}} \quad (3)$$

em que,  $C(S)$  é a curva característica de dano que associa a integridade do material ( $C$ ) ao dano acumulado  $S$ , e  $C_{11}$  and  $C_{12}$  são coeficientes de ajuste.

$$G^R = Y(N_f)^\Delta \quad (4)$$

em que,  $G^R$  é a taxa de variação média da energia de pseudo-deformação liberada (por ciclo) durante todo o processo de danificação;  $Y$  e  $\Delta$  são coeficientes de ajustes e  $N_f$  é o número de ciclos até a falha.

As curvas mestras de  $|E^*|$  das quatro misturas asfálticas investigadas foram construídas pela função polinomial. A função sigmoidal se ajustou bem aos dados experimentais. Os coeficientes das referidas funções são mostrados na Tabela 1, assim como os coeficientes das

curvas características de dano de cada mistura. Todos os parâmetros mostrados na Tabela 1 são utilizados como dados de entrada do CAP3D-D.

Tabela 1: Parâmetros usados na simulação do %AT no CAP3D-D

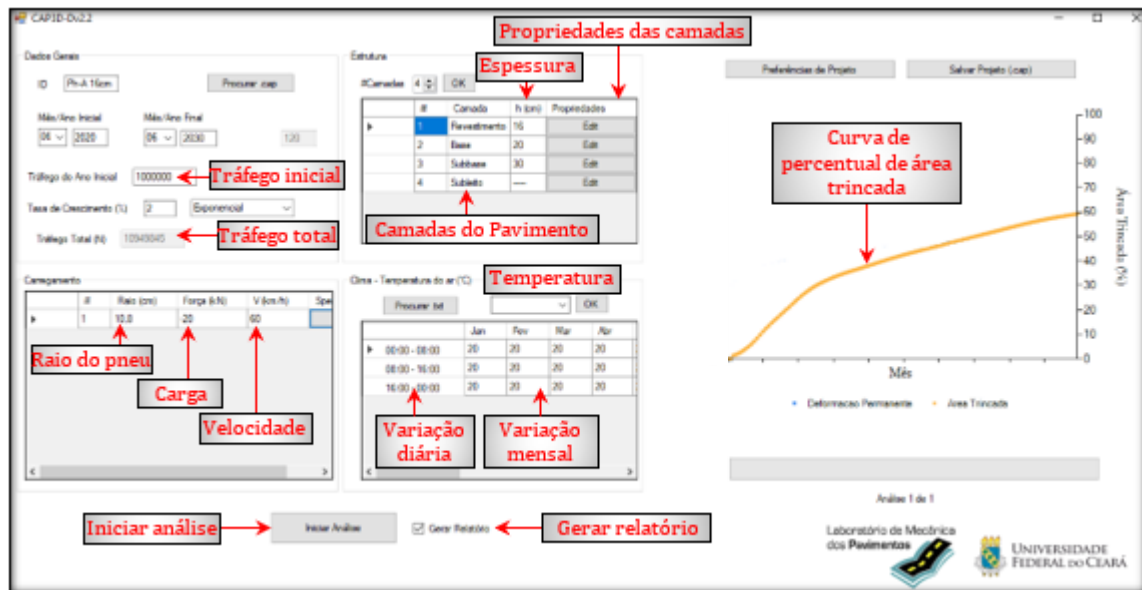
Modelagem	Parâmetro	Mistura Asfáltica			
		Ph-N	Ph-A	G-N	G-A
<i>Shift factor</i> Função Polinomial	$a_1$	8,64E-04	8,36E-04	8,26E-04	8,35E-04
	$a_2$	-0,172	-0,170	-0,169	-0,170
	$a_3$	3,234	3,237	3,224	3,219
Função Sigmoidal	$a$	1,248	1,570	0,964	1,385
	$b$	3,279	2,906	3,564	3,076
	$d$	1,185	1,221	1,203	1,034
	$g$	0,594	0,681	0,554	0,650
Taxa de evolução de dano	$\alpha$	3,191	3,197	3,088	2,971
$G^R$ vs. $N_f$ (S-VECD)	$Y$	4,59E+11	5,82E+08	3,41E+09	8,07E+07
	$\Delta$	-2,687	-1,983	-2,068	-1,535
$C$ vs $S$ . (S-VECD)	$C_{11}$	3,29E-04	1,37E-04	8,68E-04	4,50E-04
	$C_{12}$	6,37E-01	7,37E-01	5,71E-01	6,33E-01

$\alpha$ =taxa de evolução de dano (constante relacionada às propriedades de fluência ou relaxação do material).

#### 4.2.3. Simulação no CAP3D-D

A simulação de área trincada foi realizada utilizando o CAP3D-D versão 2.2 (que utiliza calibrações apresentadas por Santiago *et al.*, 2020). Esse *software* é capaz de executar análises de fadiga e deformação permanente, mas neste artigo apenas a análise de fadiga foi considerada. A Figura 2 mostra a interface do programa e as principais variáveis que podem ser modificadas para a análise desejada.

Figura 2 – Interface do CAP3D-D com as principais entradas requeridas pelo programa



Para determinar o %AT se faz necessária uma translação dos dados experimentais (por

meio de uma função  $S$ ) de dano médio ( $D_{med}$ ), transformando-os em dano médio reduzido ( $D_{red_s}$ ) e uma calibração e validação da Função de Transferência (Santiago *et al.*, 2020; Santos *et al.*, 2020). A Função de Transferência (FT) foi calibrada com 27 trechos e validada com outros 17 trechos que fazem parte do monitoramento de pavimentos da Rede de Tecnologia em Asfalto da Petrobras, um projeto que, entre outras coisas, subsidiou dados para o novo método de dimensionamento nacional de pavimentos brasileiros (MeDiNa). A Função  $S$  e a FT calibrada e validada apresentadas por Santiago *et al.* (2020) são mostradas nas Equações 5 e 6.

$$S = 0,00002(T_{0,35})^2 + 0,00872(T_{0,35}) + 0,65294 \quad (5)$$

$$\%AT = 721,96589 \left( \frac{N_{red}}{N_{f_{red}}} \right)^{3,76808} \quad (6)$$

em que,  $T_{0,35}$  é o mês em que o revestimento tem dano médio de 0,35 e  $N_{red}/N_{f_{red}}$  é a taxa média de dano reduzido.

As principais entradas solicitadas pelo CAP3D-D são o tráfego inicial, a taxa de crescimento, o raio do pneu, a força aplicada pelas cargas, a temperatura e a velocidade. Em relação às camadas granulares, foram informadas as espessuras, o coeficiente de Poisson e o módulo de elasticidade da base, da sub-base e do subleito (para esta última a espessura não precisa ser informada). Para o revestimento asfáltico, o CAP3D-D requer dados extraídos dos testes do módulo dinâmico por compressão axial (AASHTO T342) e fadiga à tração-compressão (AASHTO TP107) associados ao modelo S-VECD (Underwood *et al.*, 2012). Foi necessário informar os seguintes parâmetros:  $a_1$ ,  $a_2$  e  $a_3$  da função polinomial de ajuste do fator de transladação;  $\delta$ ,  $\alpha$ ,  $\beta$  e  $\gamma$  da função sigmoidal usada para ajustar a curva mestra de  $|E^*|$ ;  $Y$  e  $\Delta$  da curva  $G^R$  vs.  $N_f$ ,  $C_{11}$  e  $C_{12}$  da curva característica de dano  $C(S)$  e o parâmetro de dano  $\alpha$ . As análises foram realizadas com um nível de confiança de 95%. A Figura 3 mostra quais variáveis foram mantidas fixas e quais variaram a cada análise. As variáveis analisadas foram temperatura, espessura da camada asfáltica, força aplicada pelas cargas e velocidade de tráfego. A Figura 4 mostra um esquema da metodologia usada para analisar os resultados.

Figura 3 – Cenários e variáveis utilizadas na simulação

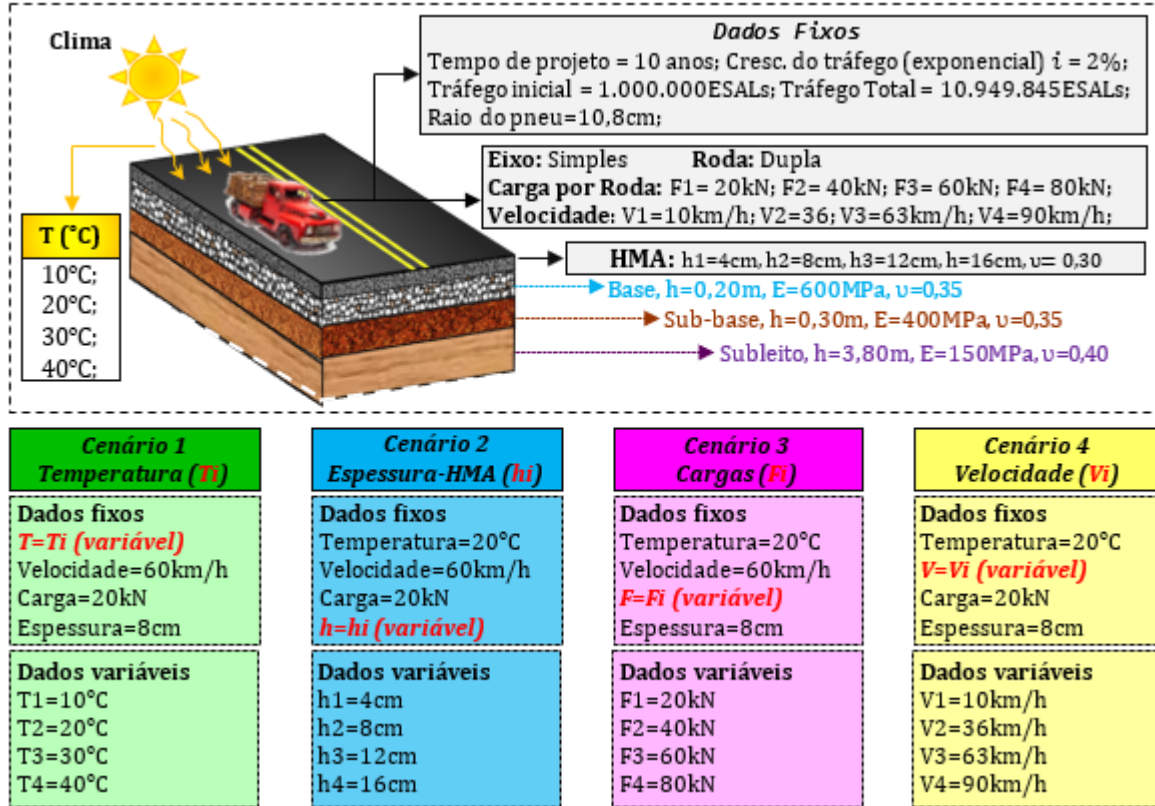
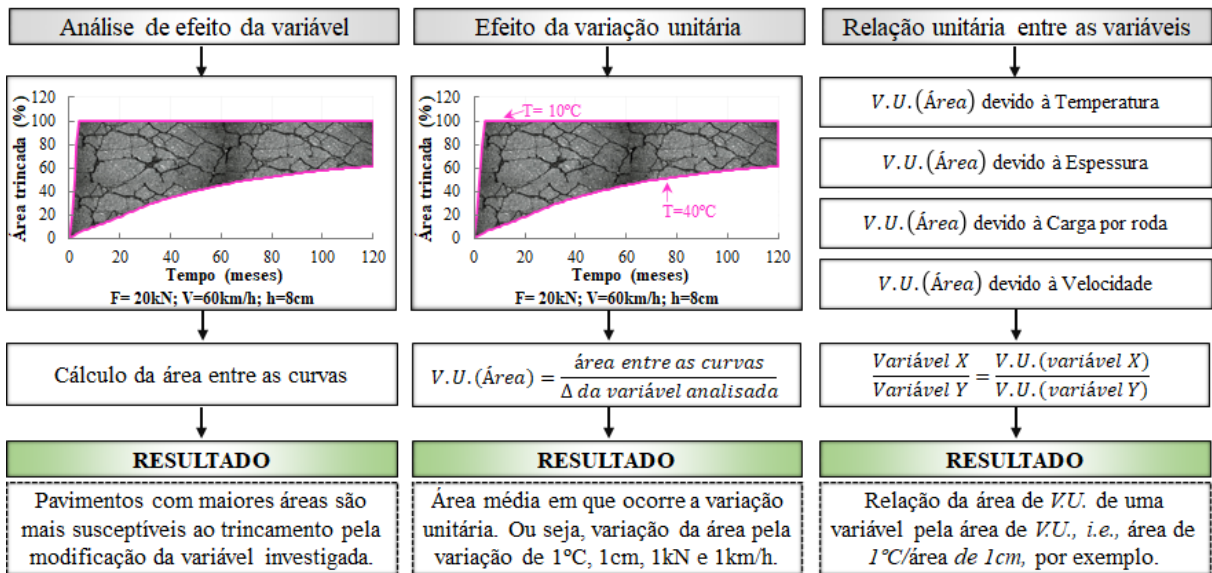


Figura 4 – Desenho esquemático da metodologia de análise dos resultados



### 4.3. Resultados e Discussões

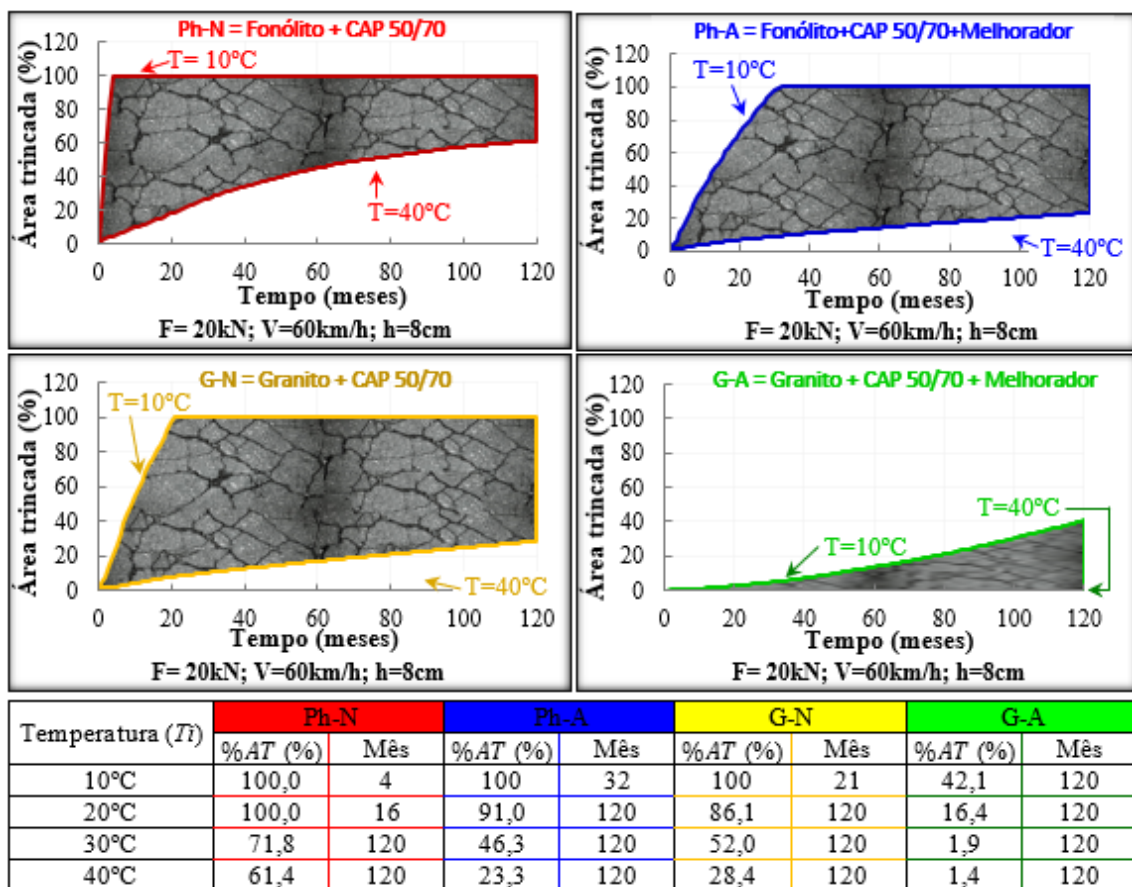
#### 4.3.1 Efeito da Temperatura na Previsão da Área Trincada

As misturas asfálticas apresentaram grande sensibilidade à mudança de temperatura (10 a 40°C). Temperaturas mais baixas apresentaram valores mais altos de %AT (semelhante

aos resultados encontrados por Minhoto *et al.*, 2005; Santos *et al.*, 2019), para carga de 20kN, velocidade 60km/h e espessura de 8cm (cf. Figura 5). Baek (2010) atribuiu os maiores danos em climas mais frios aos valores mais altos de pseudo-rigidez na falha ( $C_f$ ), quando se utiliza a análise com S-VECD. Outra explicação é a de que com maior rigidez do revestimento em climas mais frios, há mais tensão na camada de revestimento, cujo efeito não sendo compensado por maior resistência à fadiga, provocará maior trincamento.

As misturas com ligante puro apresentaram %AT mais elevado do que as misturas com melhorador de adesividade à base de amina à 10°C (ver Figura 5). As misturas Ph-N, Ph-A, G-N apresentaram, respectivamente, 100% de %AT para 4, 32 e 21 meses, enquanto G-A foi menos suscetível à variação de temperatura e apresentou 42,1% de %AT para 120 meses. A maior diferença de %AT, entre 10 e 40°C, foi de 95, 90, 92 e 41%, nos meses 4, 32, 21 e 120, para as misturas Ph-N, G-N, Ph-A e G-A, respectivamente. As misturas mais suscetíveis à variação de temperatura, em ordem decrescente, foram G-N, Ph-A, Ph-N e G-A. Esta análise foi baseada no cálculo da área entre curvas, de 10 e 40°C, para cada mistura. As áreas (em meses·%) das misturas G-N, Ph-A, Ph-N e G-A foram, respectivamente, 9118, 9005, 6999 e 1914.

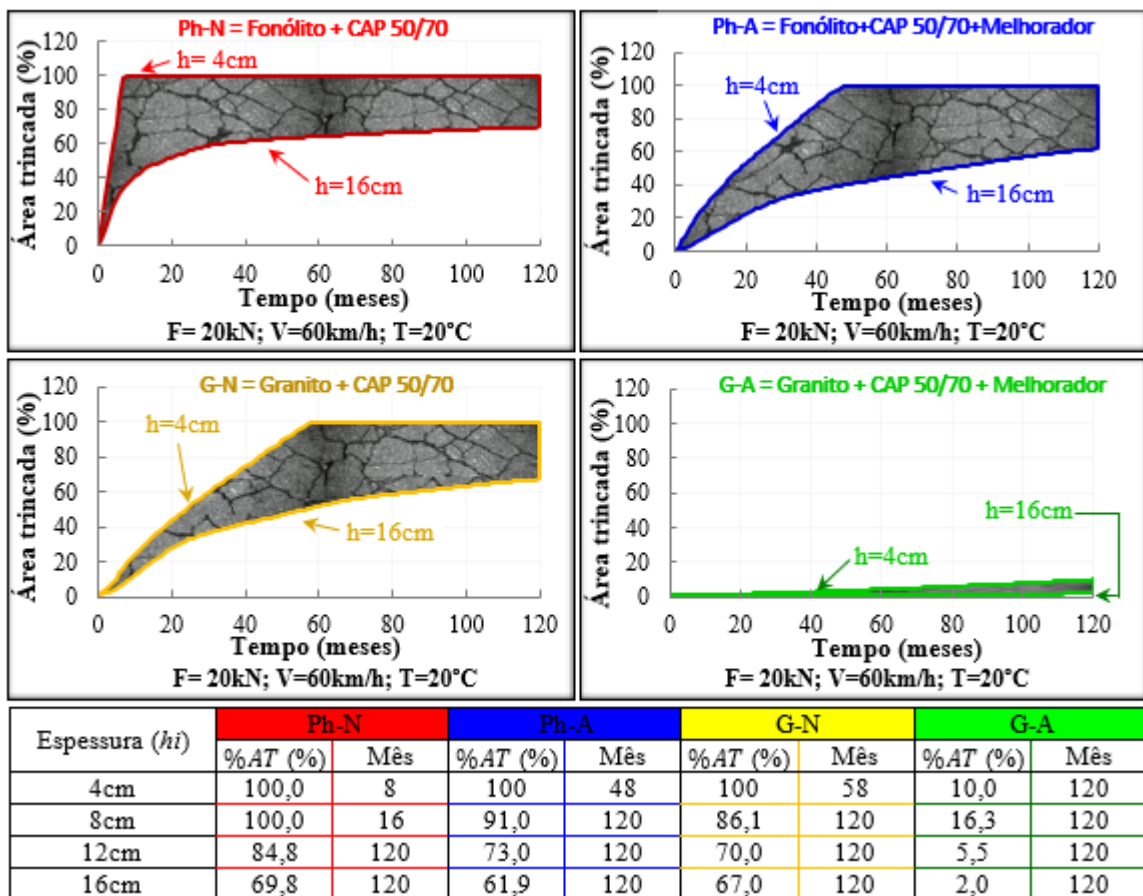
Figura 5 – Efeito da variação da temperatura na área trincada



#### 4.3.2 Efeito da Espessura da Camada Asfáltica na Previsão da Área Trincada

Analizando a Figura 6, como esperado, espessuras menores (4cm) produzem maior %AT que espessuras maiores (16cm), para carga de 20kN, velocidade 60km/h e temperatura de 20°C (resultado similar ao encontrado por Al-Qadi *et al.*, 2008; Nascimento, 2015). Para uma espessura de 4cm, a mistura G-A teve 10% de %AT, aos 120 meses, enquanto Ph-N, Ph-A e G-N atingiram 100% de %AT em 8, 48 e 58 meses, respectivamente. Ao analisar a espessura de 16cm, nenhuma das misturas atingiu 100% de %AT. Aos 120 meses as misturas Ph-N, Ph-A, G-N e G-A tiveram %AT de 70, 62, 67 e 2%, respectivamente. As misturas com melhorador de adesividade demonstraram %AT menor em comparação às misturas com ligante puro, tanto para espessuras mais esbeltas quanto para espessuras robustas. As maiores diferenças de %AT foram 64, 60, 49 e 8%, nos meses 7, 48, 58 e 120, para as misturas Ph-N, Ph-A, G-N e G-A, respectivamente. As áreas (em meses·%) relativas a Ph-A, Ph-N, G-N e G-A foram, respectivamente, 5107, 4486, 3882 e 396.

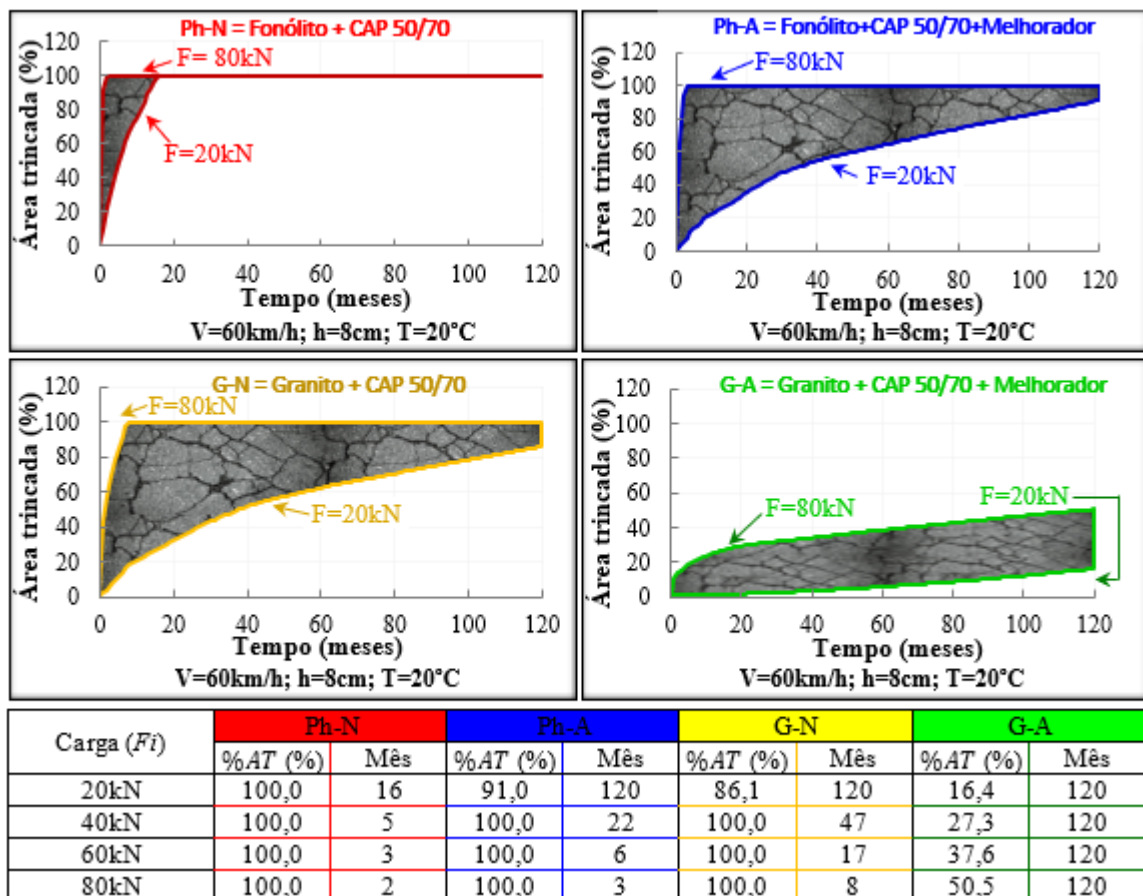
Figura 6 – Efeito da variação da espessura na área trincada



#### 4.3.3 Efeito da Carga na Previsão da Área Trincada

Cargas mais elevadas por eixo produziram valores mais altos de %AT, conforme esperado (Zhao *et al.*, 2012; Rys *et al.*, 2015). As misturas com ligante puro apresentaram um %AT mais alto do que as misturas com melhorador de adesividade para 120 meses, 30°C e 60 km/h (ver Figura 7). Para uma carga de 80kN, as misturas Ph-N, Ph-A e G-N apresentaram 100% de %AT nos meses 2, 3 e 8, respectivamente, enquanto que G-A apresentou 50% de %AT aos 120 meses. As maiores diferenças de %AT foram de 91, 82, 81 e 34%, nos meses 1, 3, 8 e 120, para Ph-A, Ph-N, G-N e G-A, respectivamente. As misturas mais sensíveis às mudanças nas cargas de 20 a 80kN foram G-N, Ph-A, G-A e Ph-N, respectivamente, com área (meses · %) de 4914, 4692, 3692 e 564.

Figura 7 – Efeito da variação da carga na área trincada

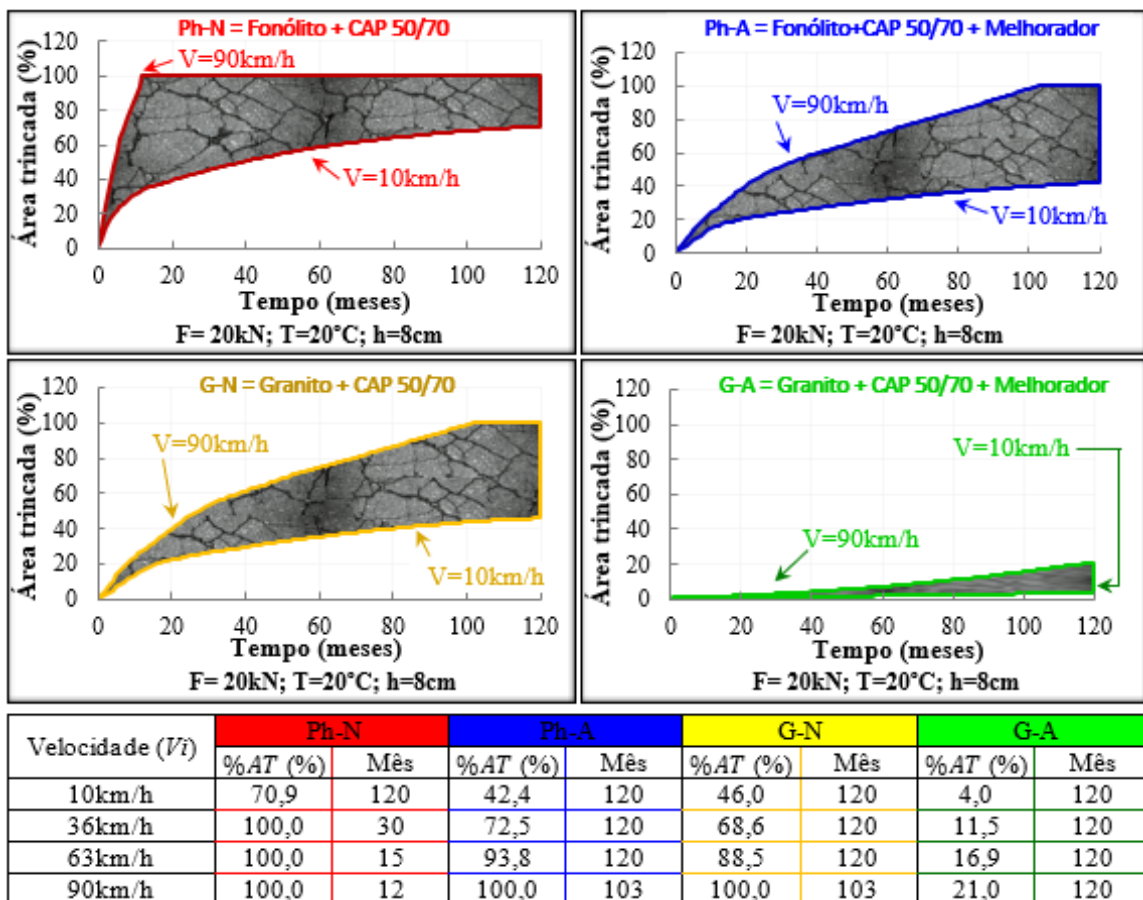


#### 4.3.4 Efeito da Velocidade na Previsão da Área Trincada

Analizando o espectro de velocidade investigado (40 a 100km/h), é possível notar que velocidades mais altas produzem valores mais altos de %AT (resultado similar ao de Santos *et al.*, 2020). As misturas com ligante puro apresentaram %AT mais alta do que aquelas com

melhorador de adesividade (Ph-N vs Ph-A e G-N vs G-A), a 120 meses, para carga de 20kN, espessura de 8cm e temperatura de 20°C (ver Figura 8). Para uma velocidade de 90km/h, Ph-N, G-N e Ph-A apresentaram, respectivamente, 100% de %AT em 12, 103 e 103 meses, enquanto que G-A apresentou 21% de %AT aos 120 meses. As maiores diferenças de %AT foram 66, 59, 56 e 17%, nos meses 12, 103, 103 e 120, para Ph-N, Ph-A, G-N e G-A, respectivamente. As misturas mais suscetíveis às mudanças na velocidade foram Ph-N, Ph-A, G-N e G-A, com áreas (meses · %) de 5012, 4633, 4422 e 772, respectivamente.

Figura 8 – Efeito da variação da velocidade na área trincada



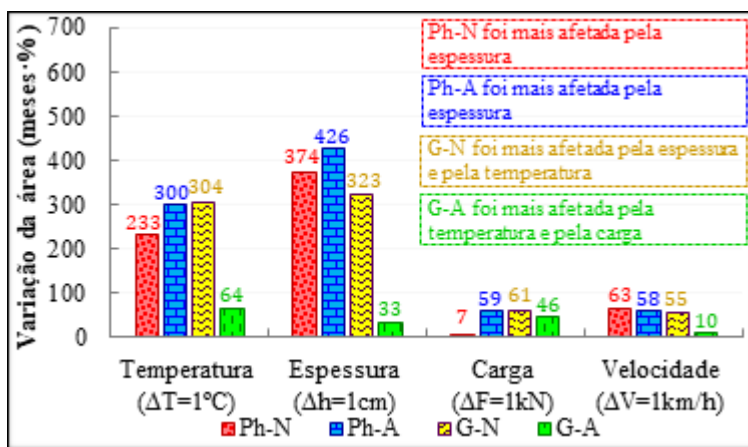
#### 4.3.5. Avaliação do Efeito Unitário das Diferentes Variáveis Analisadas na Área Trincada

Nessa análise, a área total de cada mistura foi dividida pela amplitude da variável analisada. Por exemplo, para saber qual o efeito médio da variação de  $\pm 1^\circ\text{C}$  para a mistura Ph-N, a área total entre as curvas de 10 e 40°C da mistura Ph-N foi dividida pela diferença entre 40 e 10°C, dessa forma determinou-se qual a variação média de área para a variação de cada  $\pm 1^\circ\text{C}$ . O uso dos sinais “ $\pm$ ” indicam que os valores são baseados na média da variável analisada usando a área total, ou seja, tanto pode ser analisada a variação de área iniciando em 30°C e indo até 31°C (variação +) quanto iniciando-se em 30°C e indo até 29°C (variação -), por isso a

utilização dos sinais “±”. Isso foi replicado para as demais misturas e para as outras variáveis.

Para as condições analisadas, as misturas com agregado fonolítico (Ph-N e Ph-A) tiveram valor numérico da variação unitária indicando maior sensibilidade à variação da espessura, e em seguida da temperatura. A mistura G-N foi afetada igualmente pela temperatura e pela espessura, enquanto que G-A foi mais afetada pela carga, seguida da temperatura, conforme Figura 9. Em resumo, as misturas foram, em ordem decrescente, mais sensíveis às variações unitárias de espessura, temperatura, carga aplicada e velocidade.

Figura 9 – Avaliação da variação unitária das diferentes variáveis



#### 4.3.6 Relação Unitária entre Temperatura, Espessura, Carga e Velocidade

Nessa análise, para se avaliar comparativamente os efeitos de cada variável, dividiu-se a área - considerando a unidade “meses·%” - devido à mudança de uma variável pela área, também em “meses·%”, de outra variável. Por exemplo, a razão entre a área devida à variação de  $\pm 1\text{cm}$  de espessura pela área devida à variação de  $\pm 1^{\circ}\text{C}$  de temperatura. Isso foi replicado para todas as misturas e todas as variáveis analisadas. O intuito foi entender o quanto uma variável pode ser mais prejudicial do que outra para o trincamento por fadiga.

Na Figura 10(a) se relacionou quantas vezes a variação de  $\pm 1^{\circ}\text{C}$  produziu uma área em meses·% maior se comparada à área em meses·% produzida pela variação de  $\pm 1\text{km/h}$ . Analisando-se a Figura 10(a), pode-se notar que a mistura Ph-N foi 3,7 vezes mais afetada por  $\pm 1^{\circ}\text{C}$  se comparado à variação de  $\pm 1\text{km/h}$ . Quando se adicionou o aditivo melhorador de adesividade (mistura Ph-A) essa mesma relação aumentou para 5,2 vezes. O mesmo ocorreu para os pavimentos com as misturas contendo agregado granítico (G-N e G-A), com 5,5 e 6,6 vezes mais afetadas pela variação de  $\pm 1^{\circ}\text{C}$  quando comparadas a variação de  $1\text{km/h}$ , respectivamente.

Na Figura 10(b), foi comparado o efeito da variação de  $\pm 1^{\circ}\text{C}$  com o efeito da variação

de 1kN de carga. A mistura Ph-N se mostrou ser, aproximadamente, 34 vezes mais afetada pela variação de  $\pm 1^{\circ}\text{C}$  se comparada a 1kN. As misturas Ph-A e G-N foram, aproximadamente, 5 vezes mais afetadas por  $1^{\circ}\text{C}$  que por 1km/h e a mistura G-A se mostrou mais afetada 1,4 vezes por  $\pm 1^{\circ}\text{C}$  que por  $\pm 1\text{kN}$ .

Na Figura 10(c), a relação é feita com base na área trincada devido à variação de  $\pm 1\text{cm}$  de revestimento asfáltico em comparação à variação produzida por mudança de  $\pm 1^{\circ}\text{C}$  de temperatura. Essas duas variáveis se mostraram próximas em suas influências nos resultados. A proximidade dos resultados entre espessura e temperatura é surpreendente, mostrando que a temperatura pode afetar a vida de fadiga do pavimento tanto quanto a espessura do revestimento. Mesmo que o projetista não tenha como limitar as temperaturas como tem o poder de dimensionar a espessura do revestimento asfáltico, essa informação mostra como o material asfáltico é complexo e que as abordagens experimentais mais avançadas associadas às ferramentas computacionais mais robustas podem melhor caracterizar as misturas asfálticas, refletindo-se em um dimensionamento dos pavimentos asfálticos mais adequado. Nessa análise, a mistura G-A foi a única que foi 2 vezes mais afetada pela variação de  $\pm 1^{\circ}\text{C}$  do que pela variação de  $\pm 1\text{cm}$  de espessura do revestimento asfáltico, enquanto Ph-N, Ph-A e G-N foram mais afetadas pela variação de  $\pm 1\text{cm}$ , com valores de 1,6; 1,4 e 1,1, respectivamente.

Na Figura 10(d) as misturas Ph-N, Ph-A e G-N foram mais afetadas pela variação de  $\pm 1\text{cm}$  de revestimento do que pela variação de 1kN, 53, 7 e 4 vezes, respectivamente. Por sua vez, a mistura G-A se mostrou mais afetada pela variação de 1kN do que pela variação de  $\pm 1\text{cm}$ . Nesse caso, a carga pode ser uma variável controlada pela pesagem dos veículos, mostrando que em alguns casos, como o do pavimento com a mistura G-A, pode ser mais confiável e econômico manter uma espessura intermediária e impor limites às cargas que trafegam no pavimento com estratégias de pesagem e controle.

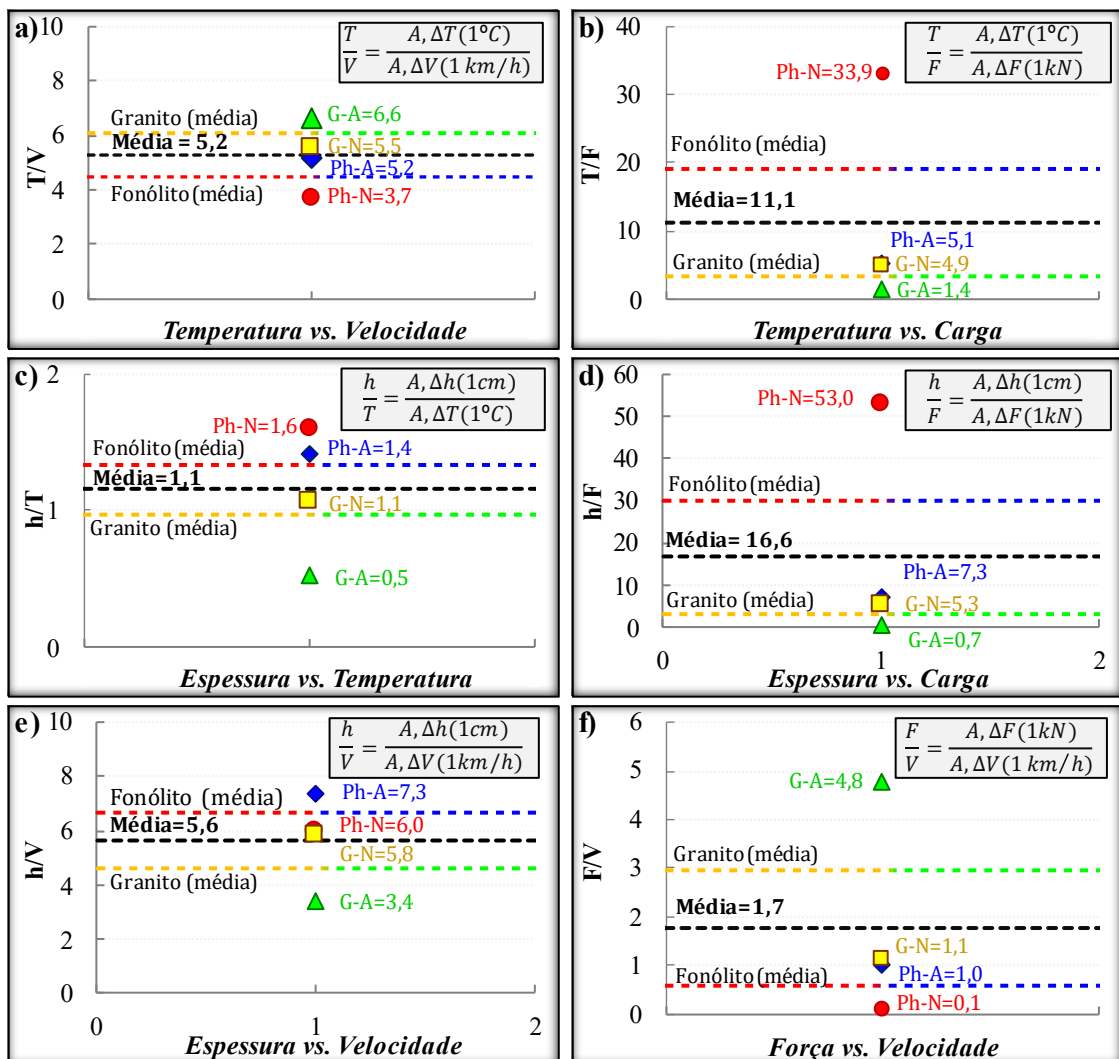
Na Figura 10(e), observa-se que todas as misturas investigadas se mostraram mais afetadas pela variação de  $\pm 1\text{cm}$  de espessura do revestimento do que pela variação de  $\pm 1\text{km/h}$ . Variações de 3,4 a 7,3 vezes foram observadas e em média, aproximadamente 5 vezes. Em relação aos resultados da Figura 10(f), as misturas foram mais afetadas pela variação de 1kN do que pela variação de  $\pm 1\text{km/h}$ , em média 1,7 vezes, todavia o pavimento com a mistura Ph-N foi mais afetado pela velocidade do que pela carga. A mistura G-A foi 4,8 vezes mais afetada pela variação de  $\pm 1\text{kN}$  do que pela variação de  $\pm 1\text{km/h}$ .

Considerando os pavimentos investigados e os valores médios de cada propriedade notou-se que: (i) cada variação de  $\pm 1\text{cm}$  de espessura do revestimento asfáltico produziu o

mesmo efeito na área trincada que, aproximadamente, as variações de  $\pm 1,1^{\circ}\text{C}$ ,  $\pm 5,6\text{km/h}$  ou  $\pm 16,6\text{kN}$  de carga por roda; (ii) cada variação de  $\pm 1^{\circ}\text{C}$  de temperatura teve o mesmo efeito que  $\pm 5,2\text{km/h}$ ,  $\pm 11,1\text{kN}$  ou  $\pm 0,9\text{cm}$  no %AT; e (iii) cada  $\pm 1\text{kN}$  teve o mesmo efeito no %AT que  $\pm 1,7\text{km/h}$ ,  $\pm 0,09^{\circ}\text{C}$  ou  $\pm 0,07\text{cm}$ .

Mesmo que os resultados numéricos sugeriram que as variáveis que mais afetaram o trincamento por fadiga foram, na ordem, espessura, temperatura, carga e velocidade, ponderese que a discussão desses resultados se baseou na variação unitária das variáveis, que têm unidades diferentes, e que têm valores numéricos que dependem da própria escolha arbitrária dessas unidades. Além disso, na prática, em campo a variação de  $\pm 1\text{km/h}$  é irrelevante e imperceptível ao condutor, enquanto  $\pm 1^{\circ}\text{C}$  já tem efeito relevante no comportamento das misturas asfálticas e é perfeitamente plausível em campo. Tomando-se como parâmetro uma variação de  $\pm 10\text{km/h}$ , a velocidade passa a ter um efeito na vida de fadiga do pavimento muito mais importante, além de ser mais realístico em relação ao que ocorre em campo.

Figura 10 – Relação das diferentes variáveis investigadas na previsão de área trincada



Os resultados apresentados nesta seção mostram a importância da implementação de uma previsão de desempenho quanto à fadiga considerando as características viscoelásticas e termo-sensíveis das misturas asfálticas. Isso só é possível com a utilização de ensaios laboratoriais que levem em conta as variações de frequência e de temperatura e com ferramentas computacionais que permitam a utilização desses dados, com adequada calibração às observações de campo. As observações de campo a serem utilizadas, por sua vez, devem guardar semelhança com as situações futuras que se pretende analisar.

Convém sublinhar informações acerca da evolução da legislação quanto a sobrecargas de veículos nas rodovias brasileiras. O Artigo 1º da Lei nº 7.408 (1985) permitiu a tolerância máxima para o peso bruto transmitido por eixo de 5% à superfície de vias públicas. Por meio da Resolução nº 104 (1999), o CONTRAN (Conselho Nacional de Trânsito) alterou a tolerância máxima para o peso bruto transmitido por eixo de 5 para 7,5%. Em 2015, promulgou-se a Lei nº 13.103 (2015), onde ficou estabelecido que a tolerância máxima para o peso bruto transmitido por eixo passaria a ser 10%. Em 2021, o Departamento Nacional de Infraestrutura de Transportes (DNIT) aprovou a resolução nº 1 (2021) que instituiu novos limites máximos de peso bruto por eixo para veículo de carga. Como exemplo, um veículo de dois pneumáticos por eixo passou a ter limite máximo de 7,5 toneladas frente às 6 toneladas regulamentadas anteriormente. Esse novo limite representa, nesse caso, uma tolerância máxima para o peso bruto transmitido por eixo de 12,5%. Os resultados apresentados neste trabalho mostram que, a depender do pavimento analisado, como o escolhido aqui, o aumento da carga tem a capacidade de deteriorar os pavimentos precocemente e que o aumento da tolerância máxima para o peso bruto pode ser um importante componente que está interferindo na qualidade das rodovias brasileiras. Essa análise deve ser feita de maneira racionalizada e com os melhores modelos disponíveis atualmente.

#### **4.4. Conclusões**

Este trabalho avaliou o efeito da temperatura, da espessura, da carga e da velocidade de passagem dos veículos considerando características viscoelásticas das misturas asfálticas, que diferiram também em termos de adesividade agregado-ligante. Com base nos resultados obtidos, foi possível formular as seguintes conclusões:

- As misturas com aditivo melhorador de adesividade à base de amina apresentaram menores valores de área de trincada prevista quando comparadas às misturas de controle com CAP puro.

- Misturas com agregado granítico apresentaram menores valores de área trincada prevista quando comparadas às misturas com agregado fonolítico.
- A mistura com agregado granítico e aditivo mostrou melhor comportamento à fadiga e foi a única mais afetada pela carga do que pelas demais variáveis analisadas (temperatura, espessura e velocidade).
- As misturas com agregado fonolítico foram mais afetadas pela variação da espessura, seguida da variação da temperatura.
- A espessura, seguida da temperatura, mostrou afetar mais a área trincada, enquanto a velocidade foi a que menos afetou, nas análises de variação unitária; todavia quando se considera uma variação de 10km/h, condizente com a variação em campo, a velocidade também se torna uma variável com grande efeito na vida de fadiga dos pavimentos asfálticos.
- Para as misturas analisadas neste trabalho, cada variação de  $\pm 1\text{cm}$  de espessura do revestimento asfáltico produz efeito semelhante na área trincada que, aproximadamente, as variações de  $\pm 1,1^\circ\text{C}$ ,  $\pm 5,6\text{km/h}$  ou  $\pm 16,6\text{kN}$  de carga por roda em um eixo simples.
- Para cada mistura em cada pavimento, a relação dos efeitos das diferentes variáveis pode mudar, modificando a ordem de prioridade das principais variáveis a serem consideradas. Ainda assim, os resultados deste trabalho, que fixou a estrutura das subcamadas, apontam para uma relevância conjunta dos efeitos da carga, da temperatura, da velocidade dos veículos e da espessura do revestimento. No caso do efeito das cargas, convém observar-se a evolução de danos em pavimentos em função da nova flexibilização de sobrecargas nas vias brasileiras conforme nova resolução nº 1 do DNIT de 2021.

## REFERÊNCIAS

- [1] AASHTO T 342 (2011) Standard Method of test for Determining Dynamic Modulus of Hot-Mix Asphalt Concrete Mixtures, American Association of State Highway and Transportation Officials, Washington, DC.
- [2] AASHTO TP 107-14 (2018) Standard Method of Test for Determining the Damage Characteristic Curve of Asphalt Mixtures from Direct Tension Cyclic Fatigue Tests, American Association of State Highway and Transportation Officials, Washington, DC.
- [3] ABNT (2017) NBR 12583: Agregado Graúdo - Determinação da adesividade ao ligante betuminoso. Associação Brasileira de Normas Técnicas.
- [4] Al-Qadi I.L., Wang H., Yoo P.J., Dessouky S.H. (2008) Dynamic Analysis and In-Situ Validation of Perpetual Pavement Response to Vehicular Loading. In Transportation Research Record: Journal of the Transportation Research Board, No. 2087, Transportation Research Board of the National Academies, Washington, D.C., pp. 29–39.

- [5] Araújo P.C., Soares J.B., Holanda A.S., Parente E.P., Evangelista F. (2010) Dynamic Viscoelastic Analysis of Asphalt Pavements using Finite Element Formulation. *Road Materials and Pavement Design*, v. 11, p. 409–433.
- [6] Azarhoosh A.R., Nejad M.F., Khodaii A. (2016) The influence of cohesion and adhesion parameters on the fatigue life of hot mix asphalt. *The Journal of Adhesion*, 93(13). <https://doi:10.1080/00218464.2016.1201656>.
- [7] Baek C.M. (2010) An Investigation of Top-Down Cracking Mechanisms Using Viscoelastic Continuum Damage Finite Element Program". Ph.D. dissertation, North Carolina State University.
- [8] Cheng D.X., Little D., Lytton R., Holste J. (2002) Surface Energy Measurement of Asphalt and Its Application to Predicting Fatigue and Healing in Asphalt Mixtures. *Transportation Research Record: Journal of the Transportation Research Board* 1810, 44–53. doi:10.3141/1810-06.
- [9] Hou Y., Xiaoping J., Jia L., Xianghang L. (2018) Adhesion between Asphalt and Recycled Concrete Aggregate and Its Impact on the Properties of Asphalt Mixture. *Materials*, 11(12). <https://doi:10.3390/ma11122528>.
- [10] Lucas Júnior J.L.O., Babadopoulos L.F.A.L., Soares J.B. (2019) Moisture-induced damage resistance, stiffness and fatigue life of asphalt mixtures with different aggregate-binder adhesion properties. *Construction and Building Material* 216: 166-175. <https://doi.org/10.1016/j.conbuildmat.2019.04.241>
- [11] Lucas Júnior J.L.O., Babadopoulos L.F.A.L., Soares J.B. (2020a) Influence of Aggregate-Binder Adhesion on Fatigue Life of Asphalt Mixtures. *Journal of Testing and Evaluation* 48 (1): 150-160. <https://doi.org/10.1520/JTE20190109>.
- [12] Lucas Júnior, J.L.O., Babadopoulos, L.F.A.L., Soares, J.B. (2020b) Effect of aggregate shape properties and binder's adhesiveness to aggregate on results of compression and tension/compression tests on hot mix asphalt. *Materials and Structures* 53 (43). <https://doi.org/10.1617/s11527-020-01472-1>.
- [13] Minhoto M.J.C., Pais J.C., Pereira P.A.A., Santos L.G.P. (2005) The influence of temperature variation in the prediction of the pavement overlay life. *Road Materials and Pavement Design* 6(3), 365-384.
- [14] Nascimento L.A.H. (2015) Implementation and Validation of the Viscoelastic Continuum Damage Theory for Asphalt Mixture and Pavement Analysis in Brazil. Tese de Doutorado. North Carolina State University. Raleigh-USA.
- [15] Holanda A.S., Parente Júnior E., Melo T.D.B., Evangelista Júnior F., Soares J.B. (2006) Finite Element of Flexible Pavements. XXVII Iberian Latin-American Congress on Computational Methods in Engineering (CILAMCE). Belém, PA.
- [16] Pais J.C., Amorim S.I.R., Minhoto M.J.C. (2013) Impact of traffic overload on road pavement performance. *Journal of Transportation Engineering*, 139 (9), 873–879. doi:10.1061/(ASCE)TE.1943-5436.0000571.
- [17] Rys D., Judycki J., Jaskula P. (2015) Analysis of effect of overloaded vehicles on fatigue life of flexible pavements based on weigh in motion (WIM) data. *International Journal of Pavement Engineering*. <https://doi:10.1080/10298436.2015.1019493>.
- [18] Rocha Segundo I.R., Castelo Branco V.T.F., Vasconcelos K.L., Holanda A.S. (2016) Misturas asfálticas recicladas a quente com incorporação de elevado percentual de fresado como alternativa para camada de módulo elevado. *Transportes*, v. 24, n. 4, p. 85-94.
- [19] Santiago L.S., Torquato e Silva S.A., Soares J.B. (2018) Determinação do dano em pavimentos asfálticos por meio da combinação do modelo S-VECD com análises elásticas. *Revista Transportes*. v. 26, n. 2, p. 31-43.
- [20] Santiago, L.S.; Babadopoulos, L. F. A. L; Soares J.B. (2019) Desenvolvimento de função de transferência para previsão de área trincada em pavimentos asfálticos por meio da

- simulação do dano por fadiga utilizando modelo S-VECD e análises elásticas. Revista Transportes. v. 28, n. 3, p. 121-136. <https://doi:10.14295/transportes.v28i3.1900..>
- [21] Santos A.B.V., Soares J.B., Babadopoulos L.F.A.L. (2020) Influência da temperatura e da velocidade de tráfego na previsão de área trincada de pavimentos asfálticos. Transportes 28 (4). <https://doi.org/10.14295/transportes.v28i4.2394>
- [22] Underwood B.S., Baek C., Kim Y.R. (2012) Simplified viscoelastic continuum damage model as platform for asphalt concrete fatigue analysis. Transportation Research Record 2296, 36–45.
- [23] Zhao Y., Tan Y., Zhou C. (2012) Determination of axle load spectra based on percentage of overloaded trucks for mechanistic-empirical pavement design. Journal of Road Materials and Pavement Design, 13 (4), 850–863. <https://doi:10.1080/14680629.2012.735796>.

## **5. EFEITO DA REOLOGIA E DA ADESIVIDADE DE LIGANTES ASFÁLTICOS EM DIFERENTES SUBSTRATOS NA RESISTÊNCIA AO CONDICIONAMENTO POR UMIDADE**

Submetido ao *The Journal of Adhesion*

### **Effects of rheology and adhesiveness of asphalt binders to different substrates on the resistance to moisture conditioning**

Jorge L.O. Lucas Júnior<sup>a\*</sup>, Lucas S.V. da Silva<sup>a</sup>, Wesley S. Rocha<sup>a</sup>,  
Lucas F.A.L. Babadopoulos<sup>b</sup>, Jorge B. Soares<sup>a</sup>

<sup>a</sup> Department of Transportation Engineering, Federal University of Ceará at Fortaleza, Brazil

<sup>b</sup> Department of Structural Engineering and Civil Construction, Federal University of Ceará at Fortaleza, Brazil

\* Corresponding author.

E-mail addresses: [j.lucas.j@det.ufc.br](mailto:j.lucas.j@det.ufc.br) (Jorge L.O. Lucas Júnior), [lucassvs2@gmail.com](mailto:lucassvs2@gmail.com) (Lucas S.V. da Silva), [wesley63@gmail.com](mailto:wesley63@gmail.com) (Wesley S. Rocha), [babadopoulos@ufc.br](mailto:babadopoulos@ufc.br) (Lucas F.A.L. Babadopoulos), [jsoares@det.ufc.br](mailto:jsoares@det.ufc.br) (Jorge B. Soares)

#### **ABSTRACT**

Adhesiveness is a property that directly affects the service life of asphalt pavements. Over the years, different materials, research methods and tests have been used to investigate different adhesiveness aspects of materials. This paper investigated two asphalt binders, one with and one without amine-based anti-stripping agent, as well as two aggregate sources, one phonolitic and another granitic. The objective was to investigate the effects of rheology and adhesiveness of asphalt binders to different substrates on the resistance to moisture conditioning. For this purpose, complex modulus and permanent deformation tests were performed on the binders in dry and moisture conditioning, adhesion was measured by the Asphalt Bond Strength (ABS) test, and the percentage of aggregate area of the substrate in contact with the binder-stub interface was obtained by digital image processing (DIP) prior to all ABS tests. Procedures were performed before and after moisture conditioning, which consisted of submerging the binders alone into 40°C water for 24h. The purposes of DIP analysis were to determine whether the aggregate area in contact with binder affects adhesion, and how these results can help understanding the phenomenon of aggregate-binder adhesiveness. The results indicated that the moisture conditioning reduced the average stiffness of the binders by about 15% for both binders. The addition of amine-based anti-stripping agent reduced the stiffness of the neat binder by approximately 9%, and at 82°C the neat binder presented higher rutting resistance if compared to the modified binder using anti-stripping agent. The aggregate area of the HMAs in contact with asphalt binder did not show a good correlation with the pull-off tensile strength in the dry condition, but it showed good correlations after moisture conditioning. This suggests that adhesion force itself may not be influenced by the proper contact between the aggregate and the binder, but this proper contact does prevent moisture damage in the interface.

**Keywords:** asphalt binders, adhesiveness, rheological properties, moisture damage, anti-stripping agent.

#### **5.1. Introduction**

Adhesiveness is a property that directly impacts the service life of asphalt pavements. In the literature, four theories describe aggregate-binder adhesiveness: (i) mechanical adhesion, (ii) molecular orientation, (iii) surface energy, and (iv) chemical reaction (Majidzadeh and Brovold, 1968; Terrel and Shute, 1989; Hicks, 1991).

High silica content ( $\text{SiO}_2$ ) on the aggregate's surface (Little and Jones IV, 2003) and the formation of the silanol ( $\text{SiOH}$ ) functional groups (Harnish, 2010) are pointed out as harmful to adhesiveness. Other authors observe that aggregates with higher content of iron oxide (Woodhams, 1998) and calcium oxide (McCann et al., 2005) are beneficial to aggregate-binder adhesiveness.

Several materials have been used to improve adhesion and to reduce the effects of moisture on pavements, such as nanosize hydrated lime (Diab et al., 2014), Portland cement (Pasandín and Pérez, 2015), styrene–butadiene–styrene and polyethylene polymers (Huang et al., 2016), zycosoil additive (Hamed and Tahami, 2017), polyphosphoric acid (Ghabchi et al., 2019), amine-based anti-stripping agent (Lucas Júnior et al., 2021) among others.

There are numerous tests used to assess aggregate-binder adhesiveness and the effects of moisture damage on asphalt pavements, such as the modified Lottman test (Kringos et al., 2009), the peel test (Cui et al., 2014), asphalt film coating dislocation (stripping) test (Lucas Júnior et al., 2019), surface free energy (SFE) test (Zhang and Luo, 2019), and the water boiling test (Caputo et al., 2020). Kanitpong and Bahia (2003) and Santagata et al. (2009) used the Pneumatic Adhesion Tensile Testing Instrument (PATTI) for the measurement of the pull-off tensile strength (adhesion) of the asphalt binder attached to an aggregate substrate. Bringel et al. (2011) evaluated the adhesiveness of conditioned and unconditioned specimens using a similar equipment and in 2013 the adhesion test was standardized by the AASHTO TP 91 (2013) as the Asphalt Bond Strength (ABS) test.

Many studies have used a mineral aggregate as a substrate to investigate the interaction with the asphalt binder by means of the ABS test (Yin et al., 2017; Ahmed et al., 2017; Lucas Júnior et al., 2019; Habal and Singh, 2019), but it has not yet been answered whether there is a possibility to use samples of compacted Hot Mix Asphalts (HMAs) as a substrate in place of the mineral aggregate. Another important unanswered question is whether the binder rheology can interfere with ABS results. There are a number of questions still open for research when it comes to aggregate-binder adhesiveness and how it relates to moisture resistance.

The objective of this paper was to investigate the effects of rheology and adhesiveness of asphalt binders to different substrates on the resistance to moisture conditioning. For this purpose, complex modulus and permanent deformation tests were performed on the binders in dry and moisture conditioning. Adhesion was measured by the ABS test, and the contact area of the asphalt binder with the aggregate part of the substrates' surface was obtained by digital image processing prior to all ABS tests. The purpose of DIP analysis was to determine whether

the aggregate area in contact with the binder affects adhesion, and how these results can help understanding the phenomenon of aggregate-binder adhesiveness.

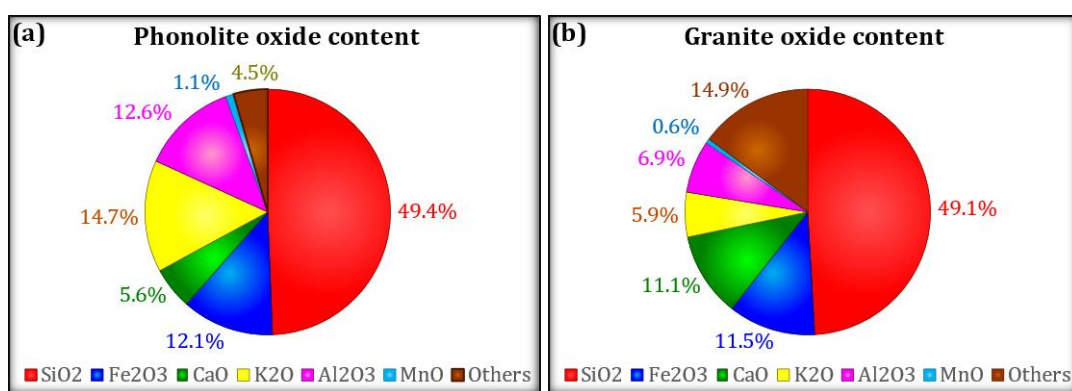
## 5.2. Experiments description

### 5.2.1. Materials

In this research, the investigated materials are a neat asphalt binder (noted N) classified by penetration as a 50/70, the same binder but modified by an amine-based anti-stripping agent (noted A), and two mineral aggregate sources (phonolite, noted Ph; and granite, noted G). The chemical composition of the mineral aggregate particles was determined using X-Ray Fluorescence. The contents of main oxides are shown in Figure 1(a) for the phonolitic aggregate and in Figure 1(b) for the granitic aggregate. It is observed that both aggregate sources have similar SiO<sub>2</sub> and Fe<sub>2</sub>O<sub>3</sub> contents, while the granitic source has more CaO. Literature suggests that this higher calcium oxide may help adhesiveness properties (Jamieson et al., 1995; Pasandín and Pérez, 2015). According to Lucas Júnior et al. (2019), who investigated the same aggregate sources, the granitic aggregate presents better adhesiveness because it has higher calcium oxide content than the phonolitic aggregate.

The modification procedure used to mix the binder with the anti-stripping agent was as follows: 0.2% w/w additive was added into a 500g sample of neat binder using a paddle agitator at 130°C, 1000rpm for 90min. In addition, both neat and modified binders were aged using the Rolling Thin Film Oven (RTFO) in accordance with ASTM D 2872 (2019).

Figure 1 – Oxide content measured by the X-Ray Fluorescence



Four HMAs materials were produced combining the phonolite (Ph) and granite (G) aggregates with the neat binder (N) and the binder modified by 0.2% amine-based antistripping agent (A). The produced materials were designated as follows: PhN (phonolitic aggregate particles + neat binder), PhA (phonolitic aggregate particles + neat binder + amine-based anti-

stripping agent), GN (granitic aggregate particles + neat binder), GA (granitic aggregate particles + neat binder + amine-based anti-stripping agent). After these four mixtures were compacted in a 10cm diameter and 15cm height cylindrical geometry with 5.0% binder content and 4% air voids, the resulting specimens were sawn down to approximately 5cm height.

Sawn specimens of the four mixtures, and not aggregate substrates, were used to measure the pull-off tensile strength of both asphalt binders, in accordance to the Asphalt Bond Strength test. Tests were performed in triplicate and all combinations (HMAs + asphalt binders) were covered, designated as follows:

- PhN HMA + Neat binder (PhN-1-N, PhN-2-N, PhN-3-N);
- PhA HMA + Neat binder (PhA-1-N, PhA-2-N, PhA-3-N);
- GN HMA + Neat binder (GN-1-N, GN-2-N, GN-3-N);
- GA HMA + Neat binder (GA-1-N, GA-2-N, GA-3-N);
- PhN HMA + Neat binder with anti-stripping agent (PhN-1-A, PhN-2-A, PhN-3-A);
- PhA HMA + Neat binder with anti-stripping agent (PhA-1-A, PhA-2-A, PhA-3-A);
- GN HMA + Neat binder with anti-stripping agent (GN-1-A, GN-2-A, GN-3-A);
- GA HMA + Neat binder with anti-stripping agent (GA-1-A, GA-2-A, GA-3-A).

In addition to check the HMA-binder adhesiveness, the investigated mineral aggregates were also used as substrate themselves, and the aggregate-binder combinations are designated as follows:

- Phonolite + Neat binder (Ph-N);
- Phonolite + Neat binder with anti-stripping agent (Ph-A);
- Granite + Neat binder (G-N);
- Granite + Neat binder with anti-stripping agent (G-A);

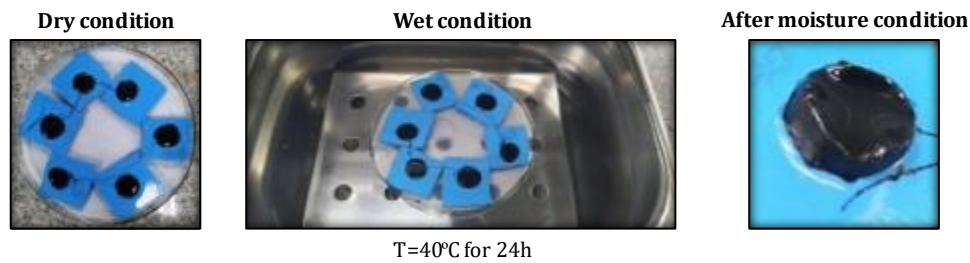
Furthermore, a moisture conditioning procedure was employed for all the tested material combinations. The utilized procedure is part of the full ABS test procedure presented in more details in Section 5.2.5.

### **5.2.2. Moisture conditioning procedure for the rheological tests**

After the post-RTFO aging procedure, performed to all samples, some binder samples were subjected to a moisture conditioning procedure for the investigation of the rheological properties and how they change upon the deleterious effect of water. At the end, asphalt binder specimens in the rheological tests are either dry or moisture conditioned. Moisture conditioning of the binders was performed according to the procedure in Figure 2. Six samples were

prepared, three neat and three modified binder samples. The conditioning method proposed is divided into five steps: (i) heating binders in an 150°C oven for 30min; (ii) pouring binder in silicone mold with 25mm-diameter and 5mm-depth arranged in a glass plate with paper on its bottom preventing adhesion; (iii) 30min air conditioning at room temperature; (iv) 24h water bath at 40°C; (v) removal from water bath and drying in lab conditions.

Figure 2 – Asphalt binder moisture conditioning procedure employed in this paper before rheological testing



### 5.2.3. Tests with the Dynamic Shear Rheometer

The Dynamic Shear Rheometer (DSR) was used to test some of the rheological properties of the asphalt binders. Two tests were performed: (i) Complex modulus ( $G^*$ ) tests obtained in Frequency Sweeps (FS), which is a stiffness test, and (ii) Multiple Stress Creep and Recovery (MSCR), which is a permanent deformation test.

From the  $G^*$  test, the dynamic modulus ( $|G^*|$ , which is the absolute value of the complex modulus) and the phase angle ( $\delta$ ) were obtained using FS (ASTM D 7175, 2015). FS was performed using parallel plates geometry in different sinusoidal frequencies of rotational loading (0.10, 0.16, 0.25, 0.40, 0.63, 1.0, 1.6, 2.5, 4.0, 6.3, 10.0, 15.9, 25.0, 40.0, 63.0 and 100Hz) and different temperatures (4, 10, 16, 22, 28, 34, 40, 46, 52, 58, 64, 70, 76 and 82°C). From 4 to 40°C, 8.0mm diameter and 2.0mm gap geometry was used, while from 46 to 82°C it was 25.0mm diameter and 1.0mm gap. The results presented are  $|G^*|$  and  $\delta$  master curves, after time-shifting isotherms by applying the time-temperature superposition principle commonly used to interpret rheological data for viscoelastic materials.

MSCR (ASTM D7405, 2020) was used to measure the permanent deformation of asphalt binders. Tests were performed at 52, 58, 64, 70, 76, 82 and 88°C with short-term aged binders (RTFO), and 25.0-mm diameter and 1.0-mm parallel plates geometry were used. Non-recoverable creep compliance ( $J_{nr}$ ) was used to investigate rutting for both 100 and 3200Pa max shear stress in each loading cycle on the specimens.  $J_{nr}$  is defined by Equation 1. The percentage differences between the non-recoverable creep compliances at the two stress levels

$(J_{nr,diff})$  was also determined, according to Equation 2. In Equation 3 it is presented the percentage of recovery.

$$J_{nr} = \frac{\varepsilon_{nr}}{\sigma} \quad (1)$$

$$J_{nr,diff} = \frac{J_{nr,3200} - J_{nr,100}}{J_{nr,100}} \cdot 100\% \quad (2)$$

$$R = \frac{\varepsilon_r}{\varepsilon_t} \cdot 100\% \quad (3)$$

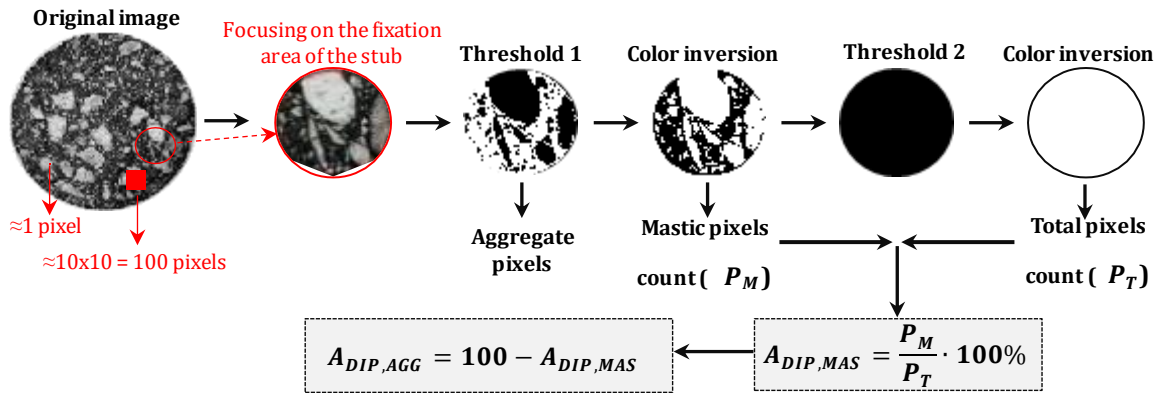
Where,  $\varepsilon_{nr}$  is the non-recoverable deformation after the rest period of 9s;  $\sigma$  is the maximum shear stress applied in a loading cycle following step loadings that last for 1s (Pa);  $J_{nr,diff}$  is the difference between the non-recoverable creep compliances at two different stress levels;  $J_{nr,3200}$  is the non-recoverable creep compliance at 3200Pa ( $\text{Pa}^{-1}$ );  $J_{nr,100}$  is the non-recoverable creep compliance at 100Pa ( $\text{Pa}^{-1}$ );  $R$  is percentage of recovery (%);  $\varepsilon_r$  is the recoverable deformation;  $\varepsilon_t$  is total deformation.

For the 3200Pa shear stress, 10 repetitions of loading and rest are applied, whereas for the 100Pa shear stress, 20 repetitions are applied. The last 10 repetitions of each stage are used for calculations.

#### 5.2.4. Digital image processing (DIP)

Prior to all ABS tests, a digital image processing (DIP) technique was performed. This was done before fixing the metal stubs on the aggregates or on HMAs using the asphalt binder as adhesive. DIP was used to determine the percentage area of mastic ( $A_{DIP,MAS}$ ) and aggregate ( $A_{DIP,AGG}$ ) in contact with the asphalt binder adhesive during the ABS test. Lucas Júnior and Soares (2019) developed the methodology used in this paper. After taking a photograph of the sawn substrate, it consists of the following steps: (i) gray scale transformation of image, (ii) threshold determination for mastic pixels, (iii) colors inversion of mastic's pixels, (iv) counting of mastic pixels ( $P_M$ ), (v) threshold determination for total pixels (mastic + aggregates), (vi) colors inversion of total pixels, (vii) counting of total pixels ( $P_T$ ), (viii) mastic and aggregates area percentages determination. Figure 3 presents an example of how the DIP procedure works. Each pixel of the processed images is approximately  $0.07\text{mm}^2$ . In Figure 3 shows an example of DIP focusing on the fixation area of the stub.

Figure 3 – Digital image processing (DIP) steps for determining mastic and aggregates area percentages on the ABS test substrates



### 5.2.5. Asphalt Bond Strength (ABS)

Two mineral aggregate types and four HMAs were used as substrates (cf. Section 5.2.1). All substrates are placed in an ultrasonic bath at 60°C for 1h and dried up after, before testing. For drying, the clean mineral aggregate substrates were heated for 30min at 150°C. To prevent the mixture from breaking up during drying, the HMAs were air dried at room temperature for 30min and then placed in an oven at 60°C for 60min. The post-RTFO aged asphalt binder specimen and metal stubs were taken to another oven at 150°C for 30min. The binder was then placed in a silicone mold for 30min in laboratory conditions. After this time, the stubs were fixed to the mineral and to the HMA substrates, using the asphalt binder as adhesive. The dry specimens were acclimated in laboratory conditions (25°C) for 24h before testing. Figure 4 shows the stubs fixed to the mineral aggregate substrates and the disposition of the tested combinations. Figure 5 presents the sample preparation and test procedure using HMA substrates.

Figure 4 – Stubs fixed on mineral aggregate substrates and representation of the different combinations of interfaces tested

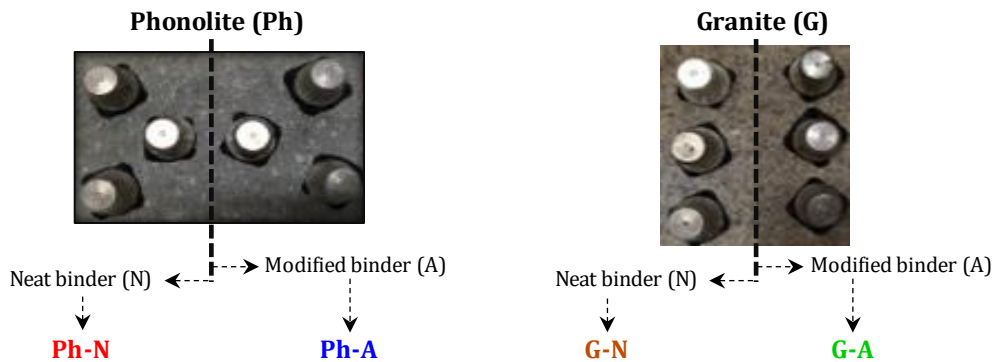
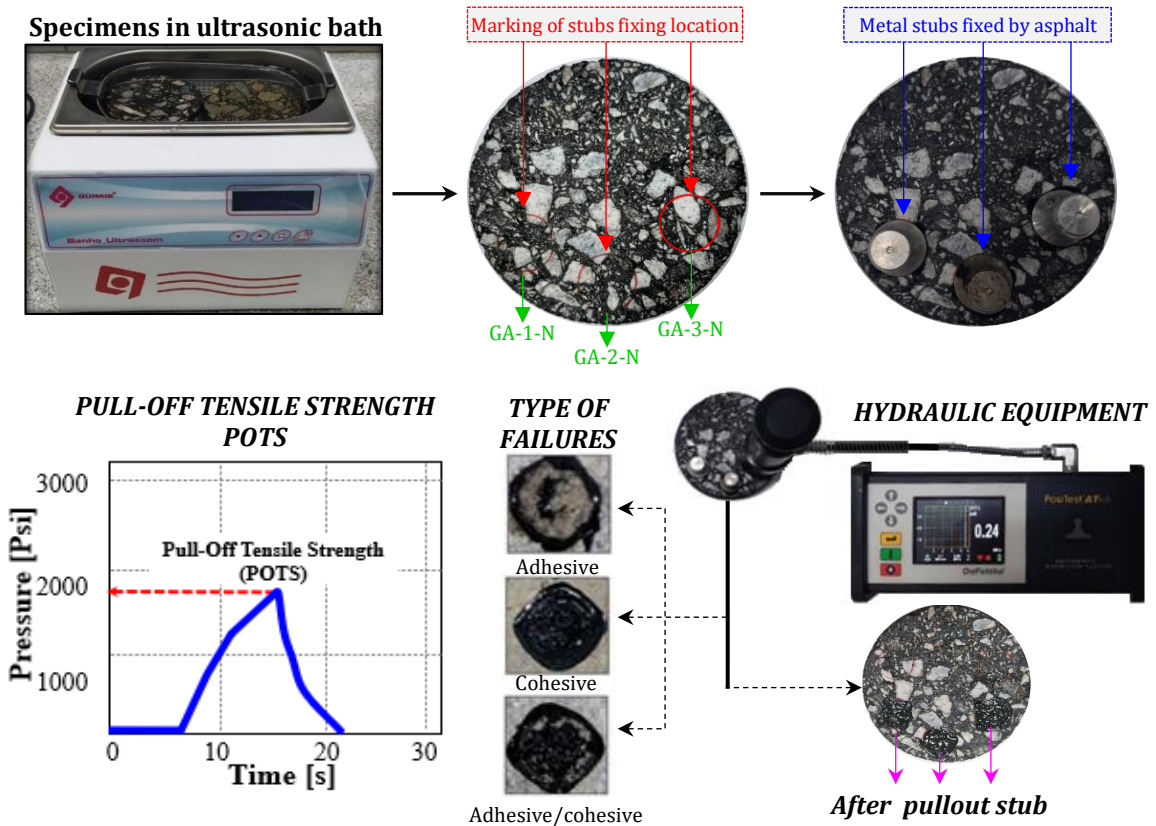


Figure 5 – Sample preparation and test procedure using HMAs substrates, and analysis of adhesive and cohesive failures during ABS tests



In order to assess moisture damage due to moisture conditioned, the specimens were acclimated in laboratory conditions ( $25^{\circ}\text{C}$ ) for 1h before moisture conditioning. The specimens were submerged in distilled water bath at  $40 \pm 2^{\circ}\text{C}$  for 20h. This temperature was chosen to be the same as for the asphalt binders conditioning in the rheology part of the investigation, while the time of conditioning was chosen as close as possible to the 24h used in the rheology part, but discounting the additional time needed for specimen cleaning and preparation. Subsequently, moisture conditioned specimens were acclimated in laboratory ( $25^{\circ}\text{C}$ ) for 1h before testing, in accordance to AASTHO TP91 (2013). The pull-off tensile strength ( $POTS$ ), which is the maximum applied pull-off tensile stress, is then determined. The ABS equipment used was a hydraulic pressure system that reports  $POTS$  automatically. To determine the effect of moisture on adhesiveness,  $R_{POTS}$  was determined, according to Equation 4.

$$R_{POTS} = \frac{POTS_{WET}}{POTS_{DRY}} \cdot 100\% \quad (4)$$

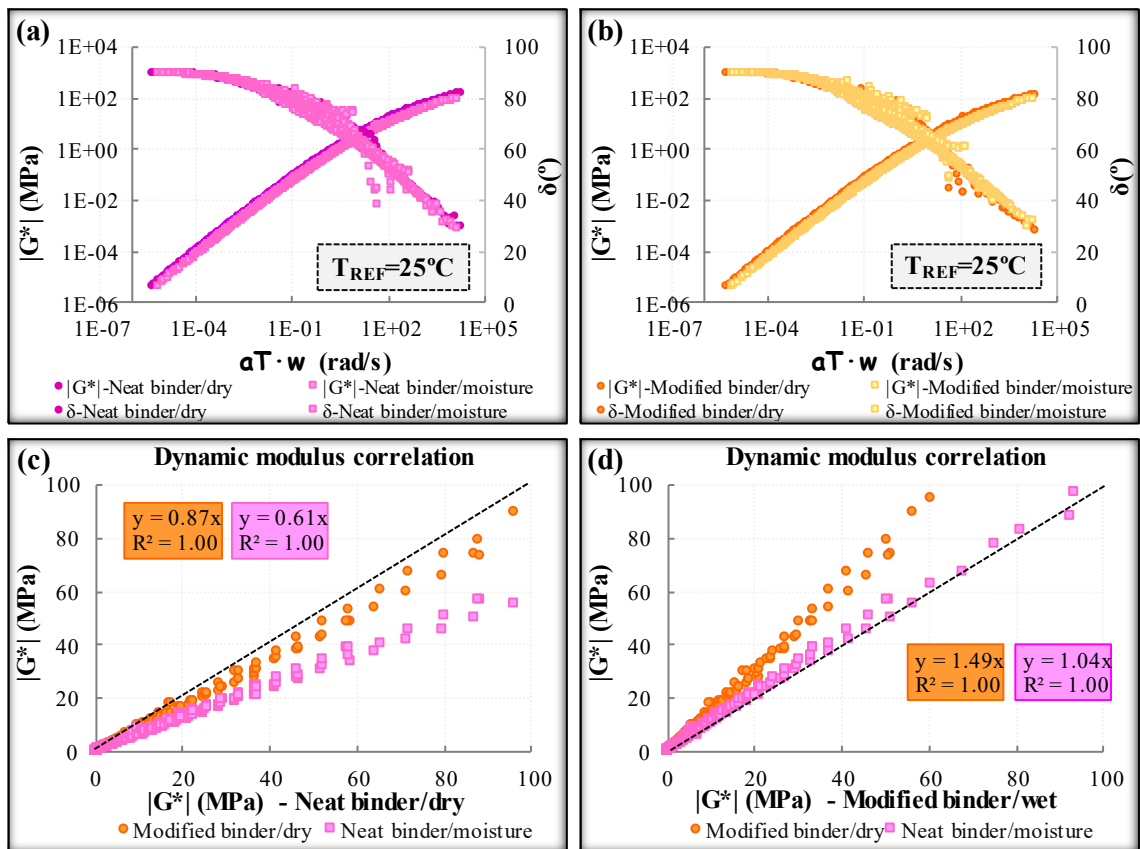
Where,  $R_{POTS}$  is the relation between  $POTS_{WET}$  and  $POTS_{DRY}$ ;  $POTS_{WET}$  is the pull-off tensile strength of the moisture conditioned specimens, and  $POTS_{DRY}$  is the pull-off tensile strength of the non-conditioned specimens, in MPa.

### 5.3. Results and discussion

#### 5.3.1. Linear viscoelastic characterization

Surprisingly, moisture conditioning affected the bulk stiffness of both asphalt binders in exactly the same way, i.e., a 15.2% reduction in the stiffness of both the neat and the modified binder using the amine-based anti-stripping agent (Figures 6(c) and 6(d)). When analyzing only the dry condition, the binder modification reduced the stiffness of the neat binder by 9.5%. When the moisture conditioning is analyzed, the modification resulted in an 8.7% decrease in stiffness when compared to the neat binder, cf. Figure 6(a). These results show that although the amine-based anti-stripping agent reduces binder stiffness, moisture similarly affected the stiffness of the two binders. Since the modulus is a bulk property of the binder, this suggests that the mechanism of preventing moisture damage of the anti-stripping agent is not on the bulk volume of the binder. The values of phase angle were not relevantly affected neither by binder modification nor by moisture conditioning, varying at most 0.3° on average, cf. Figure 6(b).

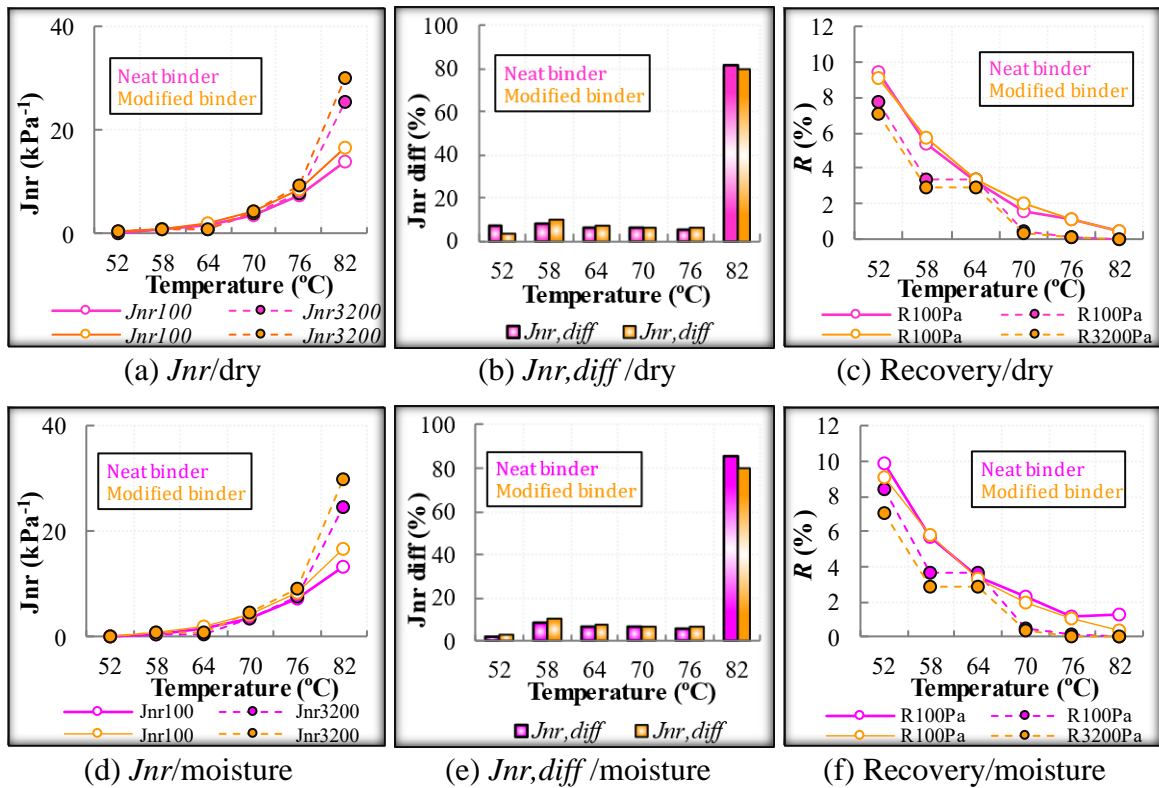
Figure 6 – Linear viscoelastic characterization results for the two tested asphalt binders at both conditions (before and after moisture conditioning): (a) Neat binder; (b) Modified binder; (c) Dynamic modulus correlation with neat binder in dry condition in x-axis and (d) Dynamic modulus correlation with modified binder in moisture conditioning in x-axis



### 5.3.2. Multiple Stress Creep Recovery (MSCR)

Figures 7(a), 7(b) and 7(c) present, in the dry condition, the  $J_{nr}$ ,  $J_{nr,diff}$  and  $R$  results, respectively, for both asphalt binders investigated. Smaller values of  $J_{nr}$  indicate smaller susceptibility to rutting after loading repetitions, while  $J_{nr,diff}$  values below 75% in high PG temperature should not present a high sensitivity to stress levels, and it is supposedly not very susceptible to the accumulation of permanent deformation (Bastos et al., 2017). Up to the temperature of 76°C, the  $J_{nr}$  results were similar, but at 82°C the neat binder presented higher rutting resistance if compared to the neat binder with anti-stripping agent (similar to that found by Zhu et al., 2018). Such small difference was only noticed at 82°C, for both 100 and 3200kPa. Both binders presented very close  $R$  values. The moisture conditioned specimens show similar behavior to dry specimens.

Figure 7 – Obtained MSCR parameters for both tested asphalt binders after RTFO



### 5.3.3. Digital Image Processing of HMA substrates

The 20mm diameter specimens were photographed before the stubs were fixed using the asphalt binder as adhesive. In Figure 8, the 24 specimens used for the dry condition testing are presented. They were divided into 2 groups of 12 specimens: (i) specimens with neat binder fixing the stubs; (ii) specimens with amine-based anti-stripping modified binder fixing the stubs. Within each group, the 4 different HMAs (PhN, PhA, GN, GA) are represented in

triplicates (12 specimens total). These images were processed in MatLab (using the described DIP procedure, cf. Section 5.2.4) and their  $A_{DIP,AGG}$  (percentage area of aggregate in HMA in contact with binder-stub) were obtained, as shown in Figure 8. It is noticed that there was a great variation in the  $A_{DIP,AGG}$  analyzed. The lowest value of  $A_{DIP,AGG}$  was 23% and the highest value was 86%, which enabled a good distribution of areas of contact amongst the tested specimens in dry condition. In Figure 9, one can see that the  $A_{DIP,AGG}$  were also well distributed, with the lowest value of 19% and the highest value of 77% for the tested specimens in moisture conditioning. This large amplitude is important to allow the analysis of changes in adhesion due to the variation of the aggregate area in contact with binder. These results are correlated with POTS in Section 5.3.5.

Figure 8 – Photograph of the HMAs used in dry condition, zoomed on the contact area with the stub, before ABS test and their corresponding DIP images

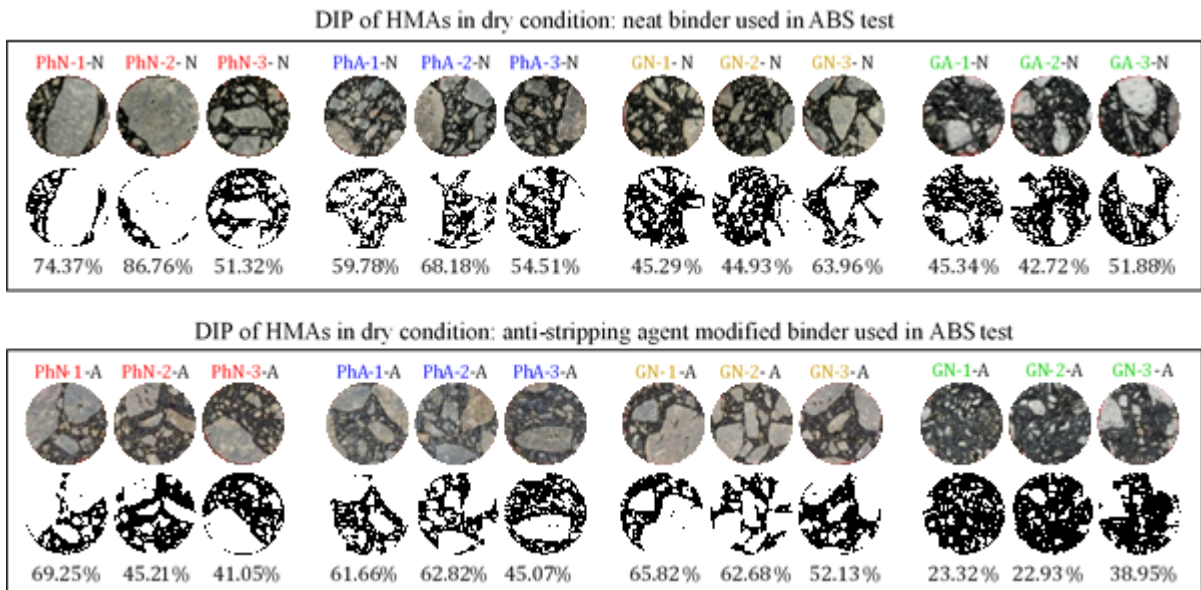
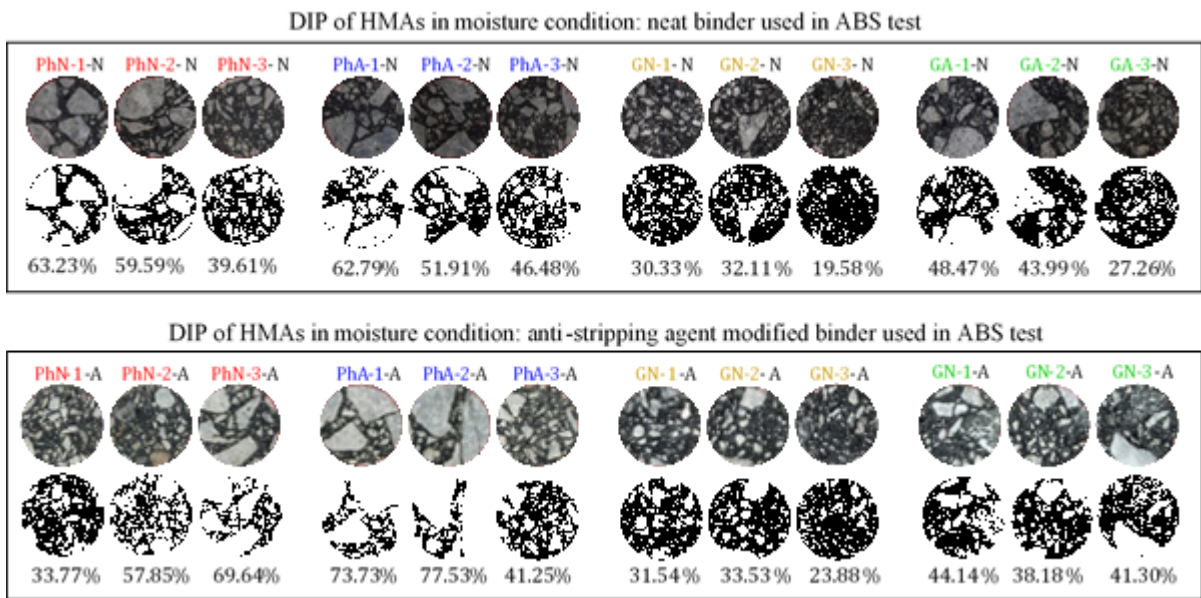


Figure 9 – Photograph of the HMAs used after moisture conditionning, zoomed on the contact area with the stub, before ABS test and their corresponding DIP images



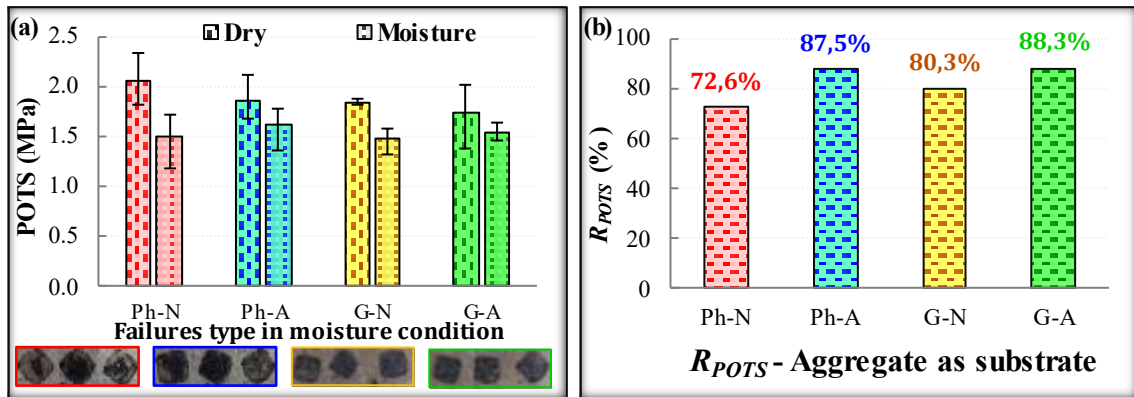
### 5.3.4. Asphalt Bond Strength (ABS) test

#### 5.3.4.1. Mineral Aggregate used as Substrate

Figure 10(a) presents the *POTS* value of the mineral aggregate used as substrate in both dry and moisture conditions. The neat binder had higher *POTS* values when compared to the modified binder, with a difference of 11% for the phonolitic aggregate (Ph-N vs. Ph-A) and 6% for the granitic aggregate (G-N vs. G-A). The phonolitic aggregate also had *POTS* values 11% higher than the granitic aggregate when comparing neat binder (Ph-N vs. G-N), and 6% higher when comparing modified binder (Ph-A vs. G-A). In moisture conditioning (Figure 10(a)) the modified binder presents higher *POTS* values than the neat binder, with 8 and 3% differences for the comparison between Ph-A and Ph-N, and between G-A and G-N, respectively.

The ranking of moisture influence on the mineral aggregates as indicated by *R<sub>POTS</sub>* values was: G-A, Ph-A, G-N, and Ph-N, cf. Figure 10(b). These results show that the modified binder had higher *R<sub>POTS</sub>* in comparison to the neat binder in 15% for the phonolitic aggregate and in 8% for the granitic aggregate. In the comparison between the aggregate sources, as they adhere the neat binder, granite had a 7% higher *R<sub>POTS</sub>*, whereas for modified binder the values were close (0.8%). In general, the granitic aggregate showed better aggregate-binder adhesiveness than the phonolitic aggregate and this may be related to its higher calcium oxide content.

Figure 10 –  $POTS$  and  $R_{POTS}$  results of the aggregate mineral substrates

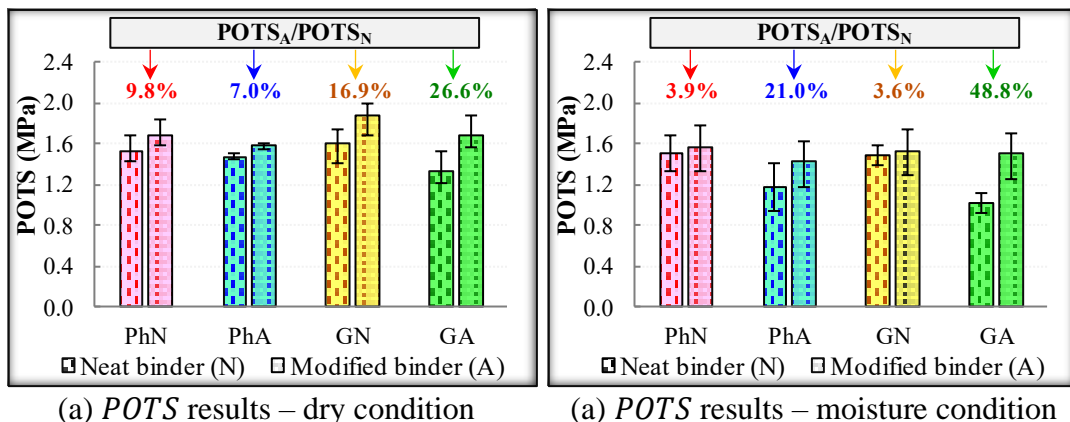


#### 5.3.4.2. HMAs used as Substrate

Figure 11(a) presents the  $POTS$  in dry condition of the 4 HMAs analyzed. For the neat binder the highest value found was 1.8MPa and the lowest value was 1.2MPa. For the binder modified by anti-stripping agent the highest value was 2.0MPa and the lowest 1.5MPa. These are 32 and 29% differences, respectively, which demonstrates that different chemical compositions of the contacts, particularly the substrates (aggregate + asphalt binder) of the four mixtures were efficient to capture differences in  $POTS$  measurement on the ABS test.

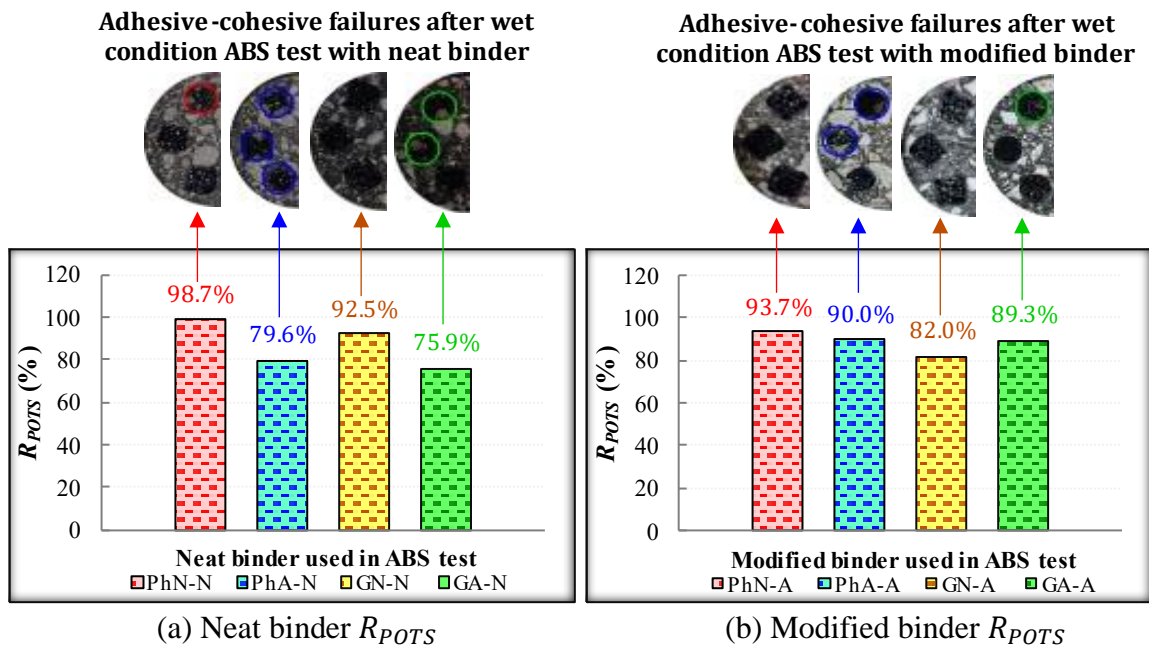
On average, HMAs with phonolitic aggregate showed  $POTS$  values 8.4% higher for the modified binder compared to the neat binder, whereas for HMAs with granitic aggregate, this difference was 21.7%, cf. Figure 11(a). This result is surprising because the neat binder had 20.7% higher average stiffness than the modified binder (cf. Figure 6), which would lead one to imagine that a greater load would be necessary to break the bond between the surfaces, since all failures were cohesive. On the other hand, a plausible explanation for these results is the better adhesion of the modified binder to the mineral aggregates, showing that the test was efficient to capture the adhesion phenomenon even in dry condition.

Figure 11 –  $POTS$  results in dry condition and after moisture conditioning



Analyzing the  $R_{POTS}$  results of the neat binder used as adhesive to fix the stubs (cf. Figure 12(a)), it is possible to notice that the highest values of  $R_{POTS}$  were obtained for mixtures compacted with phonolitic aggregate and neat binder, and with granitic aggregate and neat binder. On the other hand, for the  $R_{POTS}$  of the modified binder used as adhesive to fix the stubs (cf. Figure 12(b)), it is noted that the highest values of  $R_{POTS}$  were for mixtures with phonolitic aggregate and modified binder, and with granitic aggregate and modified binder. These results show that the  $R_{POTS}$  values are higher when the binder used in the ABS test was similar to that used in the HMAs. It is possible that the chemical characteristics of the mastic with a neat binder have greater adhesion with another neat binder and in the same way, a mixture with modified binder has better adhesion with the binder with the same modifier. It is also possible that the modifier, which should help reducing the effect of moisture, is preventing small interactions and mixture in an interphase between the mastic and the binder used as adhesive to fix the stub, reducing the anchoring in this part of the contact.

Figure 12 –  $R_{POTS}$  results and number of adhesive failures in moisture conditioning



### 5.3.5. Correlation Between POTS and $A_{DIP,AGG}$ in dry and moisture conditions

In Figure 13, it is noted that for most combinations there was no good correlation between the results of  $POTS$  in dry condition and the aggregate area ( $A_{DIP,AGG}$ ) in contact with the neat binder (cf. Figure 13(a)) and with the modified binder (cf. Figure 13(b)). When the test is performed under moisture conditioning, there is a strong correlation ( $POTS$  vs.  $A_{DIP,AGG}$ ). When the neat binder (Figure 14(a)) was in contact with larger areas of aggregate on the HMA

surface, the *POTS* values were higher. When the modified binder (Figure 14(b)) was in contact with larger areas of aggregate on the HMA surface, the *POTS* values were lower. These results lead one to imagine that due to the mastic having greater porosity than the sawn aggregate of the HMA, when moisture comes in contact with the mastic-binder interface, there is a greater tendency for the binder to detach compared to the aggregate-binder interface. The modified binder had the opposite result, i.e., it appears that the additive has a greater chemical compatibility with the mastic than with the aggregate.

Figure 13 – Correlations between *POTS* in dry condition and  $A_{DIP,AGG}$

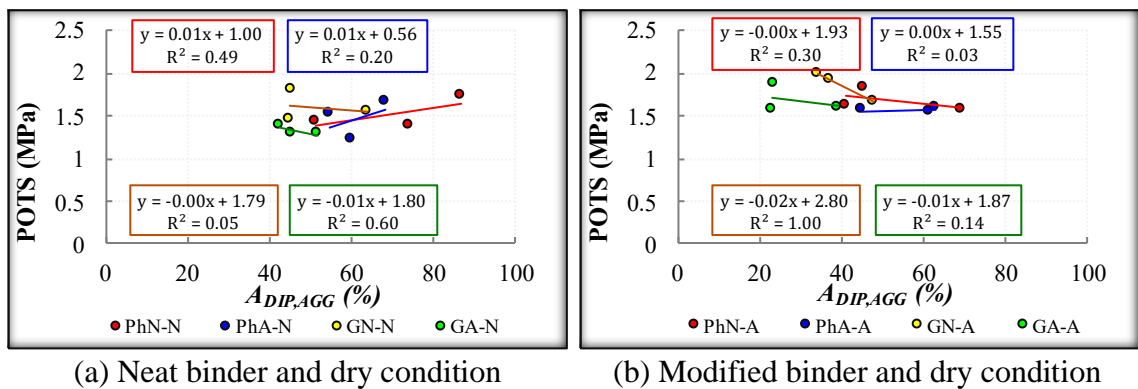
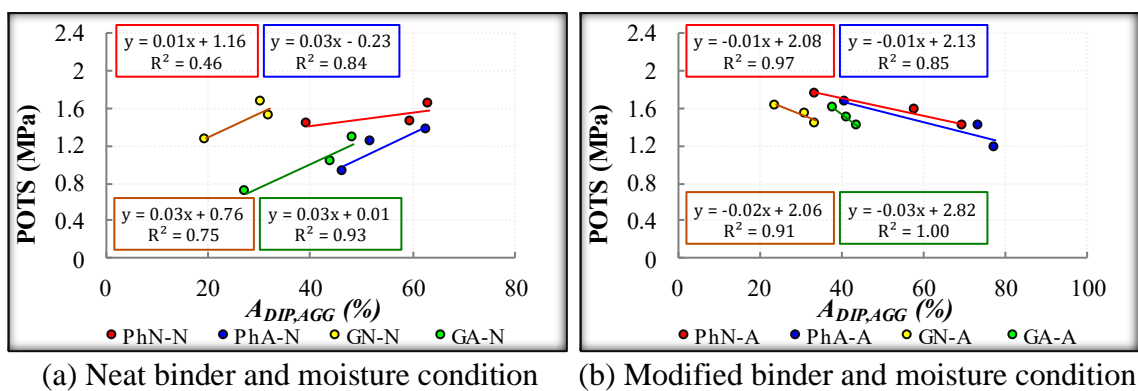


Figure 14 – Correlations between *POTS* in moisture conditioning and  $A_{DIP,AGG}$



#### 5.4. Conclusions

This paper evaluated the effects of asphalt binder's rheological properties and adhesiveness to both hot mix asphalt (HMA) and to mineral aggregate substrates on the resistance to moisture conditioning. Based on the materials and methodology used, the following conclusions were formulated:

- Moisture conditioning reduced the average stiffness by 15.2% for both neat and modified binders. Since the modulus is a bulk property of the binder, this suggests that the

mechanism of preventing moisture damage of the anti-stripping agent is not on the bulk volume of the binder;

- The addition of amine-based anti-stripping agent reduced the stiffness of the neat binder by 9.5% on dry condition and 8.7% on moisture condition;
- Up to the temperature of 76°C, the *Jnr* results were similar, but at 82°C the neat binder presented higher rutting resistance if compared to the binder with anti-stripping agent;
- The aggregate area of the HMAs in contact with asphalt binder did not show a good correlation (6 out of 8 sets of materials with  $R^2$  under 0.50) with the pull-off tensile strength in the dry condition, but it showed good correlations (7 out of 8 sets of materials with  $R^2$  above 0.75) on moisture conditioning. This suggests that adhesion force itself may not be influenced by the proper contact between the aggregate and the binder, but this proper contact does prevent moisture damage in the interface;
- When the neat binder was in contact with larger areas of aggregate of the HMA surface, the POTS values were higher, while when the modified binder was in contact with larger areas of aggregate on the HMA surface, the POTS values were lower. This suggests either one of the two things: (i) the additive has a greater chemical compatibility with the mastic than with the aggregate, or (ii) the modifier, which should help reducing the effect of moisture, is preventing small interactions and mixture in an interphase between the mastic and the binder used as adhesive to fix the stub, reducing the anchoring in this part of the contact.

## REFERENCES

- [1] AASHTO TP 91 (2013) American Association of State and Highway Transportation Officials. Determining Asphalt Binder Bond Strength by Means of the Asphalt Bond Strength (ABS) Test.
- [2] Ahmed T.A, Lee H., Williams R.C. (2017) Using a modified asphalt bond strength test to investigate the properties of asphalt binders with poly ethylene wax-based warm mix asphalt additive. International Journal of Pavement Research and Technology, (), S1996681417300858. <https://doi:10.1016/j.ijprt.2017.08.004>.
- [3] ASTM D7175-15 (2015) Standard Test Method for Determining the Rheological Properties of Asphalt Binder Using a Dynamic Shear Rheometer, ASTM International, West Conshohocken, PA. <https://doi:10.1520/D7175-15>.
- [4] ASTM D2872-19 (2019) Standard Test Method for Effect of Heat and Air on a Moving Film of Asphalt (Rolling Thin-Film Oven Test), ASTM International, West Conshohocken, PA. <https://doi:10.1520/D2872-19>.

- [5] ASTM D7405-20 (2020) Standard Test Method for Multiple Stress Creep and Recovery (MSCR) of Asphalt Binder Using a Dynamic Shear Rheometer, ASTM International, West Conshohocken, PA. <https://doi:10.1520/D7405-20>.
- [6] Bastos J.B.S., Babadopoulos L.F.A.L., Soares J.B. (2017) Relationship between multiple stress creep recovery (MSCR) binder test results and asphalt concrete rutting resistance in Brazilian roadways. *Construction and Building Materials* 145, 20–27. <https://doi:10.1016/j.conbuildmat.2017.03.216>.
- [7] Bringel R.M., Velasquez R., Bahia H.U. (2011) Measuring the Effect of Moisture on Asphalt–Aggregate Bond with the Bitumen Bond Strength Test. *Transportation Research Record: Journal of the Transportation Research Board*, n. 2209, p. 70-81.
- [8] Caputo P., Miriello D., Bloise A., Baldino N., Milet O., Ranieri G.A. (2020) A comparison and correlation between bitumen adhesion evaluation test methods, boiling and contact angle tests. *International Journal of Adhesion and Adhesives*, 102(), 102680. <https://doi:10.1016/j.ijadhadh.2020.102680>.
- [9] Cui S., Blackman B.R.K., Kinloch A.J., Taylor A.C. (2014) Durability of asphalt mixtures: Effect of aggregate type and adhesion promoters. *International Journal of Adhesion and Adhesives*, 54(), 100–111. <https://doi:10.1016/j.ijadhadh.2014.05.009>.
- [10] Diab A., You Z., Hossain Z., Zaman M. (2014) Moisture Susceptibility Evaluation of Nanosize Hydrated Lime-Modified Asphalt-Aggregate Systems Based on Surface Free Energy Concept. *Transportation Research Record: Journal of the Transportation Research Board*, 2446(), 52–59. <https://doi:10.3141/2446-06>.
- [11] Ghabchi R., Rani S., Zaman M., Ali S.A. (2019) Effect of WMA additive on properties of PPA-modified asphalt binders containing anti-stripping agent. *International Journal of Pavement Engineering*, (), 1–14. <https://doi:10.1080/10298436.2019.1614584>.
- [12] Habal A., Singh D. (2019) Effects of warm mix asphalt additives on bonding potential and failure pattern of asphalt-aggregate systems using strength and energy parameters. *International Journal of Pavement Engineering*, (), 1–13. <https://doi:10.1080/10298436.2019.1623399>.
- [13] Hamedi G.H., Tahami S.A. (2017) The effect of using anti-stripping additives on moisture damage of hot mix asphalt. *International Journal of Adhesion and Adhesives*, S014374961730067. <https://doi:10.1016/j.ijadhadh.2017.03.016>.
- [14] Harnish I.C. (2010) Liquid Anti-Strip Technology & Best Practices. Technical Manager-Aphalt Additives. ArrMaz Custom Chemicals, Overland Park, USA.
- [15] Hicks R.G. (1991) Moisture damage in asphalt concrete. National Cooperative Highway Research Program. *Synthesis of Highway Practice 175*, Transportation Research Board, Washington.
- [16] Huang W., Lv Q., Xiao F. (2016) Investigation of using binder bond strength test to evaluate adhesion and self-healing properties of modified asphalt binders. *Construction and Building Materials*, 113(), 49–56. <https://doi:10.1016/j.conbuildmat.2016.03.047>.
- [17] Jamieson I.L., Moulthrop J.S., Jones D.R. (1995) SHRP Results on Binder-Aggregate Adhesion and Resistance to Stripping. *Asphalt Yearbook 1995*, Institute of Asphalt Technology, United Kingdom.
- [18] Kanitpong K., Bahia H. (2003) Role of Adhesion and Thin Film Tackiness of Asphalt Binders in Moisture Damage of HMA. *Proceedings of the Association of Asphalt Paving Technologists*, v. 72.
- [19] Krings N., Azari H., Scarpas A. (2009) Identification of Parameters Related to Moisture Conditioning That Cause Variability in Modified Lottman Test. *Transportation Research Record: Journal of the Transportation Research Board*, 2127(), 1-11. <https://doi:10.3141/2127-01>,

- [20] Little D.N., Jones IV D.R. (2003) Chemical and Mechanical Processes of Moisture Damage in Hot-Mix Asphalt Pavements. *Moisture Sensitivity of Asphalt Pavements – A National Seminar; Transportation Research Board.*
- [21] Lucas Júnior J.L.O., Babadopoulos L.F.A.L., Soares J.B. (2019) Aggregate-Binder Adhesiveness Assessment and Investigation of the Influence of Morphological and Physico-Chemical Properties of Mineral Aggregates. *Road Materials and Pavement Design* 20 (March 2019): 1–12. <https://doi.org/10.1080/14680629.2019.1588773>.
- [22] Lucas Júnior J.L.O., Babadopoulos L.F.A.L., Soares J.B., Souza L.T. (2021) Evaluating the effect of amine-based anti-stripping agent on the fatigue life of asphalt pavements. *International Journal of Pavement Engineering.* <https://doi.org/10.1080/10298436.2020.1870687>
- [23] Lucas Júnior J.L.O., Soares J.B. (2019) Desenvolvimento de metodologia para avaliação da adesividade agregado-ligante com o uso de processamento digital de imagem. *Transportes.* <https://doi.org/10.14295/transportes.v27i1.1552> (*in Portuguese*).
- [24] Majidzadeh K., Brovold F.N. (1968) State of the art: Effect of water on bitumen aggregate mixtures. *Highway Research Board, Special Report n. 98*, p. 77.
- [25] McCann M., Anderson-Sprecher R., Thomas K.P. (2005) Statistical comparison between SHRP aggregate physical and chemical properties and the moisture sensitivity of aggregate-binder mixtures. *Road Materials and Pavement Design*, 6(2), 197–215
- [26] Pasandín A.R., Pérez I. (2015) The influence of the mineral filler on the adhesion between aggregates and bitumen. *International Journal of Adhesion and Adhesives*, 58(), 53–58. <https://doi:10.1016/j.ijadhadh.2015.01.005>.
- [27] Santagata F.A.; Cardone F., Canestrari F., Bahia H.U. (2009) Modified PATTI test for the characterization of adhesion and cohesion properties of asphalt binders. *Proceedings of the Sixth International Conference on Maintenance and Rehabilitation of Pavements and Technological Control*, v. 1, p. 124-133.
- [28] Woodhams R.T. (1998) Ferric Oxide Adhesion Promoters for Water Resistant Asphalt Pavements. *The Journal of Adhesion*, 68(1-2), 65–91. <https://doi:10.1080/00218469808029580>.
- [29] Yin Y., Huaxin C., Dongliang K., Lifang S., Lu W. (2017) Effect of chemical composition of aggregate on interfacial adhesion property between aggregate and asphalt. *Construction and Building Materials*, 146, 231–237.
- [30] Zhang D., Luo R. (2019) Using the surface free energy (SFE) method to investigate the effects of additives on moisture susceptibility of asphalt mixtures. *International Journal of Adhesion and Adhesives*, 95, 102437. <https://doi:10.1016/j.ijadhadh.2019.102437>
- [31] Zhu C., Xu G., Zhang H., Xiao F., Amirkhanian S., Wu C. (2018) Influence of different anti-stripping agents on the rheological properties of asphalt binder at high temperature. *Construction and Building Materials*, 164(), 317–325. <https://doi:10.1016/j.conbuildmat.2017.12.236>.

## **6. CONCLUSÕES E RECOMENDAÇÕES PARA TRABALHOS FUTUROS**

### **6.1. Considerações Iniciais**

O objetivo geral desta tese de doutorado foi determinar os efeitos e as inter-relações da adesividade agregado-ligante nas misturas asfálticas utilizando diferentes técnicas experimentais e o impacto desta adesividade na previsão de desempenho dos pavimentos por meio de métodos mecanístico-empíricos. Foram usados 2 ligantes asfálticos e 2 agregados com os quais foram produzidas 4 misturas asfálticas. Quatro escalas foram analisadas: ligante e agregado separados, adesividade agregado-ligante, mistura asfáltica e estrutura do pavimento. Foram usados além dos ensaios básicos: 1 método de avaliação das propriedades morfológicas dos agregados, 1 método inovador de avaliação de propriedades de misturas baseado em PDI, 2 tipos de ensaios em ligantes asfálticos, 3 diferentes ensaios de adesividade agregado-ligante, 4 diferentes ensaios em misturas asfálticas, e 2 programas computacionais de análise e dimensionamento de pavimentos asfálticos.

A tese foi apresentada na forma de artigos já publicados ou submetidos a periódicos. O artigo 1 aborda os efeitos das propriedades de forma dos agregados e da adesividade do ligante ao agregado nos resultados de ensaios em misturas asfálticas a quente. O artigo 2 avalia o efeito do melhorador de adesividade na vida de fadiga de pavimentos. O artigo 3 se destina a determinar o efeito da temperatura, da espessura, da carga e respectiva velocidade na previsão de área trincada de pavimentos. O artigo 4 trata do efeito da reologia e da adesividade de ligantes a diferentes substratos na resistência ao condicionamento por umidade.

### **6.2. Principais Contribuições da Tese**

À luz dos materiais investigados e das técnicas empregadas as principais contribuições da tese foram mostrar que a adesividade agregado-ligante impacta consideravelmente o comportamento mecânico das misturas asfálticas, e como isso se dá em função de cada parâmetro analisado em cada procedimento de análise. Misturas com melhor adesividade mostraram melhor comportamento à fadiga, e essa melhora também foi transmitida para a previsão de vida de fadiga dos pavimentos asfálticos, quando analisada a estrutura do pavimento como um todo. A seleção dos agregados e ligantes deve levar em conta as características da região, sendo variáveis importantes a se considerar a espessura do revestimento, a temperatura da região, a carga e a velocidade dos veículos que irão trafegar no pavimento. Ao se utilizarem duas camadas asfálticas, deve-se analisar com cautela a disposição de cada camada, não levando em conta apenas a menor danificação do pavimento. O ideal é que na fase de projeto já seja

prevista as manutenções preventivas e corretivas de forma que se possa decidir qual mistura deve ser aplicada na camada superior e qual mistura deve ser aplicada na camada inferior.

### **6.3. Principais Conclusões Oriundas do Programa Experimental**

#### ***6.3.1. Quanto às análises realizadas no artigo 1***

As propriedades de forma dos agregados foram importantes para os resultados de ensaios à compressão (módulo dinâmico, resistência à tração por compressão diametral e uniaxial de carga repetida), enquanto o ligante asfáltico com melhor adesividade aos agregados minerais influenciou mais fortemente os resultados do ensaio de vida de fadiga à tração/compressão de misturas asfálticas.

Agregados mais esféricos e rugosos melhoraram o intertravamento das misturas analisadas, enquanto que misturas com agregados mais lamelares e mais polidos tiveram menores diferenças entre os resultados dos ensaios de módulo dinâmico à compressão em comparação ao módulo dinâmico à tração/compressão, devido à melhor adesividade agregado-ligante.

#### ***6.3.2. Quanto às análises realizadas no artigo 2***

Misturas asfálticas contendo aditivo melhorador de adesividade à base de amina apresentaram menor dano por fadiga previsto em estruturas de pavimentos quando comparadas a misturas com CAP 50/70 puro, conforme análise pelo FlexPAVE.

Todas as estruturas analisadas mostraram trincas de baixo para cima (*bottom-up cracking*) no revestimento asfáltico. Do ponto de vista da modelagem de dano por fadiga, a investigação das diferentes combinações de misturas mostrou que é mais recomendado o uso de misturas com melhorador de adesividade à base de amina nas camadas superiores e misturas com ligante puro na parte inferior. No caso em questão essa análise foi realizada sem o condicionamento à umidade. Todavia, devido às manutenções preventivas e corretivas que serão realizadas ao longo da vida útil do pavimento a disposição das camadas deve ser analisada com cautela. Ressalta-se que as misturas com ligante puro não poderiam ser utilizadas devido a não atingirem requisitos mínimos de aceitação dos órgãos rodoviários nacionais, pois apresentaram adesividade insatisfatória e dano por umidade induzida menor que 70% .

### ***6.3.3. Quanto às análises realizadas no artigo 3***

Os pavimentos com aditivo melhorador de adesividade à base de amina apresentaram menores valores de área de trincada quando comparadas aos pavimentos com CAP 50/70 puro. Assim como os pavimentos revestidos com misturas com agregado granítico apresentaram menores valores de área trincada quando comparados aos pavimentos revestidos com misturas com agregado fonolítico.

A maioria dos pavimentos asfálticos analisados no CAP3D-D tiveram maiores valores de área trincada devido à variação de espessura do revestimento asfáltico e de temperatura quando comparados com as variações relacionadas à velocidade dos veículos e a sobrecarga, em termos de variação unitária. Para as misturas analisadas, cada variação de  $\pm 1\text{ cm}$  de espessura do revestimento produziu efeito semelhante na área trincada que, aproximadamente, as variações de  $\pm 1,1^\circ\text{C}$ ,  $\pm 5,6\text{km/h}$  ou  $\pm 16,6\text{kN}$  de carga por roda de eixo simples. Esses resultados sugerem a ordem de grandeza dos custos com sobrecargas e sublinha as importâncias dos efeitos das velocidades de tráfego e da temperatura do pavimento no seu desempenho. Para cada mistura em cada pavimento, a relação dos efeitos das diferentes variáveis pode mudar, modificando a ordem de prioridade das principais variáveis a serem consideradas. Ainda assim, os resultados deste trabalho, que fixou a estrutura das subcamadas, apontam para uma relevância conjunta dos efeitos da carga, da temperatura, da velocidade dos veículos e da espessura do revestimento.

### ***6.3.4. Quanto às análises realizadas no artigo 4***

Apesar de o aditivo melhorador de adesividade ter melhorado as propriedades adesivas do ligante asfáltico ao agregado ele ocasionou uma redução média de 9,5% na rigidez do ligante na condição seca e 8,7% após condicionamento à umidade e uma menor resistência à deformação permanente a  $82^\circ\text{C}$ .

A área de agregado dos substratos em contato com o ligante de asfalto não mostrou uma boa correlação (6 de 8 conjuntos de materiais com  $R^2$  abaixo de 0,50) com a *POTS* na condição seca, mas mostrou boas correlações (7 de 8 conjuntos de materiais com  $R^2$  acima de 0,75) no condicionamento de umidade. Isso sugere que a força de adesão em si pode não ser influenciada pelo contato adequado entre o agregado e o ligante, mas esse contato adequado pode evitar danos por umidade na interface.

#### 6.4. Recomendações para Trabalhos Futuros

- Utilizar a microscopia eletrônica de varredura de campo amplo para entender como os componentes químicos dos agregados minerais e da interface agregado-ligante e a espessura do filme asfáltico de diferentes combinações de agregados e ligantes afetam o comportamento das misturas asfálticas.
- Desenvolver um ensaio de adesividade com uma película fina, confinada entre os agregados e que seja capaz de reproduzir o fenômeno da adesividade.
- Investigar o efeito do condicionamento à umidade de misturas asfálticas na rigidez, na deformação permanente e no trincamento por fadiga.
- Usar resultados laboratoriais de amostras de misturas asfálticas condicionadas à umidade para calibrar e validar as funções de transferência campo-laboratório com o intuito de melhorar a previsão de desempenho dos pavimentos.
- Identificar o efeito da viscoelasticidade do ligante no ensaio *Asphalt Bond Strength* (ABS) modificando sua execução e tratamento dos dados para captar as diferenças de adesividade em diferentes temperaturas e frequência de carregamento.
- Desenvolver ferramentas computacionais capazes de considerar misturas asfálticas como um compósito, com constituintes interligados por meio de elementos de interface, visando simulações de ensaios em misturas de modo a investigar diferentes aspectos apontados como relevantes para a adesividade agregado-ligante.
- Desenvolver algoritmos baseados em aprendizado de máquina (*machine learning*) para a geração de amostras virtuais e elementos de volume representativo (EVR) 3D a partir de imagens de corpos de prova, de modo a considerar um grande número de possibilidades de interface agregado-ligante.

## REFERÊNCIAS BIBLIOGRÁFICAS

- AASHTO T 350-14 (2018) American Association of State Highway and Transportation Officials. Multiple stress creep recovery (MSCR) test of asphalt binder using a dynamic shear rheometer (DSR). Standard Method of Test, Washington.
- AASHTO T 283 (2014) American Association of State and Highway Transportation Officials - Standard Method of Test for Resistance of Compacted Asphalt Mixtures to Moisture Induced Damage.
- AASHTO T 342 (2011) Standard Method of test for Determining Dynamic Modulus of Hot-Mix Asphalt Concrete Mixtures, American Association of State Highway and Transportation Officials, Washington, DC.
- AASHTO TP 101-14 (2014) American Association of State Highway and Transportation Officials. Estimating damage tolerance of asphalt binders using the linear amplitude sweep . Standard Method of Test, Washington.
- AASHTO TP 107-18 (2018) Standard Method of Test for Determining the Damage Characteristic Curve of Asphalt Mixtures from Direct Tension Cyclic Fatigue Tests, American Association of State Highway and Transportation Officials, Washington, DC.
- AASHTO TP 91 (2013) American Association of State and Highway Transportation Officials. Determining Asphalt Binder Bond Strength by Means of the Asphalt Bond Strength (ABS) Test.
- ABNT NBR 12583 (2017) Agregado Graúdo - Determinação da adesividade ao ligante betuminoso. Associação Brasileira de Normas Técnicas.
- ABNT NBR 15617 (2015) Misturas Asfálticas – Determinação do dano por Umidade Induzida, Associação Brasileira de Normas Técnicas.
- Aguiar-Moya J.P., Baldi-Sevilla A., Salazar-Delgado J., Pacheco-Fallas, J.F., Loria-Salazar L., Reyes-Lizcano F., & Cely-Leal N. (2016). Adhesive properties of asphalts and aggregates in tropical climates. International Journal of Pavement Engineering, 19(8), 738–747. <https://doi:10.1080/10298436.2016.1199884>.
- Aguiar-moya, J.P.; Salazar-Delgado, J., Baldi-Sevilla, A.; Leiva Villacorta, F.; Loria-Salazar, L. (2015) Effect of Aging on Adhesion Properties of Asphalt Mixtures with the Use of Bitumen Bond Strength and Surface Energy Measurement Tests. Transportation Research Record: Journal of the Transportation Research Board, n. 2505, p. 57-65.
- Ahmed T.A, Lee H., Williams R.C. (2017) Using a modified asphalt bond strength test to investigate the properties of asphalt binders with poly ethylene wax-based warm mix asphalt additive. International Journal of Pavement Research and Technology, (), S1996681417300858. <https://doi:10.1016/j.ijprt.2017.08.004>.
- Alexander M., Mindess S. (2005) Aggregates in concrete. New York: Taylor and Francis, p. 439.
- Al-Qadi I.L., Wang H., Yoo P.J., Dessouky S.H. (2008) Dynamic Analysis and In-Situ Validation of Perpetual Pavement Response to Vehicular Loading. In Transportation Research Record: Journal of the Transportation Research Board, No. 2087, Transportation Research Board of the National Academies, Washington, D.C., pp. 29–39.
- Al-Rousan T.M. (2004) Characterization of aggregate shape properties using a computer automated system (Doctoral dissertation). Department of Civil Engineering. Texas A&M University, College Station, TX.
- Arabani M., Roshani H., Hamed G.H. (2012) Estimating Moisture Sensitivity of Warm Mix Asphalt Modified with Zycosoil as an Antistrip Agent Using Surface Free Energy Method.

- Journal of Materials in Civil Engineering, 24(7), 889–897. [https://doi:10.1061/\(asce\)mt.1943-5533.0000455](https://doi:10.1061/(asce)mt.1943-5533.0000455).
- Araújo P.C., Soares J.B., Holanda A.S., Parente E.P., Evangelista F. (2010) Dynamic Viscoelastic Analysis of Asphalt Pavements using Finite Element Formulation. *Road Materials and Pavement Design*, v. 11, p. 409–433.
- ASTM D7175-15 (2015) Standard Test Method for Determining the Rheological Properties of Asphalt Binder Using a Dynamic Shear Rheometer, ASTM International, West Conshohocken, PA. <https://doi:10.1520/D7175-15>.
- ASTM D2872-19 (2019) Standard Test Method for Effect of Heat and Air on a Moving Film of Asphalt (Rolling Thin-Film Oven Test), ASTM International, West Conshohocken, PA. <https://doi:10.1520/D2872-19>.
- ASTM D3625-20 (2020) Standard Practice for Effect of Water on Asphalt-Coated Aggregate Using Boiling Water, ASTM International, West Conshohocken, PA.
- ASTM D7405-20 (2020) Standard Test Method for Multiple Stress Creep and Recovery (MSCR) of Asphalt Binder Using a Dynamic Shear Rheometer, ASTM International, West Conshohocken, PA. <https://doi:10.1520/D7405-20>.
- Azarhoosh A.R., Nejad M.F., Khodaii A. (2016) The influence of cohesion and adhesion parameters on the fatigue life of hot mix asphalt. *The Journal of Adhesion*, 93(13). <https://doi:10.1080/00218464.2016.1201656>.
- Babadopoulos L.F.A.L., Soares J.B., Ferreira J.L.S., Nascimento L.A.H. (2018) Fatigue cracking simulation of aged asphalt pavements using a viscoelastic continuum damage model. *Road Materials and Pavement Design*, 19(3), 546–560. <https://doi:10.1080/14680629.2018.1418715>.
- Baek C.M. (2010) An Investigation of Top-Down Cracking Mechanisms Using Viscoelastic Continuum Damage Finite Element Program". Ph.D. dissertation, North Carolina State University.
- Bagampadde U., Isacsson U., Kiggundu B.M. (2005) Influence of aggregate chemical and mineralogical composition on stripping in bituminous mixtures. *International Journal of Pavement Engineering*, 6(4), 229–239. <https://doi:10.1080/10298430500440796>.
- Baladi G. (1989) Fatigue life and permanent deformation characteristics of asphalt concrete mixes. *Transportation Research Record* 1227. Washington, DC: Transportation Research Board.
- Bastos J.B.S., Babadopoulos L.F.A.L., Soares J.B. (2017) Relationship between multiple stress creep recovery (MSCR) binder test results and asphalt concrete rutting resistance in Brazilian roadways. *Construction and Building Materials* 145, 20–27. <https://doi:10.1016/j.conbuildmat.2017.03.216>.
- Bessa I.S., Branco V.T.F.C., Soares J.B., Neto J.A.N. (2015) Aggregate Shape Properties and Their Influence on the Behavior of Hot-Mix Asphalt. *Journal of Materials in Civil Engineering*, 27(7), 04014212. [https://doi:10.1061/\(asce\)mt.1943-5533.0001181](https://doi:10.1061/(asce)mt.1943-5533.0001181)
- Bhasin A., Masad E., Little D., Lytton R. (2006) Limits on adhesive bond energy for improved resistance of hot mix asphalt to moisture damage. *Transportation Research Record* 1970: 3–13. <https://doi:10.3141/1970-03>.
- Bringel R.M., Velasquez R., Bahia H.U. (2011) Measuring the Effect of Moisture on Asphalt–Aggregate Bond with the Bitumen Bond Strength Test. *Transportation Research Record: Journal of the Transportation Research Board*, n. 2209, p. 70-81.
- Caputo P., Miriello D., Bloise A., Baldino N., Milet O., Ranieri G.A. (2020) A comparison and correlation between bitumen adhesion evaluation test methods, boiling and contact angle tests. *International Journal of Adhesion and Adhesives*, 102(), 102680. <https://doi:10.1016/j.ijadhadh.2020.102680>.

- Caro S., Masad E., Airey G., Bhasin A., Little D. (2008) Probabilistic analysis of fracture in asphalt mixtures caused by moisture damage. *Transportation Research Record* 2057, Transportation Research Board, Washington, DC, 28–36.
- Chehab G.R., Kim Y.R., Schapery R.A., Witczak M.W., Bonaquist R. (2002) Time-Temperature Superposition Principle for Asphalt Concrete Mixtures with Growing Damage in Tension State. *Journal of the Association of Asphalt Paving Technologists, AAPT* 71: 559-593.
- Chen X., Huang B. (2008) Evaluation of moisture damage in hot mix asphalt using simple performance and superpave indirect tensile tests. *Construction and Building Materials*, 22(9), 1950-1962. <https://doi:10.1016/j.conbuildmat.2007.07.014>.
- Cheng D.X., Little D., Lytton R., Holste J. (2002) Surface Energy Measurement of Asphalt and Its Application to Predicting Fatigue and Healing in Asphalt Mixtures. *Transportation Research Record: Journal of the Transportation Research Board* 1810, 44–53. doi:10.3141/1810-06.
- Cui S., Blackman B.R.K., Kinloch A.J., Taylor A.C. (2014) Durability of asphalt mixtures: Effect of aggregate type and adhesion promoters. *International Journal of Adhesion and Adhesives*, 54, 100–111. <https://doi:10.1016/j.ijadhadh.2014.05.009>.
- Diab A., You Z., Hossain Z., Zaman M. (2014) Moisture Susceptibility Evaluation of Nanosize Hydrated Lime-Modified Asphalt-Aggregate Systems Based on Surface Free Energy Concept. *Transportation Research Record: Journal of the Transportation Research Board*, 2446(), 52–59. <https://doi:10.3141/2446-06>.
- Diógenes L.M., Bessa I.S., Branco V.T.F.C., Mahmoud E. (2018) The influence of stone crushing processes on aggregate shape properties. *Road Materials and Pavement Design*, 1-18. <https://doi:10.1080/14680629.2017.1422792>.
- DNIT 136-ME (2018) Pavimentação asfáltica – Misturas asfálticas – Determinação da resistência à tração por compressão diametral – Método de ensaio, Rio de Janeiro.
- DNIT 184-ME (2018) Pavimentação - Misturas asfálticas - Ensaio uniaxial de carga repetida para determinação da resistência à deformação permanente – Método de ensaio, Rio de Janeiro.
- Dong M.; Sun W.; Li L.; Gao Y. (2020) Effect of asphalt film thickness on shear mechanical properties of asphalt-aggregate interface. *Construction and Building Materials*, 263(), 120208-. doi:10.1016/j.conbuildmat.2020.120208.
- Eslamnia M.S., Thirunavukkarasu S., Guddati M.N., Kim Y.R. (2012) Accelerated pavement performance modeling using layered viscoelastic analysis. 7th RILEM International Conference on Cracking in Pavements, 4, 497–506. [https://doi:10.1007/978-94-007-4566-7\\_48](https://doi:10.1007/978-94-007-4566-7_48).
- Etheridge R.A., Wang Y.D., Kim S.S., Kim Y.R. (2019) Evaluation of Fatigue Cracking Resistance of Asphalt Mixtures Using Apparent Damage Capacity. *Journal of Materials in Civil Engineering*, 31(11), 04019257. [https://doi:10.1061/\(asce\)mt.1943-5533.0002870](https://doi:10.1061/(asce)mt.1943-5533.0002870).
- Forough S.A., Moghadas Nejad F., Khodaii A. (2014) Comparison of tensile and compressive relaxation modulus of asphalt mixes under various testing conditions. *Materials and Structures* 49(1-2): 207-223. <https://doi:10.1617/s11527-014-0489-y>.
- Ghabchi R., Rani S., Zaman M., Ali S.A. (2019) Effect of WMA additive on properties of PPA-modified asphalt binders containing anti-stripping agent. *International Journal of Pavement Engineering*, (), 1–14. <https://doi:10.1080/10298436.2019.1614584>.
- Habal A., Singh D. (2019) Effects of warm mix asphalt additives on bonding potential and failure pattern of asphalt-aggregate systems using strength and energy parameters. *International Journal of Pavement Engineering*, (), 1–13. <https://doi:10.1080/10298436.2019.1623399>.

- Hamedi G.H., Tahami S.A. (2017) The effect of using anti-stripping additives on moisture damage of hot mix asphalt. International Journal of Adhesion and Adhesives, S014374961730067. <https://doi:10.1016/j.ijadhadh.2017.03.016>.
- Harnish I.C. (2010) Liquid Anti-Strip Technology & Best Practices. Technical Manager-Aphalt Additives. ArrMaz Custom Chemicals, Overland Park, USA.
- Hesami E., Mehdizadeh G. (2017) Study of the amine-based liquid anti-stripping agents by simulating hot mix asphalt plant production process. Construction and Building Materials, 157, 1011–1017. <https://doi:10.1016/j.conbuildmat.2017.09.168>.
- Hicks R.G. (1991) Moisture damage in asphalt concrete. National Cooperative Highway Research Program. Synthesis of Highway Practice 175, Transportation Research Board, Washington.
- Holanda A.S., Parente Júnior E., Melo T.D.B., Evangelista Júnior F., Soares J.B. (2006) Finite Element of Flexible Pavements. XXVII Iberian Latin-American Congress on Computational Methods in Engineering (CILAMCE). Belém, PA.
- Hou Y., Xiaoping J., Jia L., Xianghang L. (2018) Adhesion between Asphalt and Recycled Concrete Aggregate and Its Impact on the Properties of Asphalt Mixture. Materials, 11(12). <https://doi:10.3390/ma11122528>.
- Huang W., Lv Q., Xiao F. (2016) Investigation of using binder bond strength test to evaluate adhesion and self-healing properties of modified asphalt binders. Construction and Building Materials, 113(), 49–56. <https://doi:10.1016/j.conbuildmat.2016.03.047>.
- Ibiapina D.S., Castelo Branco V.T.F., Diógenes L.M., Motta L.M.G., Freitas S.M. (2018) Proposição de um sistema de classificação das propriedades de forma de agregados caracterizados com o uso do processamento digital de imagens a partir de materiais oriundos do Brasil. Transportes 26(4). <https://doi:10.14295/transportes.v26i4.1510>.
- Jamieson I.L., Moulthrop J.S., Jones D.R. (1995) SHRP Results on Binder-Aggregate Adhesion and Resistance to Stripping. Asphalt Yearbook 1995, Institute of Asphalt Technology, United Kingdom.
- Johnson, D.R.; Freeman, R.B. (2002) Rehabilitation Techniques for Stripped Asphalt Pavements. FHWA/MT-002-003/8123. Western Transportation Institute, Bozeman, Montana, USA.
- Kanitpong K., Bahia H.U. (2003) Role of adhesion and thin film thickness of asphalt binders in moisture damage of HMA. Journal of the association of asphalt paving technologists 72: 502-528.
- Kanitpong K., Bahia H.U. (2008) Evaluation of HMA moisture damage in Wisconsin as it relates to pavement performance. International Journal of Pavement Engineering, 9(1), 9-17. <https://doi:10.1080/10298430600965122>.
- Khodary F. (2010) Evaluation of fatigue resistance for modified asphalt concrete mixtures based on dissipated energy concepts. PhD Thesis, Technische Universität Darmstadt, Darmstadt.
- Kiggundu B.M.; Roberts F.L. (1988) Stripping in HMA Mixtures: State-of-the-Art and Critical Review of Test Methods. Auburn University: National Center for Asphalt Technology.
- Kim Y.R. (2018) Advances in Materials and Pavement Performance Prediction: Proceedings of the International AM3P Conference. Edited by Masad E., Bhasin A., Scarpas T., Menapace I., Kumar A. Taylor & Francis Group, London, ISBN 978-1-138-313095.
- Kringos N., Azari H., Scarpas A. (2009) Identification of Parameters Related to Moisture Conditioning That Cause Variability in Modified Lottman Test. Transportation Research Record: Journal of the Transportation Research Board, 2127(), 1-11. <https://doi:10.3141/2127-01>.
- Kringos N., Scarpas T., Kasbergen C., Selvadurai P. (2008) Modelling of combined physical-mechanical moisture-induced damage in asphaltic mixes, Part 1: governing processes and

- formulations. International Journal of Pavement Engineering, 9(2), 115–128. <https://doi:10.1080/10298430701792185>.
- LEI nº. 13.103, de 2 de março de 2015. Acessado em 02/03/2021 em: [http://www.planalto.gov.br/ccivil\\_03/\\_ato2015-2018/2015/lei/l13103.htm](http://www.planalto.gov.br/ccivil_03/_ato2015-2018/2015/lei/l13103.htm).
- LEI nº. 7.408, DE 25 DE NOVEMBRO DE 1985. Acessado em 02/03/2021 em: [http://www.planalto.gov.br/ccivil\\_03/leis/l7408.htm](http://www.planalto.gov.br/ccivil_03/leis/l7408.htm).
- Little D.N., Jones IV D.R. (2003) Chemical and Mechanical Processes of Moisture Damage in Hot-Mix Asphalt Pavements. Moisture Sensitivity of Asphalt Pavements – A National Seminar; Transportation Research Board.
- Liu Y., Huang Y., Sun W., Nair H., Lane D.S., Wang L. (2017) Effect of coarse aggregate morphology on the mechanical properties of stone matrix asphalt. Construction and Building Materials 152: 48–56. <https://doi:10.1016/j.conbuildmat.2017.06.062>.
- Lucas Júnior J.L.O., Soares J.B. (2019) Desenvolvimento de metodologia para avaliação da adesividade agregado-ligante com o uso de processamento digital de imagem. Transportes. <https://doi.org/10.14295/transportes.v27i1.1552>.
- Lucas Júnior J.L.O., Babadopoulos L.F.A.L., Soares J.B. (2019a) Aggregate-Binder Adhesiveness Assessment and Investigation of the Influence of Morphological and Physico-Chemical Properties of Mineral Aggregates. Road Materials and Pavement Design 20 (March 2019): 1–12. <https://doi.org/10.1080/14680629.2019.1588773>.
- Lucas Júnior J.L.O., Babadopoulos L.F.A.L., Soares J.B. (2019b) Moisture-induced damage resistance, stiffness and fatigue life of asphalt mixtures with different aggregate-binder adhesion properties. Construction and Building Material 216: 166-175. <https://doi.org/10.1016/j.conbuildmat.2019.04.241>.
- Lucas Júnior J.L.O., Babadopoulos L.F.A.L., Soares J.B (2020a) Influence of Aggregate-Binder Adhesion on Fatigue Life of Asphalt Mixtures. Journal of Testing and Evaluation 48: 1, 150-160. <https://doi:10.1520/JTE20190109>.
- Lucas Júnior J.L.O., Babadopoulos L.F.A.L., Soares J.B. (2020b) Effect of aggregate shape properties and binder's adhesiveness to aggregate on results of compression and tension/compression tests on hot mix asphalt. Materials and Structures 53, 1–15. <https://doi.org/10.1617/s11527-020-01472-1>.
- Lucas Júnior J.L.O., Babadopoulos L.F.A.L., Soares J.B., Souza L.T. (2021) Evaluating the effect of amine-based anti-stripping agent on the fatigue life of asphalt pavements. International Journal of Pavement Engineering. <https://doi.org/10.1080/10298436.2020.1870687>.
- Lytton R.L., Gu F., Zhang Y., Luo X. (2017) Characteristics of undamaged asphalt mixtures in tension and compression. International Journal of Pavement Engineering 19(3): 192-204. <https://doi:10.1080/10298436.2017.1279489>.
- Mahmoud E., Gates L., Masad E., Erdogan S., Garboczi E. (2010) Comprehensive evaluation of AIMS texture, angularity, and dimension measurements. Journal of Materials in Civil Engineering 22(4): 369-379. [https://doi:10.1061/\(asce\)mt.1943-5533.0000033](https://doi:10.1061/(asce)mt.1943-5533.0000033).
- Majidzadeh K., Brovold F.N. (1968) State of the art: Effect of water on bitumen aggregate mixtures. Highway Research Board, Special Report n. 98, p. 77.
- Masad E. (2004) Aggregate imaging system (AIMS): basics and applications (Report nº FHWA/TX-05/5- 1707-01-1). College Station, TX: Texas Transportation Institute. Retrieved from <http://tti.tamu.edu/documents/5-1707-01-1.pdf>
- McCann M., Anderson-Sprecher R., Thomas K.P. (2005) Statistical comparison between SHRP aggregate physical and chemical properties and the moisture sensitivity of aggregate-binder mixtures. Road Materials and Pavement Design, 6(2), 197–215

- Minhoto M.J.C., Pais J.C., Pereira P.A.A., Santos L.G.P. (2005) The influence of temperature variation in the prediction of the pavement overlay life. *Road Materials and Pavement Design* 6(3), 365-384.
- Monismith C.L. (1970) Influence of shape, size, and surface texture on the stiffness and fatigue response of asphalt mixtures. Technical Report 109, Transportation Research Record, National Research Council.
- Nascimento L.A.H. (2015) Implementation and Validation of the Viscoelastic Continuum Damage Theory for Asphalt Mixture and Pavement Analysis in Brazil. Tese de Doutorado. North Carolina State University. Raleigh-USA.
- Nascimento L.A.H. (2016) Apresentação realizada no Departamento de Engenharia de Transportes na Universidade Federal do Ceará. Data: 21/12/2016, Fortaleza-CE.
- Nguyen Q.T., Di Benedetto H., Sauzéat C., Nguyen M.L., Hoang T.T.N. (2016) 3D complex modulus tests on bituminous mixture with sinusoidal loadings in tension and/or compression. *Materials and Structures* 50(1). <https://doi:10.1617/s11527-016-0970-x>
- Norouzi A., Kim Y.R. (2015) Mechanistic evaluation of fatigue cracking in asphalt pavements. *International Journal of Pavement Engineering*, 18(6), 530–546. doi:10.1080/10298436.2015.1095909.
- Olard F., Di Benedetto H. (2003) General “2S2P1D” model and relation between the linear viscoelastic behaviours of bituminous binders and mixes, *Road Material and Pavement Design* 4 (2). <https://doi.org/10.1080/14680629.2003.9689946>.
- Pais J.C., Amorim S.I.R., Minhoto M.J.C. (2013) Impact of traffic overload on road pavement performance. *Journal of Transportation Engineering*, 139 (9), 873–879. doi:10.1061/(ASCE)TE.1943-5436.0000571.
- Park H.J., Eslaminia M., Kim Y.R. (2014) Mechanistic evaluation of cracking in in-service asphalt pavements. *Materials and Structures*, 47(8), 1339–1358. <https://doi:10.1617/s11527-014-0307-6>.
- Park S.W., Kim Y.R., Schapery R.A. (1996) A viscoelastic continuum damage model and its application to uniaxial behavior of asphalt concrete. *Mechanics of Materials* 24: 241-255. [https://doi.org/10.1016/S0167-6636\(96\)00042-7](https://doi.org/10.1016/S0167-6636(96)00042-7).
- Pasandín A.R., Pérez I. (2015) The influence of the mineral filler on the adhesion between aggregates and bitumen. *International Journal of Adhesion and Adhesives*, 58(), 53–58. <https://doi:10.1016/j.ijadhadh.2015.01.005>.
- Resolução nº. 1, de 8 de janeiro de 2021. Departamento Nacional se Infraestrutura De Transportes, DNIT. Acessado em 02/03/2021 em: <https://www.in.gov.br/web/dou/-/resolucao-n-1-de-8-de-janeiro-de-2021-298507898#:~:text=Estabelece%20normas%20so bre%20o%20uso,pelo%20Conselho%20Nacional%20de%20Tr%C3%A2nsito>.
- Resolução nº. 104 (1999) Dispõe sobre a tolerância máxima do peso bruto dos veículos. Conselho Nacional de Trânsito, CONTRAN.
- Rocha Segundo I.R., Castelo Branco V.T.F, Vasconcelos K.L., Holanda A.S. (2016) Misturas asfálticas recicladas a quente com incorporação de elevado percentual de fresado como alternativa para camada de módulo elevado. *Transportes*, v. 24, n. 4, p. 85-94.
- Rys D., Judycki J., Jaskula P. (2015) Analysis of effect of overloaded vehicles on fatigue life of flexible pavements based on weigh in motion (WIM) data. *International Journal of Pavement Engineering*. <https://doi:10.1080/10298436.2015.1019493>.
- Sabouri M. (2020) Evaluation of performance-based mix design for asphalt mixtures containing Reclaimed Asphalt Pavement (RAP). *Construction and Building Materials*, 235, 117545. <https://doi:10.1016/j.conbuildmat.2019.117545>.
- Sabouri M., Kim Y.R. (2014) Development of a failure criterion for asphalt mixtures under different modes of fatigue loading. *Transportation Research Record: Journal of the Transportation Research Board*, 2447(4), 117–125. <https://doi:10.3141/2447-13>.

- Santagata F.A.; Cardone F., Canestrari F., Bahia H.U. (2009) Modified PATTI test for the characterization of adhesion and cohesion properties of asphalt binders. Proceedings of the Sixth International Conference on Maintenance and Rehabilitation of Pavements and Technological Control, v. 1, p. 124-133.
- Santiago L.S., Torquato e Silva S.A., Soares J.B. (2018) Determinação do dano em pavimentos asfálticos por meio da combinação do modelo S-VECD com análises elásticas. Revista Transportes. v. 26, n. 2, p. 31-43.
- Santiago, L.S.; Babadopoulos, L. F. A. L; Soares J.B. (2019) Desenvolvimento de função de transferência para previsão de área trincada em pavimentos asfálticos por meio da simulação do dano por fadiga utilizando modelo S-VECD e análises elásticas. Revista Transportes. v. 28, n. 3, p. 121-136. <https://doi:10.14295/transportes.v28i3.1900>.
- Santos A.B.V., Soares J.B., Babadopoulos L.F.A.L. (2020) Influência da temperatura e da velocidade de tráfego na previsão de área trincada de pavimentos asfálticos. Transportes 28 (4). <https://doi.org/10.14295/transportes.v28i4.2394>.
- Schapery R.A. (1984) Correspondence Principles and a Generalized J-integral for Large Deformation and Fracture Analysis of Viscoelastic Media. International Journal of Fracture 25: 195-223. <https://doi.org/10.1007/BF01140837>.
- SEINFRA-CE (2021) Secretaria da Infraestrutura do Ceará. Tabela de Custos 026/21. <http://www.seinfra.ce.gov.br/index.php>. Acessado em, 02 de março de 2021.
- Terrel R.L., Al-Swailmi S. (1994) Water sensitivity of asphalt-aggregate mixes: Test selection. SHRP-A-403, strategic highway research program. Washington, DC: National Research Council.
- Terrel, R.L.; Shute J.W. (1989) SHRP-A/IR-89-003: Summary Report on Water Sensitivity. National Research Council, Washington, D.C.
- Underwood B.S., Baek C., Kim Y.R. (2012) Simplified viscoelastic continuum damage model as platform for asphalt concrete fatigue analysis. Transportation Research Record 2296, 36–45.
- User Guide (2018) Layered viscoelastic pavement analysis for critical distresses FlexPAVE 1.1<sup>Alpha</sup>. Department of Civil, Construction, and Environmental Engineering North Carolina State University. Accessed in: [http://onlinepubs.trb.org/Onlinepubs/nchrp/docs/FlexPAVE1.1Standalone\\_UserManual.docx](http://onlinepubs.trb.org/Onlinepubs/nchrp/docs/FlexPAVE1.1Standalone_UserManual.docx).
- Valdés-Vidal G., Calabi-Floody A., Miró-Recasens R., Norambuena-Contreras J. (2015) Mechanical behavior of asphalt mixtures with different aggregate type. Construction and Building Materials 101: 474–481. <https://doi:10.1016/j.conbuildmat.2015.10.050>.
- Wang Y., Norouzi A., Kim Y.R. (2016) Comparison of Fatigue Cracking Performance of Asphalt Pavements Predicted by Pavement ME and LVECD Programs. Transportation Research Record: Journal of the Transportation Research Board, 2590, 44–55. <https://doi:10.3141/2590-06>.
- Wang Y.D., Keshavarzi B., Kim Y.R. (2018) Fatigue Performance Analysis of Pavements with RAP Using Viscoelastic Continuum Damage Theory. KSCE Journal of Civil Engineering, 22(6), 2118–2125. <https://doi:10.1007/s12205-018-2648-0>.
- Woodhams R.T. (1998) Ferric Oxide Adhesion Promoters for Water Resistant Asphalt Pavements. The Journal of Adhesion, 68(1-2), 65–91. <https://doi:10.1080/00218469808029580>.
- Yin Y., Huaxin C., Dongliang K., Lifang S., Lu W. (2017) Effect of chemical composition of aggregate on interfacial adhesion property between aggregate and asphalt. Construction and Building Materials, 146, 231–237.
- Zhang D., Luo R. (2019) Using the surface free energy (SFE) method to investigate the effects of additives on moisture susceptibility of asphalt mixtures. International Journal of Adhesion and Adhesives, 95, 102437. <https://doi:10.1016/j.ijadhadh.2019.102437>.

- Zhao Y., Tan Y., Zhou C. (2012) Determination of axle load spectra based on percentage of overloaded trucks for mechanistic-empirical pavement design. *Journal of Road Materials and Pavement Design*, 13 (4), 850–863. <https://doi:10.1080/14680629.2012.735796>.
- Zhu C., Xu G., Zhang H., Xiao F., Amirkhanian S., Wu C. (2018) Influence of different anti-stripping agents on the rheological properties of asphalt binder at high temperature. *Construction and Building Materials*, 164(), 317–325. <https://doi:10.1016/j.conbuildmat.2017.12.236>.